

**NASA Contractor Report 181993**

**GROUND SHAKE TEST OF THE UH-60A HELICOPTER  
AIRFRAME AND COMPARISON WITH NASTRAN  
FINITE ELEMENT MODEL PREDICTIONS**

**G. R. Howland, J. A. Durno, and W. J. Twomey**

**UNITED TECHNOLOGIES CORPORATION  
SIKORSKY AIRCRAFT DIVISION  
STRATFORD, CT 06601**

**Contract NAS1-17499  
March 1990**

(NASA-CR-181993) GROUND SHAKE TEST OF THE  
UH-60A HELICOPTER AIRFRAME AND COMPARISON  
WITH NASTRAN FINITE ELEMENT MODEL  
PREDICTIONS Final Report (Sikorsky  
Aircraft) 256 p

N90-25143

Unclas  
CSCL 01C 63/08 0293027



National Aeronautics and  
Space Administration

**Langley Research Center**  
Hampton, Virginia 23665-5225



## FOREWORD

Sikorsky Aircraft has been conducting a study of finite element modeling of helicopter airframes to predict vibration. This work is being performed under U.S. Government Contract NAS1-17499. The contract is monitored by the NASA Langley Research Center, Structures Directorate.

This report summarizes the test plan, test results, and a comparison of test results with results obtained from analysis using a NASTRAN finite element model. These results will serve as the basis for validation of a finite element vibration model of the Sikorsky UH-60A helicopter airframe. Key NASA and Sikorsky personnel are listed below.

### NASA LANGLEY

1 Panice H. Clark, Contracting Officer  
Joseph W. Owens, Contract Specialist  
John H. Cline, Technical Representative  
Raymond G. Kvaternik, Leader, Rotorcraft  
Structural Dynamics Group

### SIKORSKY

Dennis Prebenson, Contract  
Administrator  
Wen-Liu Miao, Chief of Dynamics  
David O. Adams, Chief of Structural  
Test  
Hugh Kearney, Senior Test Engineer  
William Twomey, Senior Dynamics  
Engineer  
Guy Howland, Structural Dynamics  
Test Engineer  
Jason Durno, Dynamics Engineer



## TABLE OF CONTENTS

<u>Section</u>	<u>Page</u>
1.0 Introduction	7
2.0 Aircraft Description	11
3.0 Test and Comparison Plan	23
3.1 Introduction	25
3.2 Test Article Configuration	33
3.3 Method of Excitation	39
3.4 Instrumentation and Data Analysis	51
3.5 Comparison of Test Results with NASTRAN	81
4.0 Shake Test Description	91
4.1 Test Article Configuration	93
4.2 Aircraft Excitation	105
4.3 Instrumentation and Measurement Procedures	113
5.0 Shake Test Results	123
5.1 Rigid Body Modes	125
5.2 Suspension System Modes	131
5.3 Nonlinear Response Investigation	139
5.4 Summary of Test Results	151



TABLE OF CONTENTS (Continued)

<u>Section</u>	<u>Page</u>
6.0 NASTRAN Analysis	177
7.0 NASTRAN vs Shake Test: Frequency Response	185
8.0 NASTRAN vs Shake Test: Modal Properties	225
9.0 Schedule and Resources	249
10.0 Conclusions	255
11.0 References	259

PRECEDING PAGE BLANK NOT FILMED

5

~~PAGE 4~~ INTENTIONALLY BLANK





# **SECTION 1.0**

## **INTRODUCTION**



## INTRODUCTION

The NASA Langley Research Center is sponsoring a rotorcraft structural dynamics program with the overall objective to establish in the United States a superior capability to utilize finite element analysis models for calculations to support industrial design of helicopter airframe structures. Viewed as a whole, the program is planned to include efforts by NASA, Universities and the U.S. Helicopter Industry. In the initial phase of the program, teams from the major U.S. manufacturers of helicopter airframes will apply extant finite element analysis methods to calculate static internal loads and vibrations of helicopter airframes of both metal and composite construction, conduct laboratory measurements of the structural behavior of these airframes and perform correlations between analysis and measurements to build up a basis upon which to evaluate the results of the applications. To maintain the necessary scientific observation and control, emphasis throughout these activities will be on advance planning, documentation of methods and procedures, and thorough discussion of results and experiences, all with industry-wide critique to allow maximum technology transfer between companies. The finite element models formed in this phase will then serve as the basis for the development, application, and evaluation of both improved modeling techniques and advanced analytical and computational techniques, all aimed at strengthening and enhancing the technology base which supports industrial design of helicopter airframe structures. Here again, procedures for mutual critique have been established and these procedures call for a thorough discussion among the program participants of each method prior to the applications and of the results and experiences after the applications. The aforementioned rotorcraft structural dynamics program has been given the acronym DAMVIBS (Design Analysis Methods for VibrationS).

The present report presents the results of that phase of the DAMVIBS contract devoted to validating the NASTRAN finite-element model of the Sikorsky UH-60A helicopter. This validation process involved: (1) ground shake testing of a UH-60A airframe, (2) analysis of the test configuration using the NASTRAN Model, and (3) comparison of test and analytical results. No attempt has been made as yet to correlate the two sets of data, that is "to combine them, quantitatively, in order to identify specifically the causes of the discrepancies between predicted and measured properties" (Ref. 1). This report includes: (1) Introduction, (2) Vehicle Description, (3) Test and Comparison Plan, 4) Shake Test Description, (5) Shake Test Results, (6) NASTRAN Analysis, and (7) Comparison of Test and Analysis.



# **SECTION 2.0**

## **AIRCRAFT DESCRIPTION**

## UH-60A VEHICLE DESCRIPTION

The UH-60A is a single rotor helicopter designed for transport of troops and cargo. The aircraft can operate up to 9,979 kg (22,000 lbs) gross weight and cruises at a speed of 74.6 m/sec (145 kts). The primary power is provided by two General Electric T700-GE-700 turbine engines located above and on each side of the aft portion of the mid cabin. The rotor system is four-bladed, with a fully articulated elastomeric bearing main rotor head. Directional control is provided by a four-bladed tractor tail rotor mounted on the top right hand side of the tail rotor pylon. Normal main and tail rotor speeds are 258 rpm and 1,190 rpm, respectively. The horizontal stabilator is of the moveable type, the angle of attack being controlled by a linear electrical actuator mounted within the tail rotor pylon and attached to a fitting on the upper surface of the stabilator. The fuel is carried in two large crashworthy self-sealing fuel tanks located in the transition section between the cabin and the tail cone. The landing gear consists of main wheels on each side of the fuselage and a tail wheel between the cabin and the tail cone. The oleo struts of the three wheels operate as normal air-oil struts in normal landing but are designed to stroke at constant load in crash conditions with high vertical impact velocities. The struts are also used to lower the aircraft until it almost contacts the ground to allow for air transportation in an aircraft with limited ceiling height. Just aft of the tail wheel is a splice in the tailcone which allows manual folding of the tail rotor pylon. The normal crew is a pilot, copilot and crew chief. The UH-60A normally carries 11 troops, but can carry up to 14 with a high density seating arrangement. A cargo hook is provided under the main cabin for transporting cargo using an external sling.

# UH-60A VEHICLE DESCRIPTION

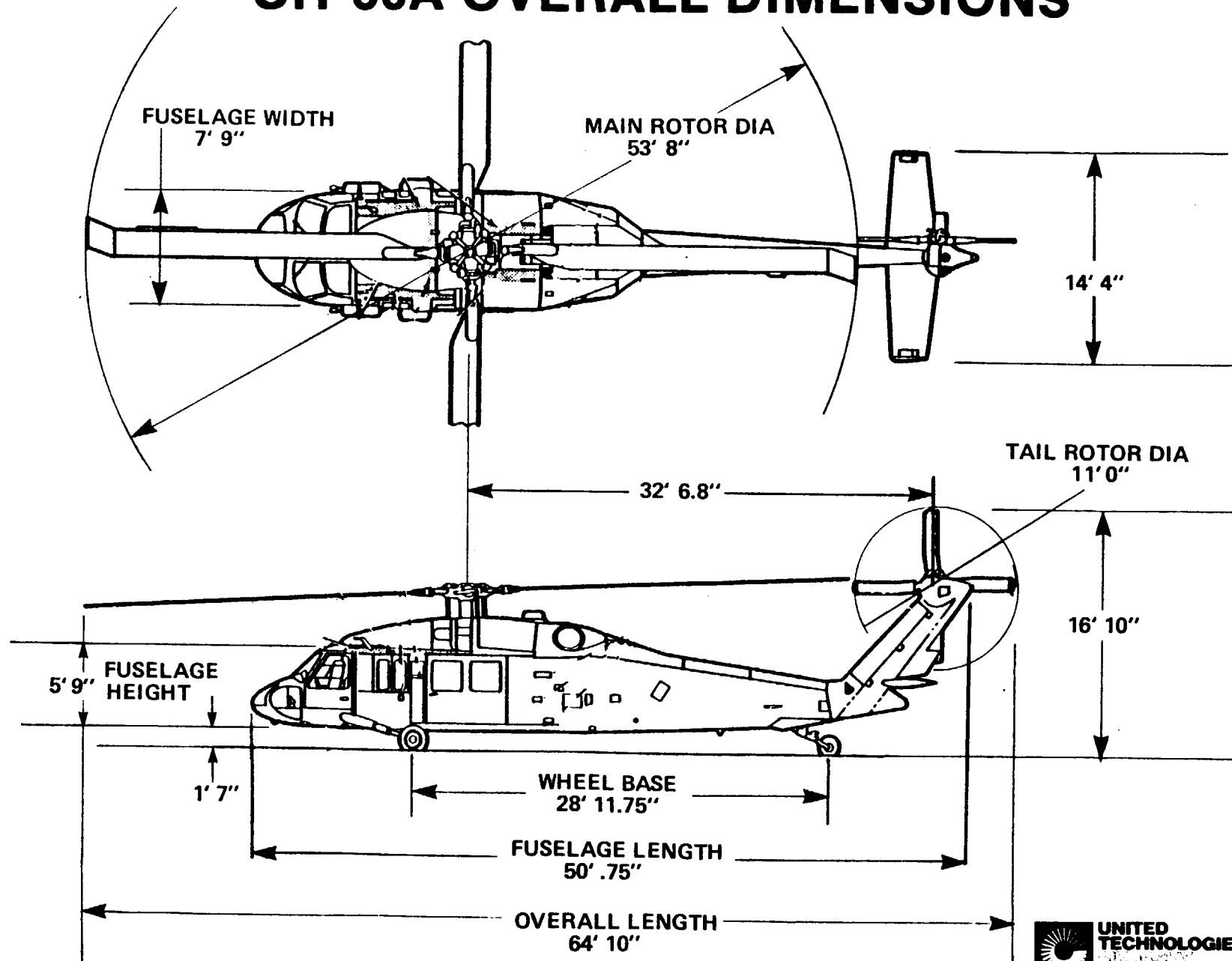


#### UH-60A OVERALL DIMENSIONS

The accompanying figure shows overall dimensions for the UH-60A. The overall length and width, exclusive of the rotor blades, are 15.24 m (50'-0.75") and 2.36 m (7'-9"), respectively. The overall length and width including rotors are 19.76 m (64'-10") and 16.21 m (53'-2"), respectively. The center to center distance of the main and tail rotor is 9.93 m (32'-6.8") and the wheel base is 8.83 m (28'-11.75").



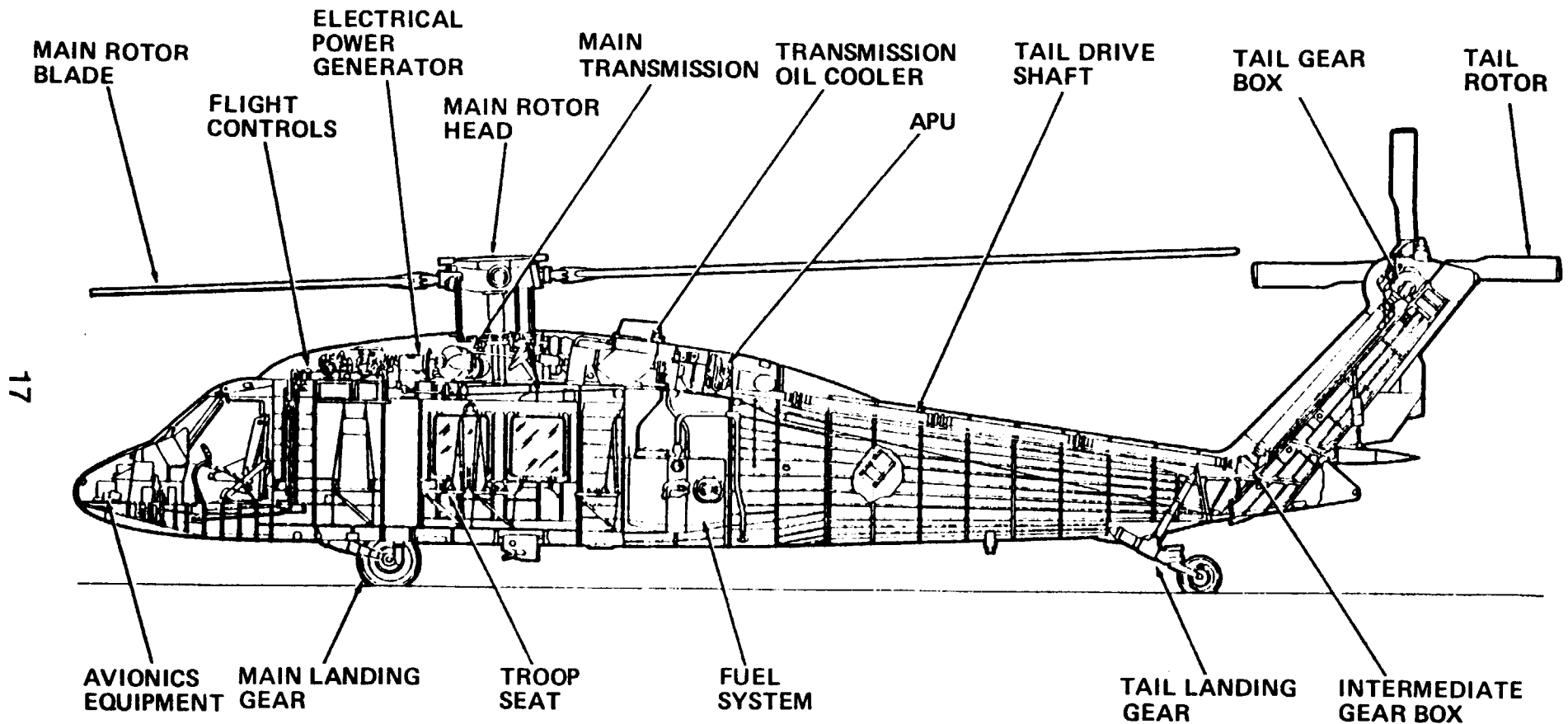
# UH-60A OVERALL DIMENSIONS



## UH-60A GENERAL ARRANGEMENT

The accompanying figure shows the general arrangement of the UH-60A and the locations of the various aircraft components.

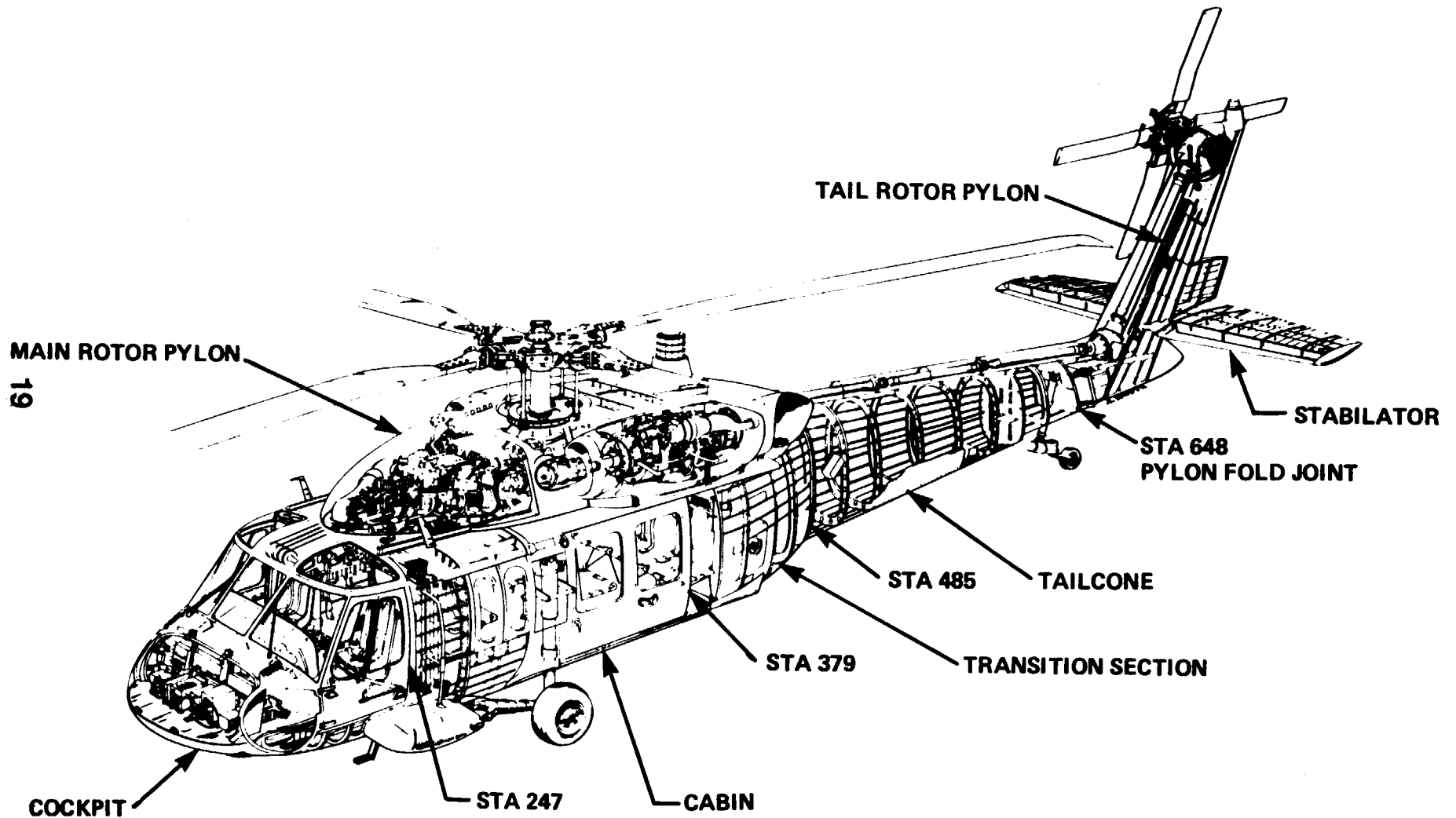
# UH-60A GENERAL ARRANGEMENT



## UH-60A PRIMARY FUSELAGE STRUCTURE

The fuselage of the UH-60A helicopter is an aluminum semi-monocoque structure 15.24 m (600.75 in.) inches long, 2.36 m (93 in.) wide and 1.75 m (69 in.) high consisting of frames, stringers, skins, beams, and bulkheads. Frames and bulkheads are the transverse members of the structure; stringers and beams are the longitudinal members. The principal material used in the airframe construction is aluminum except in high temperature areas, where titanium is used. Generally, the structure is built up from sheet and extruded stock. In areas with high concentrated loads, such as the transmission support structure, machined aluminum fittings are used.

# UH-60A PRIMARY FUSELAGE STRUCTURE

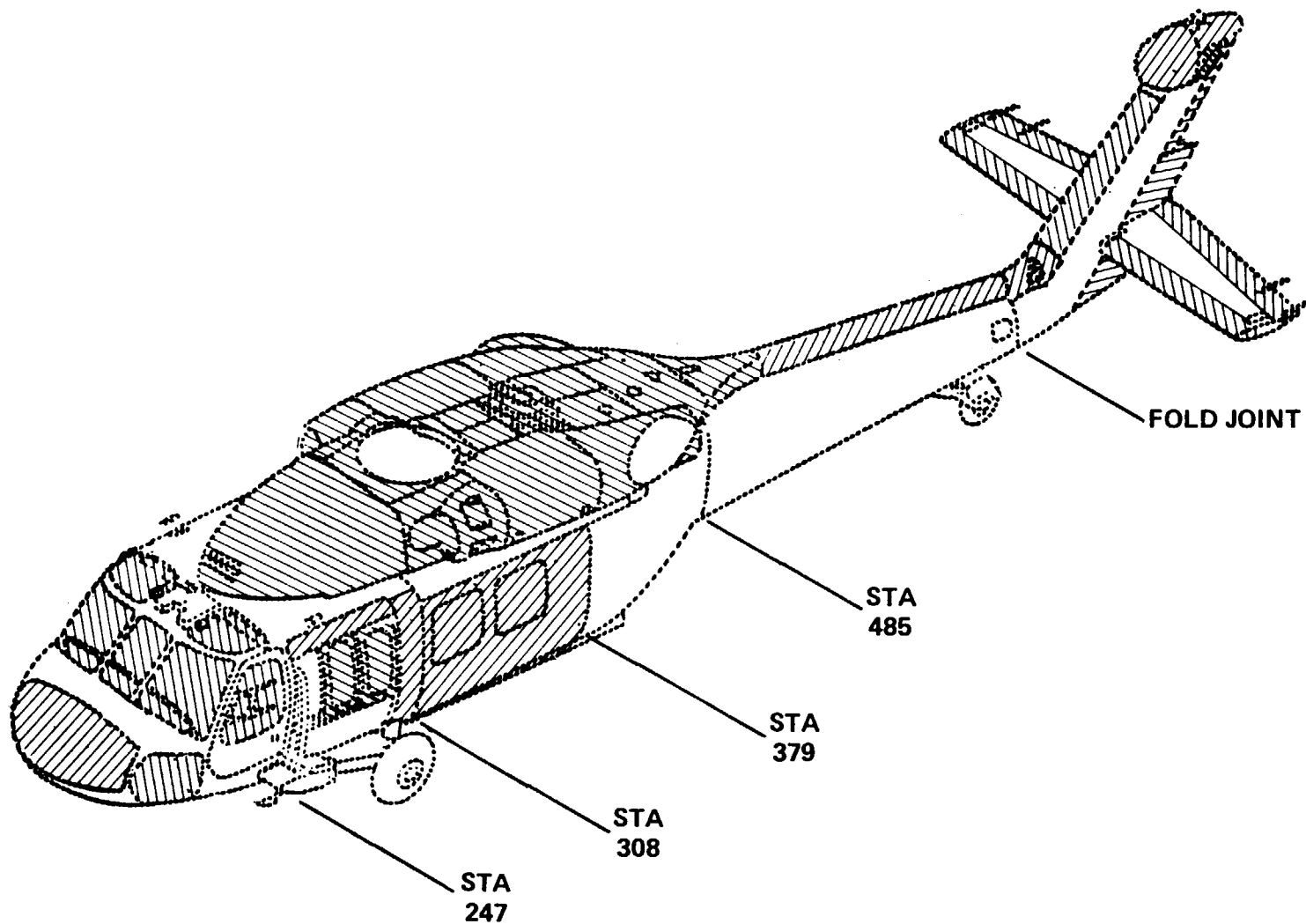


## UH-60A SECONDARY STRUCTURE

A number of elements of secondary structure are provided solely for aerodynamic fairing over mechanical components and are not relied on for other structural functions. Generally, fairings are of sandwich construction consisting of aluminum honeycomb cores with laminated fiberglass or Kevlar skins. In some instances laminated fiberglass or Kevlar is used with no core. The windows in the mid cabin and cockpit, except for the windshields in front of the pilot and copilot, are stretched plexiglass. The windshields, which have wipers, are laminated glass construction with an embedded layer of PVB plastic.

The shaded areas in the accompanying figure show the extent of secondary structure in the UH-60A.

# UH-60A SECONDARY STRUCTURE







**SECTION 3.0**

**TEST AND COMPARISON PLAN**



# **SECTION 3.1**

## **INTRODUCTION**

## TEST AND COMPARISON PLAN OBJECTIVE

The objective of the test and comparison plan is to present all aspects of the test and comparison effort which could reasonably be considered to affect the ability to validate the UH-60A NASTRAN finite element model. The report contains a detailed description of test article configuration, methods of suspension, excitation and vibratory response measurements; presentation of test results; data analysis; and comparison with results from a finite element analysis. Various data analysis techniques are compared and the impact of non-linear response is discussed. The final comparison with the finite element analysis and conclusions reflect the overall ability to meet the program objective.

## **TEST AND COMPARISON PLAN OBJECTIVE**

**The objective is to present all aspects of the test and comparison effort which could reasonably be considered to affect the results**

- **Test article configuration**
- **Method of suspension**
- **Method of excitation**
- **Vibratory response measurement**
- **Data analysis and presentation**
- **Comparison with the finite element analysis**

## SHAKE TEST REQUIREMENTS

To perform a shake test of the UH-60A aircraft with the purpose of comparing the results with the associated finite element model, the following general requirements must be satisfied: the test article configuration must correspond with that modeled in the NASTRAN analysis; the airframe must be suspended in a manner which approximates the free-free analysis condition; induced airframe vibration response, resulting from a single point excitation technique, must be accurately measured and processed to provide data which may be compared directly with the NASTRAN analysis results.

---

## **SHAKE TEST REQUIREMENTS**

**Listed below are the general measurement requirements for performing a shake test on the UH-60A aircraft and comparing the results with the associated finite element model**

**29**

- **Define the test article configuration**
- **Suspend the airframe in a free-free condition**
- **Apply excitation to the airframe**
- **Measure and record induced vibration response**
- **Process measured response data**
- **Prepare plots of processed data for comparison**

## TEST AND COMPARISON APPROACH

In addition to a detailed description of the approach planned to accomplish each of the previously outlined requirements, a number of additional test and analysis objectives will be discussed. These topics are considered to be of importance as to the quality of the measured vibratory response, the amount of information which may be extracted from this measured data, and the extent to which this information can be used to validate the corresponding theoretical model. An outline of these topics is provided below. Each will be addressed in the following sections of the test and comparison plan.

- 1) Incorporate the test methodology, data processing equipment and data analysis techniques which will best support the overall program objectives.
- 2) Investigate the extent and the effects of non-linear response and establish an approach for dealing with this behavior.
- 3) Develop a complete test based modal model (natural frequencies, damping and mode shapes), in addition to the forced response data, to allow the comparison and possible correlation effort to extend to multiple levels of analysis. There are three different levels of a dynamic model which may be developed from either experimentally or theoretically derived sets of data. The levels are equivalent for both but the order of development is reversed as shown below. Each model provides the opportunity for comparison and correlation between test and analysis.

### Theoretical

1. Spatial Model
2. Modal Model
3. Response Model

### Experimental

1. Response Model
2. Modal Model
3. Spatial Model



## **TEST AND COMPARISON APPROACH**

- **Incorporate the test methodology, data processing equipment and data analysis techniques which will best support the overall program objectives.**
- **Investigate the extent and the effects of non-linear response and establish an approach for dealing with this behavior.**
- **Develop a complete test-based modal model (natural frequencies, damping and mode shapes), in addition to the forced response data, to allow the comparison effort to extend to multiple levels of analysis.**



## SECTION 3.2

### TEST ARTICLE CONFIGURATION

## TEST ARTICLE CONFIGURATION

The test article configuration will correspond to the NASTRAN analysis where emphasis was on modeling the basic airframe structure. The aircraft will be empty, without fuel or cargo, and the vibration absorbers will be locked out.

All main rotorhead hardware will be replaced by an aircraft hub which has been modified to include attachments for shaker assembly, overhead suspension and ballast. The shake test article rotorhead mass will be equal to the static (nonflapping) mass of the aircraft rotorhead plus 50% of the main rotor blade flapping mass. Aircraft and test article rotorhead inertia properties will be kept similar.

The tail rotor hub and blades will be replaced by a hub modified to include an attachment for tail suspension and having equivalent lumped mass and center of gravity properties. The main transmission will be locked to prevent the hub from turning with respect to the aircraft.

The test article will otherwise be in delivered flight-ready configuration, with all primary and most secondary structure intact.

## **TEST ARTICLE CONFIGURATION**

- **Configuration will correspond to the NASTRAN analysis conditions of empty aircraft without fuel or cargo**
- **Rotorhead components replaced by aircraft hub modified to include attachments for shaker assembly, overhead suspension, and ballast**
- 35 ● **Test article rotorhead mass equal to the static (non-flapping) mass of the aircraft rotorhead plus 50% of the main rotor blade flapping mass**
- **Center of gravity and inertia properties for facility hubs similar to aircraft properties**
- **Test article will otherwise be in delivered flight-ready configuration, with all primary and most secondary structure installed**

## AIRCRAFT SUSPENSION

The test article is suspended during measurements in a manner which closely approximates the 'free-free' NASTRAN analysis condition. The test article is suspended from deep I-beams, attached to the roof trusses of the test bay, by suspension cables attached to integral lifting eyes in the modified rotor heads. Each suspension cable consists of spring packs fabricated from bungee elastic cords, chain hoists and long steel cables. This soft spring arrangement was designed to isolate the test article from the overhead support structure and, together with the overall pendulum length, provide for aircraft rigid body modes of less than 1.5 Hz. These are less than 20% of the lowest vertical bending mode of the aircraft to prevent significant influence on its response. The actual frequency placement of all six rigid body modes was identified to assure that the method of suspension was adequate.

## **AIRCRAFT SUSPENSION**

- **Aircraft suspended in free flight configuration which closely approximates the “Free-Free” NASTRAN analysis condition**
- **Aircraft suspended at main and tail rotorheads by means of chain hoists, spring-packs fabricated from bungee cord, and long wire cables**
- **Spring-pack stiffness and overall pendulum length designed to meet isolation requirements**
- **Highest rigid body mode frequency less than 20% of the lowest vertical bending mode frequency**
- **Suspension system serves to raise and lower aircraft and maintain proper attitude**





## **SECTION 3.3**

### **METHOD OF EXCITATION**

## AIRFRAME EXCITATION

Vibratory loads will be applied at the main rotor hub in the vertical, lateral and longitudinal directions; and in the vertical and lateral directions at the tail rotor hub. The magnitude of applied loads will be as large as possible, up to the levels of operational loads. Actual levels will be dependent on the amplitude of airframe response and on the extent of non-linear response, but are expected to be in the 100-200 pound range. The frequency range of excitation will be from 3 Hz to 40 Hz (0.17 to 2.3 times the main rotor blade passage frequency).

# AIRFRAME EXCITATION

## Main Rotor Excitation

Vertical  
Lateral  
Longitudinal

## Tail Rotor Excitation

Vertical  
Lateral

Frequency range  
Force level

3 Hz to 40 Hz  
100-200 pounds

## MAIN ROTOR HEAD EXCITATION

The primary method of airframe excitation will be swept (step) sine force input at the main rotor hub. This excitation force will be generated by dual electrohydraulic inertia shakers mounted on opposite arms of the aircraft hub. The shakers consist of high performance servo-controlled actuators, with closed-loop displacement feedback, which provide sinusoidal acceleration of external weights. The acceleration of these weights is measured and used to calculate the shaker force exerted on the hub.

Excitation direction is controlled by rotation of the shaker and hub to provide alignment of the mass acceleration in each of the three principle aircraft axes. The frequency range of excitation is from 0.2 x blade passage frequency (3.4 Hz) to 2.2 x blade passage frequency (37.8 Hz). The force level for airframe excitation will be based on the practical considerations of magnitude of response, nonlinear response, and the magnitude of the shaker response in regions of resonances involving large motions at the rotorhead.

## **MAIN ROTOR HEAD EXCITATION**

- **Primary excitation location is at the main rotor hub**
- **Excitation force supplied by dual electro-hydraulic inertial shakers**
- **Frequency range of excitation is from 0.2 x blade passage frequency (3.4 HZ) to 2.2 x blade passage frequency (37.8HZ)**
- **Applied force based on practical considerations, (nonlinear response, magnitude of response, shaker behavior)**
- **Shaker force calculated from measured acceleration of shaker moving mass**

## APPLICATION OF PURE FORCE WITH DUAL INERTIA SHAKERS

The application of a pure force with dual inertia shakers requires that the two shakers must be identical in configuration and function. They must be mounted at the same offset from the point of force application (main rotor shaft centerline) and the acceleration of each mass must be equal throughout the frequency range of excitation. The phase relationship between shaker forces must remain at  $0^\circ$  and the location of the resultant shaker force applied at the shear center of the main rotor hub arms. The static mass of the shaker system is treated as part of the main rotor head mass and is specifically included as part of the NASTRAN model.

## **APPLICATION OF PURE FORCE WITH DUAL INERTIA SHAKERS**

- **Two shakers identical in configuration and function**
- **Mounted in an identical manner at the same offset from point of force application**
- **Accelerations of each mass must be equal throughout the sweep**
- **The phase relationship between shaker forces must be  $0^\circ$  over entire sweep range**
- **Shaker force located at shear center of main rotor hub arms**
- **Shaker static mass treated as part of the main rotor head mass and is included as part of NASTRAN model**

## SECOND EXCITATION LOCATION

A second excitation location, which is well separated from the main rotor head location, provides excitation and measurement of response modes which may not be adequately defined from main rotor head excitation. A valid reciprocity check is also provided, which aids in the identification of any non-linearities in the aircraft response. A second excitation location also provides additional data for checking the extracted modal parameters.



## **2ND EXCITATION LOCATION**

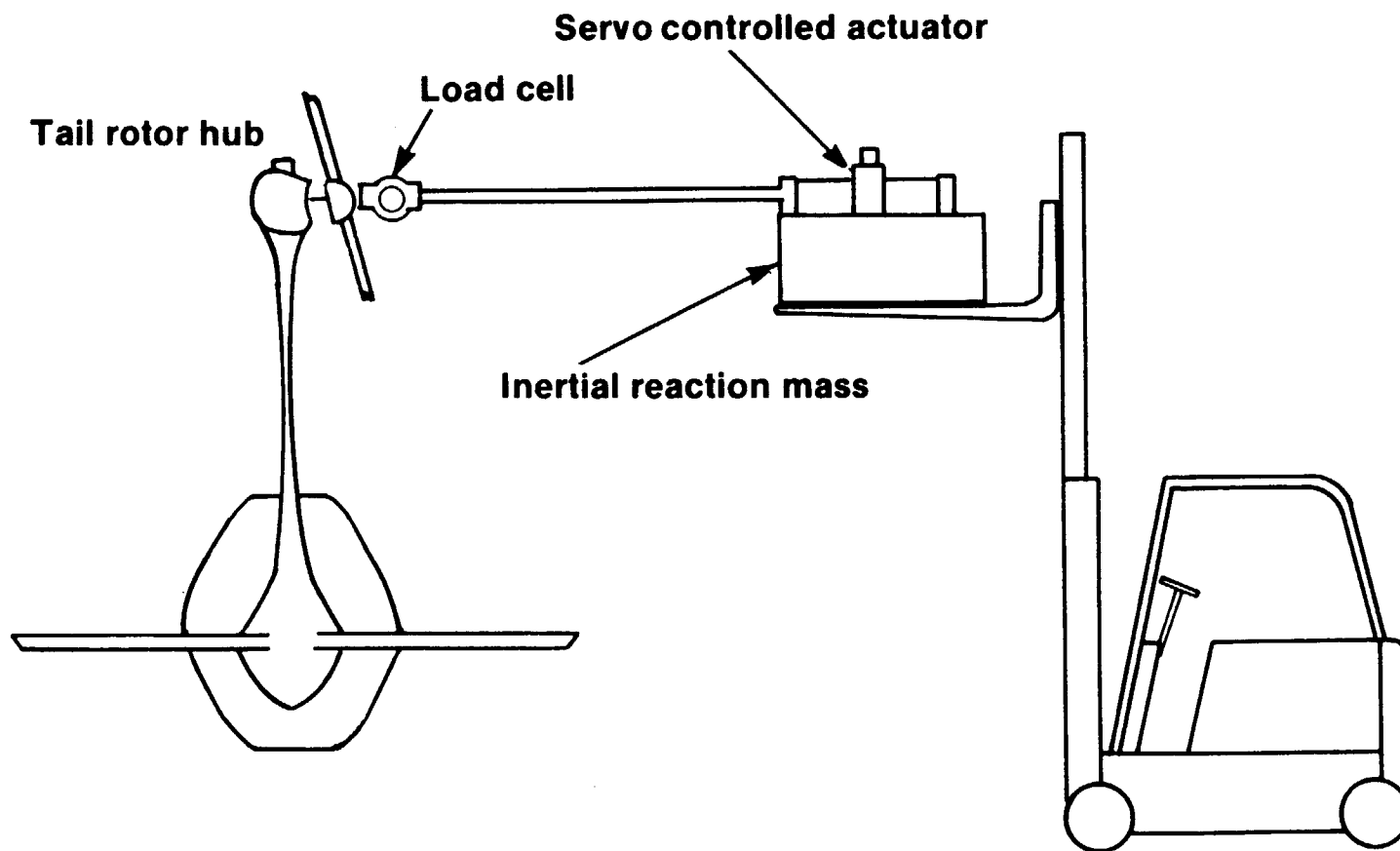
- **Provides excitation and measurement of response modes not adequately defined from main rotor head excitation**
- **Well separated on structure from primary excitation location for a valid reciprocity check**
- **Allows measurement of additional elements of the frequency response function matrix to provide an additional check of extracted modal parameters**
- **Furthers the ability to assess the extent of nonlinearity in the aircraft response**

## TAIL ROTOR EXCITATION METHOD

The following figure shows a typical tail rotor excitation set-up. The key points are as follows.

1. A servo-controlled hydraulic actuator is mounted to a weighted fork lift which provides alignment with the tail rotor hub. An inertial mass on the fork lift minimizes its response.
2. A flexible drive link and proving ring load cell are used to connect the shaker to the hub and measure input force.
3. The shaker is controlled through a closed loop force feedback system.
4. The frequency range of excitation will be from 3 Hz to 80 Hz, covering the 4/rev tail rotor forcing frequency range.

## TAIL ROTOR EXCITATION METHOD





## **SECTION 3.4**

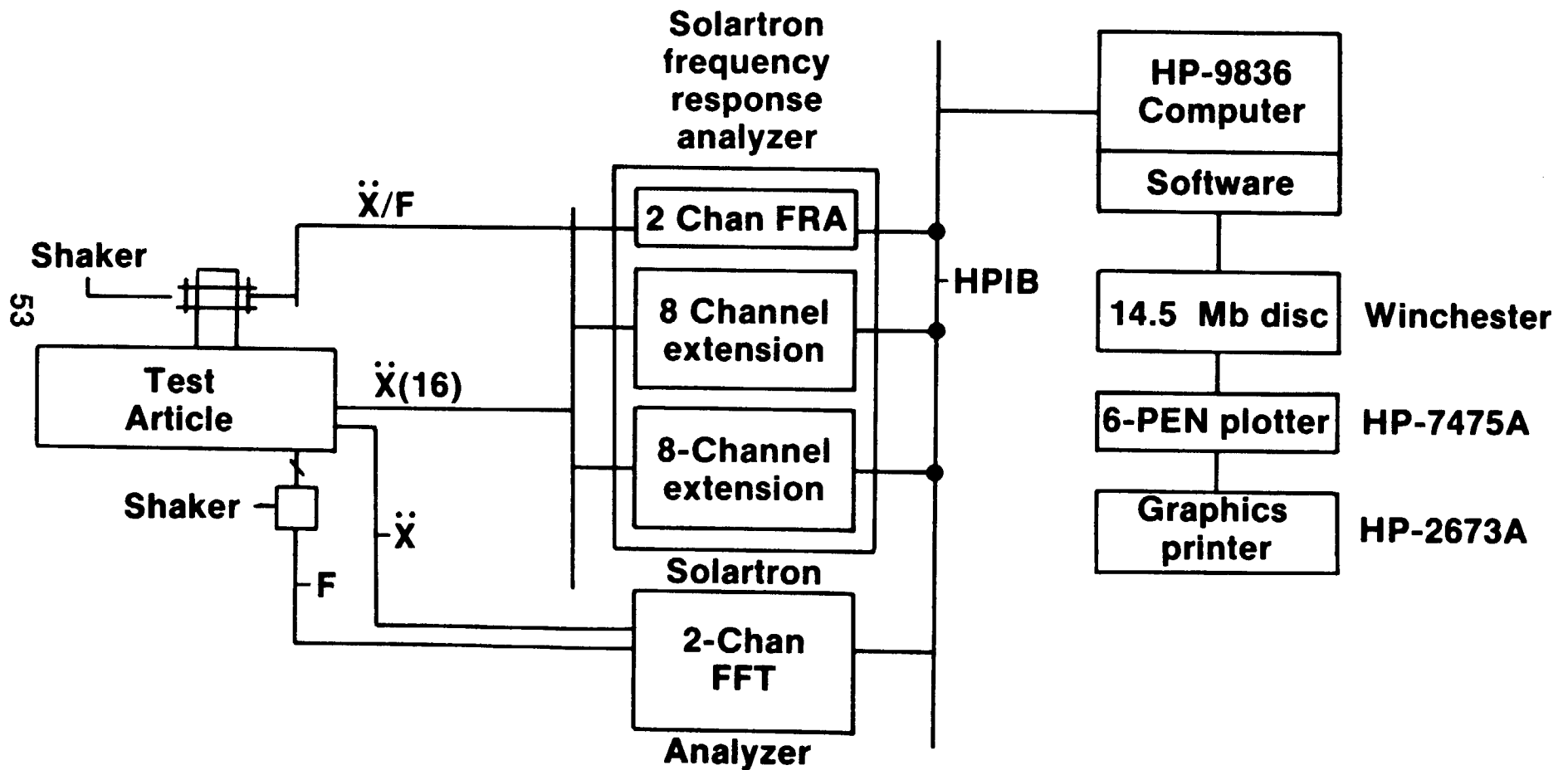
# **INSTRUMENTATION AND DATA ANALYSIS**

## DYNAMIC TEST AND ANALYSIS SYSTEM

A block diagram of the Dynamic Test and Analysis System is shown in the following figure. The major components of this system are as follows:

- SOLARTRON 18-CHANNEL FREQUENCY RESPONSE ANALYZER
- SOLARTRON 2-CHANNEL FFT SPECTRUM ANALYZER
- HEWLETT PACKARD 9836 COMPUTER AND PERIPHERALS (DISC STORAGE, PRINTER, PLOTTER)
- IMPERIAL COLLEGE OF SCIENCE AND TECHNOLOGY SYSTEM CONTROL AND ANALYSIS SOFTWARE

# DYNAMIC TEST AND ANALYSIS SYSTEM



# DYNAMIC TEST AND ANALYSIS SYSTEM (CONCLUDED)

The accompanying photograph shows the physical arrangement of the test system.



# DYNAMIC TEST AND ANALYSIS SYSTEM (CONCLUDED)



ORIGINAL PAGE  
BLACK AND WHITE PHOTOGRAPH

ORIGINAL PAGE IS  
OF POOR QUALITY

## FREQUENCY RESPONSE ANALYZER

The Solartron 1250 Frequency Response Analyzer consists of three parts:

1. A Generator which produces a sinusoidal electrical stimulus for the system being tested.
2. A Fournier analyzer which measures the response to the stimulus at 18 points in the system (one point usually being the shaker force), enabling either of the following to be calculated and displayed:
  - a. Single point measurements (e.g. the absolute voltage of either channel, and its phase with respect to the generator).
  - b. Point-to-point measurements (e.g. the response of channel 2 with respect to channel 1, in terms of gain and phase shift).
3. The Display, which shows the results of the measurements in rectangular, polar, or log polar coordinate systems.

Features of the Frequency Response Analyzer include:

- A measurement delay which allows the system to settle out following a change of frequency.
- An auto-integration feature which automatically adjusts the length of time that the measurement is continued until the running average result becomes sufficiently consistent.
- An amplitude compression feature which allows the variation in the response amplitude of the test article to be limited. It does this by varying automatically the generator output such that the signal input to one channel remains at constant amplitude.

## **FREQUENCY RESPONSE ANALYZER**

- **Consists of 3 parts:**
  - **A generator to produce the sinusoidal stimulus for the shaker**
  - **An analyzer to measure response at 18 points**
  - **The display**
- **Features include:**
  - **Measurement delay**
  - **Auto-integration**
  - **Amplitude compression**

## SYSTEM OPERATION AND ANALYSIS SOFTWARE MEASUREMENT PHASE

The software for the test system operation and analysis was developed by Imperial College of Science and Technology under contract to Sikorsky Aircraft. During the measurement phase, the software program facilitates the set-up of the 18-channel analyzer from the host computer. This includes transducer calibrations, sweep range, frequency resolution and force level. During, and at completion of, data acquisition and processing, the software provides for measured data quality checks in the form of individual channel measurement displays and single-degree-of-freedom analysis techniques. The host computer controls all display, storage and hardcopy operations.

## **SYSTEM OPERATION AND ANALYSIS SOFTWARE MEASUREMENT PHASE**

- **Facilitates set-up of 18-channel analyzer from host computer**
- **Controls acquisition and processing of data for each channel**
- **Provides for on-line and post-measurement data quality check**
- **Controls data display, storage, and hard-copy operations**

SYSTEM OPERATION AND ANALYSIS SOFTWARE  
DATA ANALYSIS PHASE

The software provides an assortment of frequency response function (FRF) analysis techniques of both the Single Degree of Freedom (mode by mode) and Multi-Degree of freedom (all modes) type (Reference 1). Also included are methods for dealing with closely coupled response modes and evaluating the extent of non-linearities. Each analysis technique uses a unique approach to providing the set of modal parameters (natural frequency, mode shape, and damping), which best describe the measured frequency response function. The mode shapes are normalized to unit generalized mass. The response function may be regenerated from the estimated parameters as a means of validating the data analysis. Residual terms, which are constants reflecting the effect of contributions outside the measured frequency range, may also be estimated and included in the regenerated FRF. The extracted modal parameters are sorted and combined with a coarse wire-frame diagram of the structure to provide both hard-copy plots and animated displays of individual modes. A statistical analysis is performed to determine the average value and degree of variance in estimations of natural frequency and damping.

## **SYSTEM OPERATION AND ANALYSIS SOFTWARE DATA ANALYSIS PHASE**

- **S.D.O.F. circle fit/M.D.O.F. curve fit analysis capability**
- **Diagnostic plot for evaluation of non-linearities**
- **Frequency response function regeneration from extracted modal parameters plus residual terms**
- **Static and dynamic display of individual modes**

## INSTRUMENTATION

The shake test instrumentation will provide for 18 simultaneous measurements, corresponding to the available channels of the data acquisition and processing system. One channel will be required for the reference input force measurement, consisting of either moving mass acceleration (for rotorhead excitation) or calibrated load cell output (for tail excitation). The remaining 17 channels will provide parallel acceleration response signals, separated into five tri-axial and two unidirectional sets. Each transducer has separate balance, gain and phase control ( $\pm 180^\circ$ ), and a traceable dynamic calibration in g's/volt. The  $180^\circ$  phase converters provide for consistent acceleration phasing when installation (base direction) of transducer is reversed due to accessibility.

Accelerometers are the piezoresistive type, dynamically calibrated over the frequency range of interest. Resistance calibrations of all transducer are performed at the beginning and end of each daily test period. In addition, 2-G turnover calibrations are performed prior to each installation, serving as a system calibration (transducer, cable, amplifier) and a verification of phasing. The complete instrumentation set-up will remain intact throughout the test to minimize the possibility of sensitivity or calibration errors.

A Multichannel Signal Conditioner/Amplifier System, will accept the low-level acceleration signals and condition and amplify them into high-level outputs suitable for multiple channel simultaneous dynamic recording. The frequency response of this system is flat from DC to above 1 KHz.



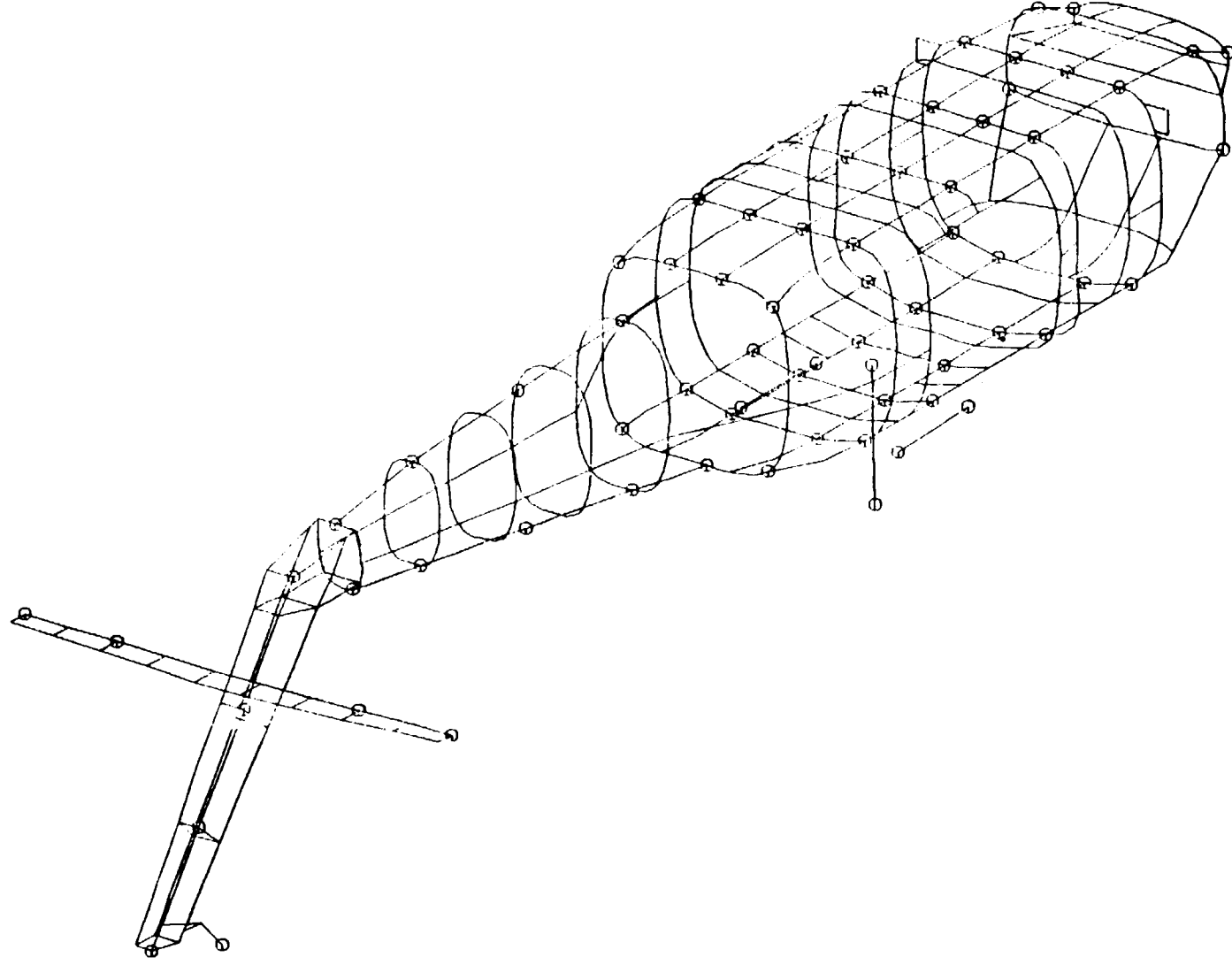
# **INSTRUMENTATION**

- **18 simultaneous measurement channels**
- **Multichannel signal conditioning/amplifier system**
- **Piezoresistive accelerometers dynamically calibrated**
- **Resistive and turnover calibrations at installation**
- **Frequency response for instrumentation is flat from DC to  $> 1000$  Hz**

## MEASUREMENT LOCATIONS

The induced vibration response will be measured at locations selected to correspond with the NASTRAN grid points and in sufficient number to fully define the fundamental mode shapes of the airframe and major components. The figure and the table show the locations selected. Accelerometer mounting blocks will be bonded throughout the airframe prior to the start of testing and the actual locations will be determined by the availability of suitable mounting surfaces and accessibility. Accelerometers are attached to the blocks with threaded studs and will be oriented in each of the principal aircraft axes. At some locations, where directional responses are expected to be similar, measurements will be restricted to the directions of unique response only. Wires will be carefully routed from the transducers to the exit point and firmly secured to prevent unwanted noise.

# MEASUREMENT LOCATIONS



MEASUREMENT LOCATIONS (CONTINUED)

Airframe Location	Location Number	NASTRAN Grid	Coordinates			Direction		
			FS	BL	WL	X,	Y,	Z
<u>Nose</u>								
Right	1	519	175	30	210	X,	Y,	Z
Left	2	530	175	-30	210			
<u>Cockpit</u>								
Floor-Right	3	919	205	30	203	Y,	Z	
Floor-Left	4	930	205	-30	203			
Panel-Right	5	907	205	41	233	X,	Y,	Z
Panel-Left	6	942	205	-41	233			
<u>STA 247</u>								
Floor	7	2119	247	30	200	Y,	Z	
.	8	2123	247	10	200			
.	9	2127	247	-10	200	Z		
.	10	2131	247	-30	200			
Overhead	11	2106	247	34.5	265	Y,	Z	
.	12	2103	247	16.5	269			
.	13	2147	247	-16.5	269	Z		
.	14	2144	247	-34.5	265			
<u>STA 295</u>								
Floor	15	2719	295	30	200	Y,	Z	
.	16	2723	295	10	200			
.	17	2727	295	-10	200	Z		
.	18	2731	295	-30	200			
Overhead	19	2706	295	34.5	265	Y,	Z	
.	20	2703	295	16.5	269			
.	21	2747	295	-16.5	269	Z		
.	22	2744	295	-34.5	265			

MEASUREMENT LOCATIONS (CONTINUED)

Airframe Location	Location Number	NASTRAN Grid	Coordinates			Direction		
			FS	BL	WL	X, Y, Z	X, Y, Z	
<u>X-Mission Beam</u>								
<u>STA 343</u> Floor . . .	23	3103	327	16.5	269	Y, Z		
	24	3147	327	-16.5	269	Z		
	25	3319	343	30	200	Y, Z		
	26	3323	343	10	200	Z		
	27	3327	343	-10	200	Z		
	28	3331	343	-30	200	Z		
<u>STA-360</u>								
X-Mission Beam . . .	29	3706	360	34.5	265	Y, Z		
	30	3703	360	16.5	269	Z		
	31	3747	360	-16.5	269	Z		
	32	3744	360	-34.5	265	Z		
<u>STA 398</u>								
Floor . . . Overhead . . .	33	4119	398	30	200	Y, Z		
	34	4122	398	10	200	Z		
	35	4128	398	-10	200	Z		
	36	4133	398	-30	200	Z		
	37	4106	398	34.5	265	Y, Z		
	38	4103	398	16.5	269	Z		
	39	4147	398	-16.5	269	Z		
	40	4144	398	-34.5	265	Z		

MEASUREMENT LOCATIONS (CONTINUED)

Airframe Location	Location Number	NASTRAN Grid	Coordinates			Direction		
			FS	BL	WL	X,	Y,	Z
<u>STA 443.5</u>								
Floor	41	5319	443.5	30	205	Y,	Z	
.	42	5322	443.5	10	201	Z		
.	43	5328	443.5	-10	201	Z		
.	44	5331	443.5	30	205	Z		
Overhead	45	5306	443.5	28	261	Y,	Z	
.	46	5344	443.5	-28	261	Z		
<u>Tailcone</u>								
485 Bottom	47	5725	485	0	203	Y,	Z	
485 Top	48	5701	485	0	259	Y,	Z	
545 Bottom	49	6325	545	0	206	Y,	Z	
545 Top	50	6301	545	0	251	Y,	Z	
605 Bottom	51	6925	605	0	208	Y,	Z	
605 Top	52	6901	605	0	243	Y,	Z	
647 Bottom	53	7711	647	0	215	Y,	Z	
647 Top	54	7501	647	0	238	Y,	Z	
IGB	55	8307	679	0	220	X,	Y,	Z
Tail Pylon	56	8504	687	0	268	X,	Y	
	57	8704	710	0	297	X,	Y	
	58	8924	732	0	325	X,	Y,	Z
TRGB	59	60016	732	14	325	X,	Y,	Z

MEASUREMENT LOCATIONS (CONTINUED)

Airframe Location	Location Number	NASTRAN Grid	Coordinates			Direction		
			FS	BL	WL	X,	Y,	Z
<u>Stabilator</u>								
Right Tip	60	9204	703	82.7	247	X,	Z	
BL 47	61	9244	703	47	247	X,	Z	
Center	62	9124	703	0	247	X,	Z	
BL -47	63	9044	703	-47	247	X,	Z	
Left Tip	64	9004	703	-82.7	247	X,	Z	
<u>MR Shaft</u>								
Top	65	9800	341	0	315	X,	Y,	Z
Bottom	66	9803	343	0	270	X,	Y,	Z
<u>Engines</u>								
RT (CG)	67	60008	373	30	279	X,	Y,	Z
RT (Input)	68	95003	350	30	279	X,	Y,	Z
LT (CG)	69	60009	373	-30	279	X,	Y,	Z
LT (Input)	70	95002	350	-30	279	X,	Y,	Z

## MEASUREMENT PROCEDURE

A general measurement procedure will be used to characterize the airframe response prior to the intensive data acquisition phase of the shake test. During this time, the essential nature of the structure's dynamic properties will be established. This will include the modal density, level of damping, and degree of non-linearity in the measured response to main rotor head excitation. The shaker system and suspension system will be checked to assure they satisfy the test requirements. The tail excitation location will be checked to assure that all modes have been identified from the main rotor excitation. Reciprocity effects of the main rotor to tail rotor excitations will be verified and data will provide additional indication of non-linear response. Once this investigation has been completed, an appropriate set of methods will be determined for performance of the test. All data to be used to construct the final modal model will be measured using an approach consistent with the above findings.



# **MEASUREMENT PROCEDURE**

**Explore and establish the essential nature of the structure's dynamic properties**

- **Modal density**
- **Level of damping**
- **Degree of non-linearity**

**Assure shaker attachment and suspension system satisfy requirements**

**Evaluate second excitation location**

- **Assure all modes are uncovered**
- **Verify reciprocity**
- **Further investigate non-linearities in response**

**Execute data acquisition phase in which all data to be used to construct the final modal model are measured using the most appropriate methods as determined from findings of above investigations.**

## NONLINEAR RESPONSE

Current finite element modeling and modal testing techniques are all founded on the assumption that the structure under investigation behaves in a linear fashion. However, experience indicates that helicopter-like structures generally manifest a certain amount of nonlinear behavior. One manifestation of nonlinear behavior is a distortion in the frequency response plot, especially in the regions around the resonances. An examination of a three-dimensional damping plot which is generated from the measured points close to a resonance can aid in assessing the amount of nonlinearity present in the resonance. A random variation in the curve-fitted damping estimates indicates noise or other measurement uncertainties. A systematic variation is caused either by the effects of adjacent modes or by a nonlinearity. Examination of trends can indicate the type of nonlinearity (e.g., cubic stiffness or Coulomb friction).

## **NONLINEAR RESPONSE**

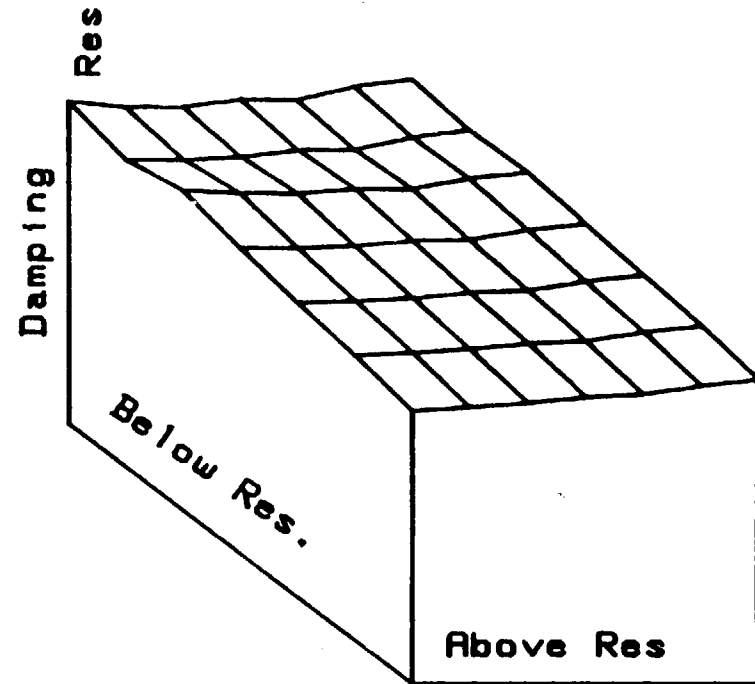
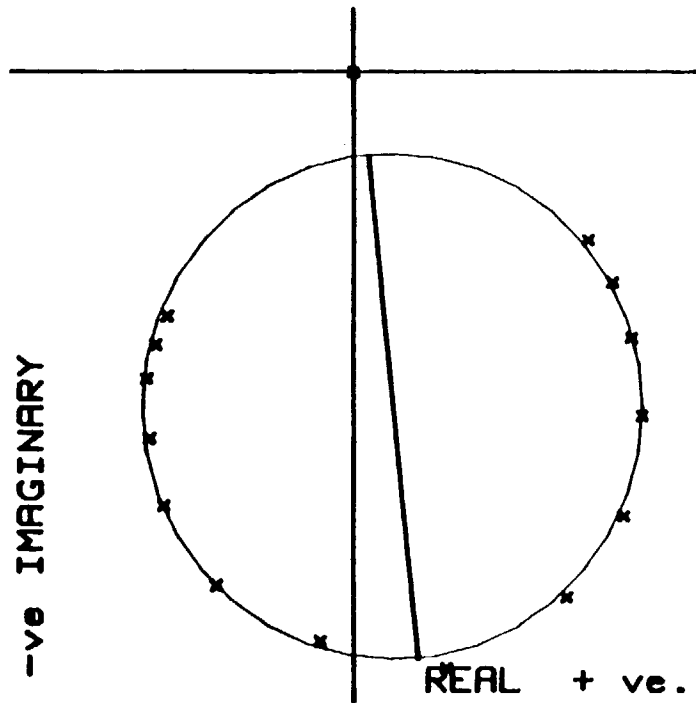
**Nonlinear effects are most significant around the resonant region. A three-dimensional damping plot which is generated from the measured points close to resonance can clearly show if the estimates of damping vary in this region.**

- **A random variation indicates noise or other measurement uncertainty**
- **A systematic variation is likely to be caused by the effects of adjacent modes or a nonlinearity**
- **Examination of trends may indicate the type of nonlinearity (e.g.) cubic stiffness or Coulomb friction**

## SDOF ANALYSIS

The figure below shows a typical single degree of freedom curve fit of a resonant region and an associated three dimensional plot of damping estimates. The points selected to perform the circle-fit are used to determine estimates for damping. For any combination of three points below and above resonance, one estimate of damping may be deduced. All possible values are calculated and the mean and standard deviation of the damping estimates are calculated and displayed. The variation in damping becomes evident when viewed graphically. A linear system, unaffected by adjacent modes, will have identical estimates of damping resulting in a uniform surface on the plot.

# SDOF ANALYSIS



RESPONSE at Point : 5

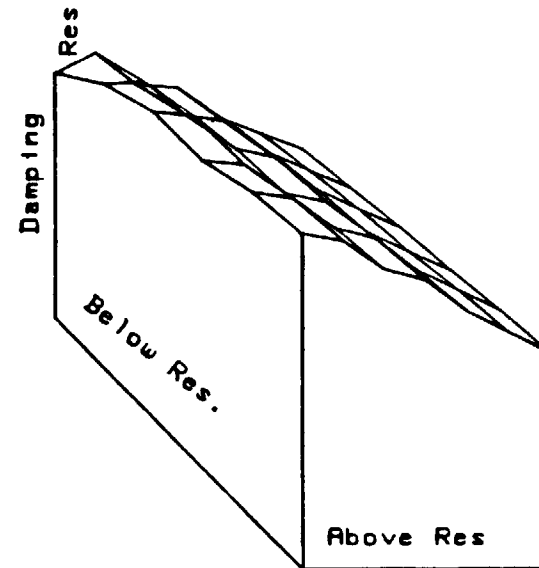
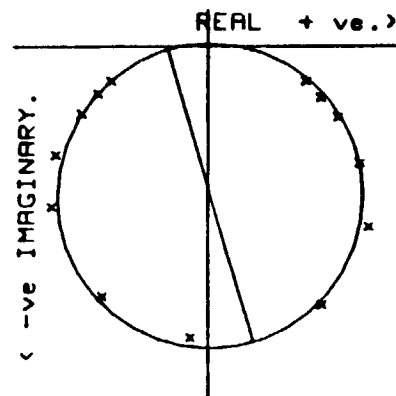
Resonance Frequency	=	42.358 hz.
Damping Loss Factor	=	.02534
Damping Variation	=	5.45 %
Phase Angle	=	+5.69 deg.
Modal Constant	=	7.21577E-02 1/

(=  $\phi_i \phi_j$ , where  $\phi_i$  and  $\phi_j$  are the eigenvector elements at the excitation and response points, respectively)

## EFFECT OF NONLINEARITY ON DAMPING PLOT

The variation in damping estimates for a nonlinear response at resonance is shown in the accompanying figure. It is clear that an average damping value from these estimates does not accurately define the damping of the structure. As the points used for damping estimates increase in frequency beyond resonance, a systematic decrease in damping value is observed. Damping plots of this type will be used to evaluate the measured response for signs of nonlinearity and to investigate excitation techniques which minimize these effects.

# EFFECT OF NON-LINEARITY ON DAMPING PLOT



Resonance Frequency	=	15.90 Hz.
Phase angle	=	+16.5 deg
Damping Loss Factor	=	.01085
Modal Constant	=	1.06994E+00 1/kg
Damping Variation	=	.0079 to .0125

## HIGH AND LOW FREQUENCY RESIDUAL TERMS

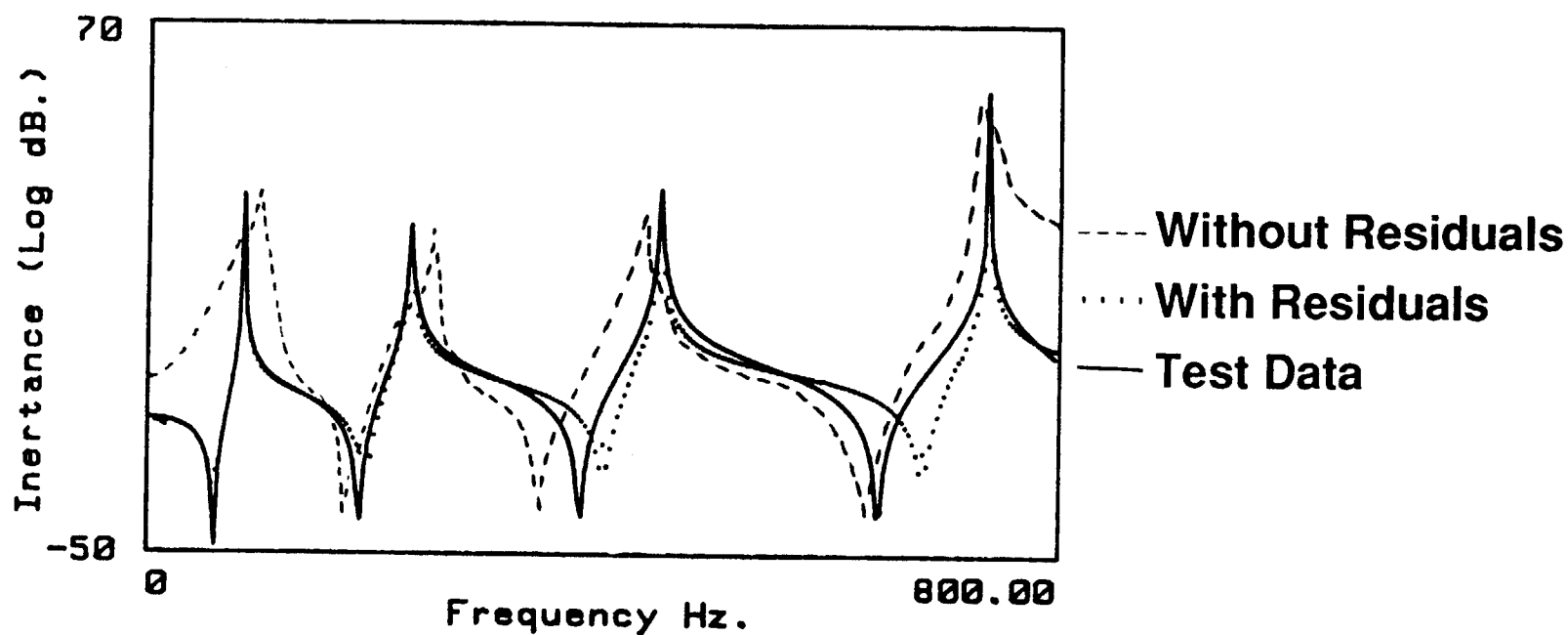
The analysis of measured frequency response functions and extraction of modal parameters can be significantly influenced by adjacent modes outside the measured frequency range. A correction may be applied which assumes that there exist two out-of-range modes, one above and one below the measured range, which affect the measured data. The response at a selected frequency is then equal to the response due to the sum of the measured modes, plus the response due to the two residual terms.

The following figure shows a multi-degree-of-freedom measurement analysis which includes a low frequency rigid body mode and a high frequency mode as residual terms in the calculation of the extracted modal parameters. The inclusion of these residual terms results in an improved estimate of modal properties and a regenerated curve which more closely reflects the original measured frequency response function.





# HIGH AND LOW FREQUENCY RESIDUAL TERMS



Frequency Hz	Modal Const (1/kg)	Phase(deg)	Damping loss factor.
84.375	1.01328E-01	0	.00286
231.250	1.02686E-01	0	.00629
450.000	1.13353E-01	0	.00270
737.500	9.69205E-02	0	.00017
1000.000	3.52189E-01	0	Hi freq residual

## SECTION 3.5

# COMPARISON OF TEST RESULTS WITH NASTRAN

## PRESENTATION OF RESULTS - COMPARISON WITH NASTRAN

The test results will be presented in the form of frequency response functions (log amplitude and phase versus excitation frequency), for a representative sample of response locations, and a set of modal properties (frequencies, dampings, and mode shapes) identified from the frequency response functions. Comparisons between test and analysis will be presented for both frequency response functions and modal frequencies and shapes.

## **PRESENTATION OF RESULTS - COMPARISON WITH NASTRAN**

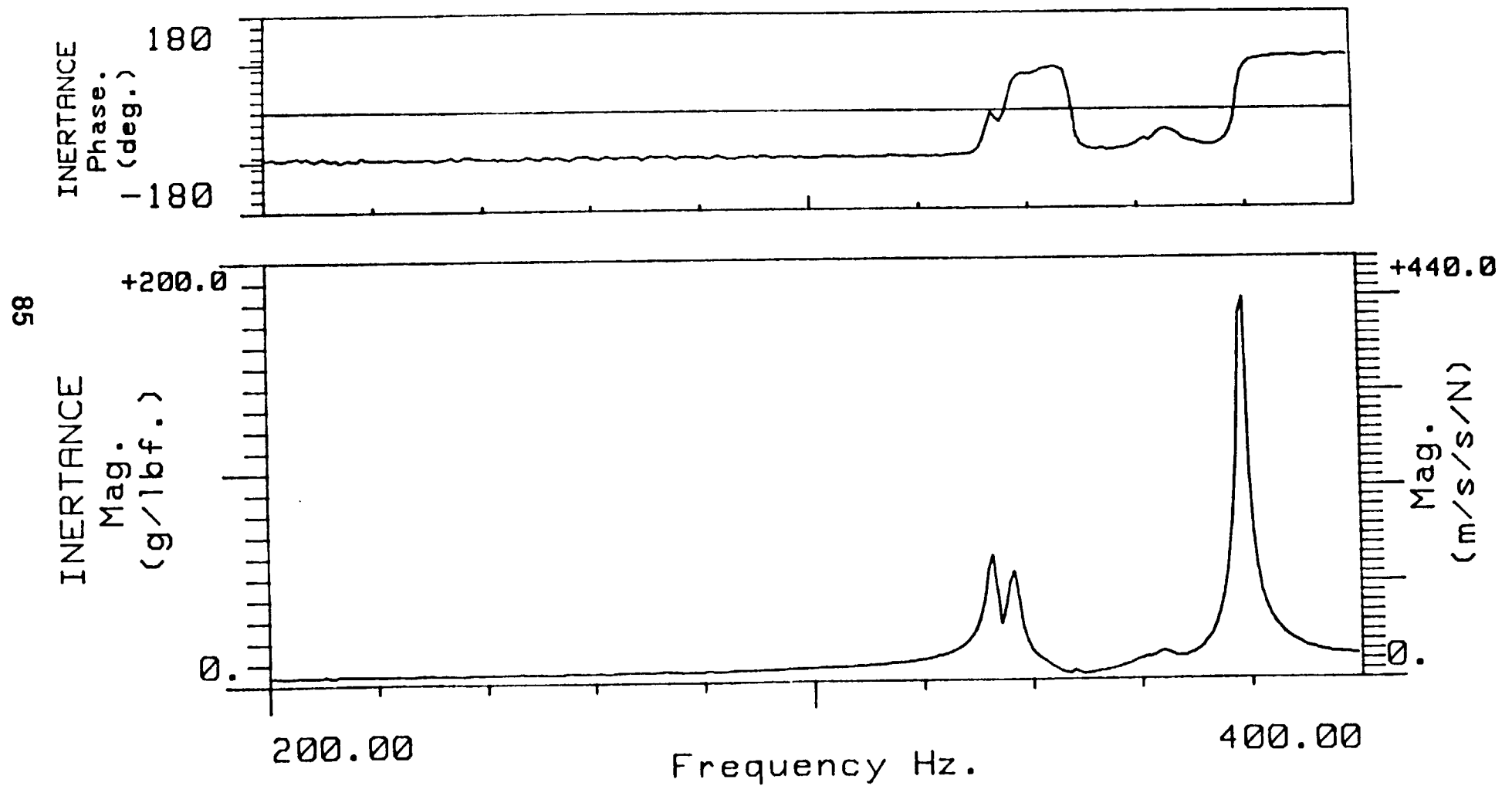
- **Response properties**
  - **Comparison plots of steady state acceleration amplitude and phase versus excitation frequency**
- **Modal properties**
  - **Comparison of measured versus predicted natural frequencies**
  - **Comparison of measured versus predicted mode shapes**

## COMPARISON OF RESPONSE PROPERTIES

Plots of steady-state acceleration amplitude and phase versus excitation frequency will be produced for all combinations of load location and direction, and measurement location and direction.

Comparison plots (side by side or overlay) will be generated for corresponding frequency response functions for a set of locations distributed over the airframe, from analysis and test. The frequency and amplitude of resonant and antiresonant regions will be examined for indications of systematic discrepancies. This will be the primary criteria for evaluating the ability of the NASTRAN model to accurately represent the structure under test.

# COMPARISON OF RESPONSE PROPERTIES



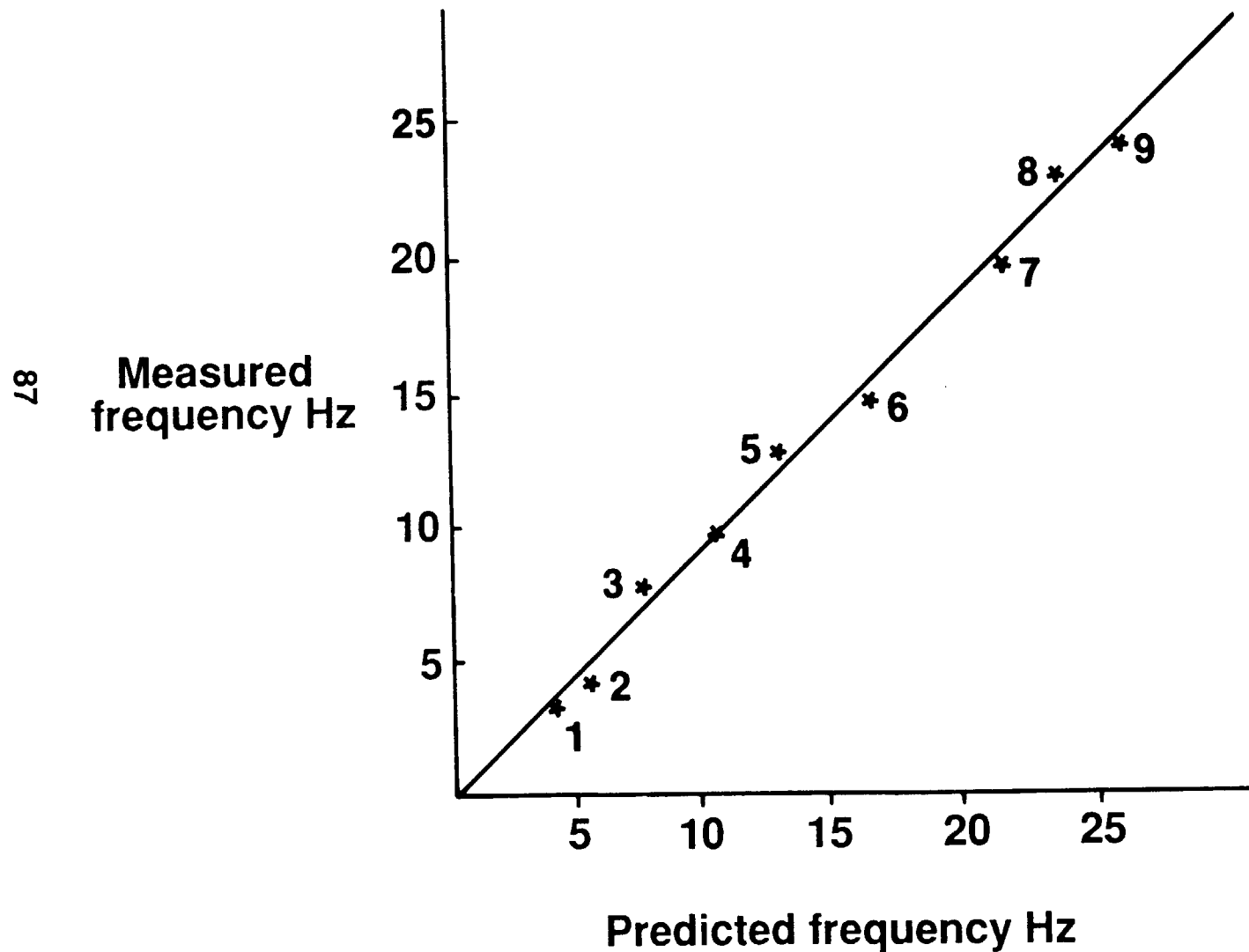
## COMPARISON OF NATURAL FREQUENCIES

A table providing predicted and measured natural frequencies will be presented. The table will allow a quick comparison of frequencies for similar modes and identification of those modes which were either measured or predicted, but not both. In addition to this tabular comparison, a plot of experimentally determined natural frequency versus the predicted value for corresponding modes included in the comparison will also be presented. Examination of this plot will provide not only the degree of correlation between the two sets of results, but also an indication of the type of any discrepancy which exists. The points of this plot should lie on a straight line, on or close to a slope of 1. Results which deviate from this form may indicate one of the following:

- Scattered widely about a straight line - indicates a serious failure of the model to represent the test structure.
- Systematic deviation (rather than random) - suggests a specific characteristic is responsible and results are not simply attributable to experimental error (e.g., close to a line of different slope indicates a material property error).



# COMPARISON OF NATURAL FREQUENCIES



## COMPARISON OF MODE SHAPES

When making comparisons between experimental versus predicted natural frequencies, it must be verified that the frequencies relate to the same mode. This is not a problem for simple structures with well separated modes. However, on complex structures with closely spaced natural frequencies, ensuring that comparisons are correctly made requires mode shape information as well as frequency.

Side by side comparison plots of the mode shapes, measured and predicted, will be presented. This will allow a comparison of the mass normalized eigen vectors from both sets of data.

## **COMPARISON OF MODE SHAPES**

- 8 Side-by-side comparison plots of the measured and predicted mode shapes will be presented**



## SECTION 4.0

# SHAKE TEST DESCRIPTION



## **SECTION 4.1**

# **TEST ARTICLE CONFIGURATION**

## TEST ARTICLE CONFIGURATION

The UH-60A helicopter used as the test specimen was production aircraft No. 640 (S/N 86-24507) assigned for use to this program under a U.S. Army bailment agreement. The aircraft was a recent production configuration, inspected and acceptance-tested to flight-worthy status prior to bailment for the test program. In preparation for shake testing, the following aircraft rotorhead components and equipment were removed:

Main Rotor Blades	Tail Rotor Blades
Spindles	Tail Rotor Hub
Bearings	Cabin Troop Seats
Dampers	Fuel
Bifilar	Tail Gearbox Cover
Main Rotor Hub	Intermediate Gearbox Cover
Nose Absorber Access Cover	Lower Pylon Fairing

The fairings and covers were removed to provide access to measurement locations and were considered as secondary structure having little or no effect on the aircraft response. The nose, forward transmission, and aft transmission vibration absorbers were installed but the leaf springs were blocked, making the absorbers inactive. Articles installed on the aircraft included a modified BLACK HAWK main rotor hub, dummy tail rotor hub, main rotor excitation hardware and the main rotor/tail rotor suspension system hardware.



## **TEST ARTICLE CONFIGURATION**

- **U.S. Army UH-60A of recent production configuration**
- **Inspected and acceptance-tested to flight worthy status**
- **Installed vibration absorbers locked out**
- **Components and equipment removed:**
  - **Main rotor blades**
  - **Spindles**
  - **Bearings**
  - **Dampers**
  - **Bifilar**
  - **Main rotor hub**
  - **Nose absorber access cover**
  - **Tail rotor blades**
  - **Tail rotor hub**
  - **Cabin troop seats**
  - **Fuel**
  - **Tail gearbox cover**
  - **Intermediate gearbox cover**
  - **Lower pylon fairing**
- **Articles installed:**
  - Modified BLACK HAWK main rotor hub**
  - Dummy tail rotor hub**
  - Main rotor excitation hardware**
  - Main rotor/tail rotor suspension hardware**

# TEST SPECIMEN - WEIGHT SUMMARY

The NASTRAN mass modeling weight, based on the empty No. 640 production BLACK HAWK, was 4501 kg (9923 lbs) at a horizontal C.G. of 9.144 (360 in.). This weight is for the aircraft with 50% of the flapping mass of the main rotor included. The test article weight, with the aircraft rotor head hardware removed and the test hub installed, was 4309 kg (9500 lbs) at a horizontal C.G. of 9.144 m (360 in). A total of 640 lbs was added to the rotor hub to simulate 50% of the flapping mass of the rotor head items removed and the bifilar mass. The added weight consisted of 108.9 kg (240 lbs) for the main rotor head shaker and hardware and 181.8 kg (400 lbs) for the steel plates attached to the hub arms. A summary is shown below.

## Weight Required:

50% of blade flapping mass	=	492 lbs
Bifilar Mass	=	<u>148 lbs</u>
Total		640 lbs

## Weight Added:

Main Rotor Head Shakers and Hardware	=	240 lbs
Steel Plates Attached to Hub Arms	=	<u>400 lbs</u>
Total		640 lbs

## NASTRAN ANALYSIS

Weight = 9923 lbs  
Horizontal C.G. = Sta 360

## TEST ARTICLE CONFIGURATION

Weight = 10,140 lbs  
Horizontal C.G. = Sta 359

# TEST SPECIMEN - WEIGHT SUMMARY

## Weight Required:

50% of rotor head flapping mass

= 492 lbs

Bifilar mass

= 148 lbs

Total

640 lbs

## Weight Added:

Main rotor head shakers and hardware

= 240 lbs

Steel plates attached to hub arms

= 400 lbs

Total

640 lbs

NASTRAN analysis

Weight = 9923 lbs

Horizontal C.G. = Sta. 360

Test article configuration

Weight = 10,140 lbs

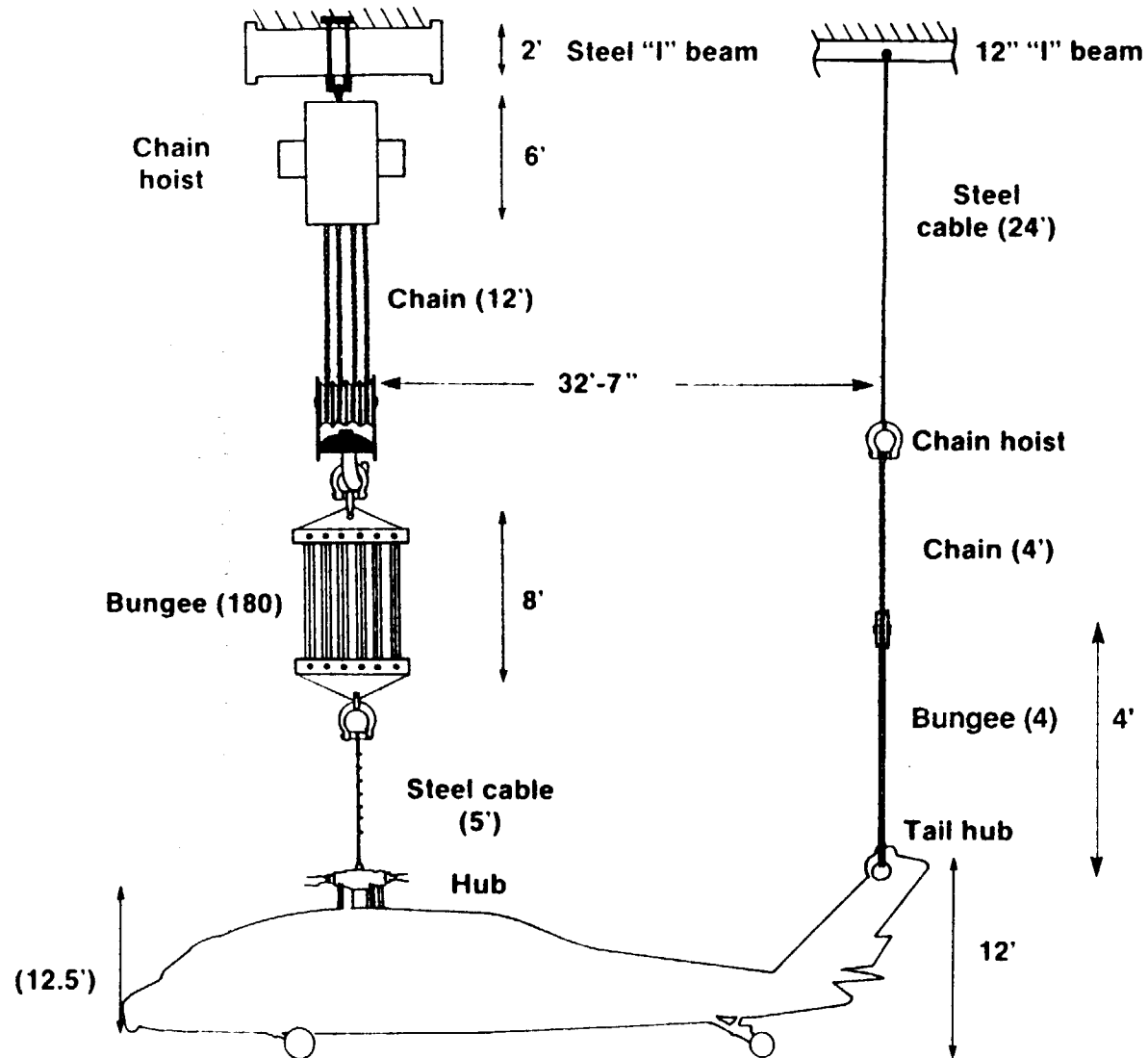
Horizontal C.G. = Sta. 359

## AIRCRAFT SUSPENSION

The test article was suspended from deep I-beams, attached to the roof trusses of the test bay, by suspension cables attached to integral lifting eyes in the modified rotor heads. Each suspension cable consists of spring packs fabricated from bungee elastic cords, chair hoists and long steel cables.

The test article was suspended during measurements in a manner which closely approximates the 'free-free' NASTRAN analysis condition. This soft spring arrangement was designed to isolate the test article from the overhead support structure and, together with the overall pendulum length, provide for aircraft rigid body modes of less than 1.5 Hz. These are less than 20% of the lowest vertical bending mode of the aircraft to prevent significant influence on its response. The actual frequency placement of all six rigid body modes was identified to assure that the method of suspension was adequate.

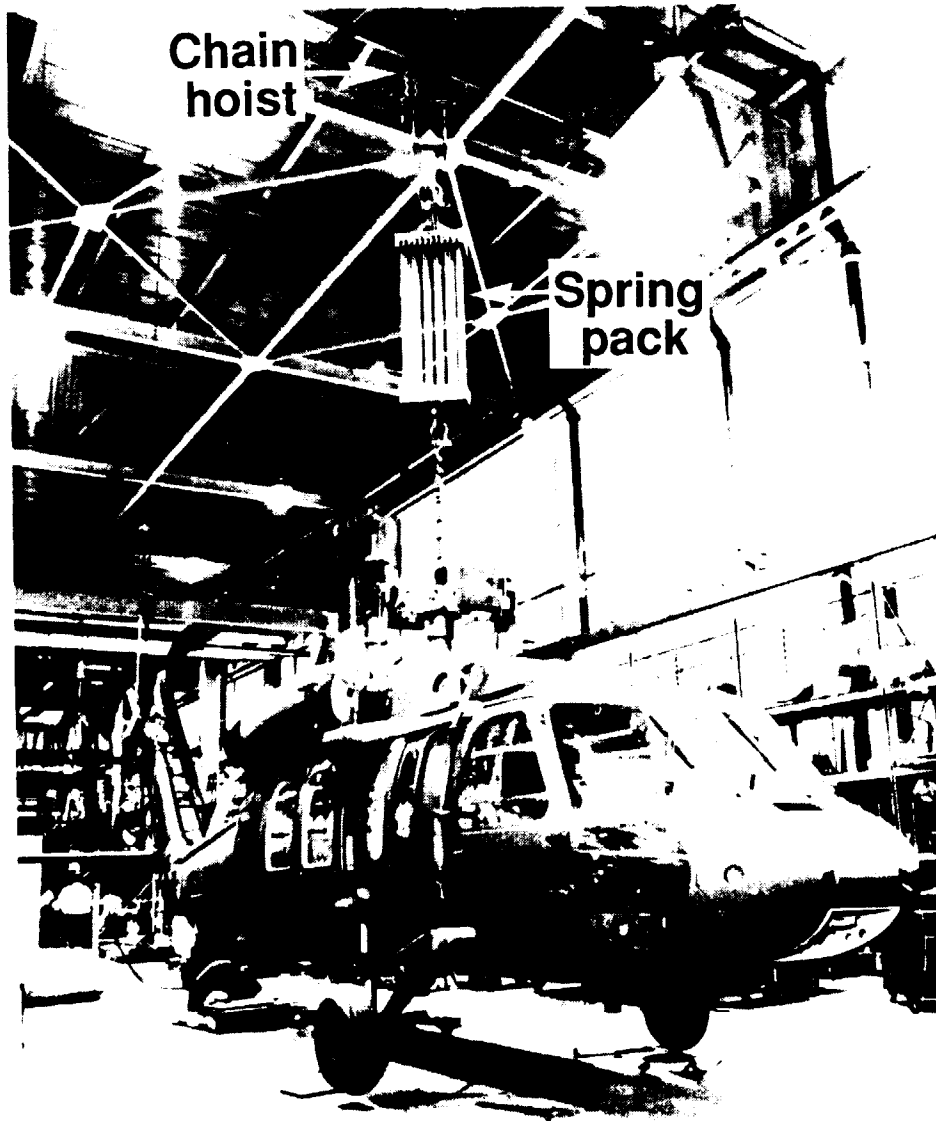
# AIRCRAFT SUSPENSION



#### AIRCRAFT SUSPENSION (CONTINUED)

The photograph below shows the aircraft suspension "spring packs" fabricated from bungee cord. Also visible are the cables and chain hoists which together make up the aircraft suspension system.

## AIRCRAFT SUSPENSION (CONT.)



Chain  
hoist

Spring  
pack

ORIGINAL PAGE  
BLACK AND WHITE PHOTOGRAPH

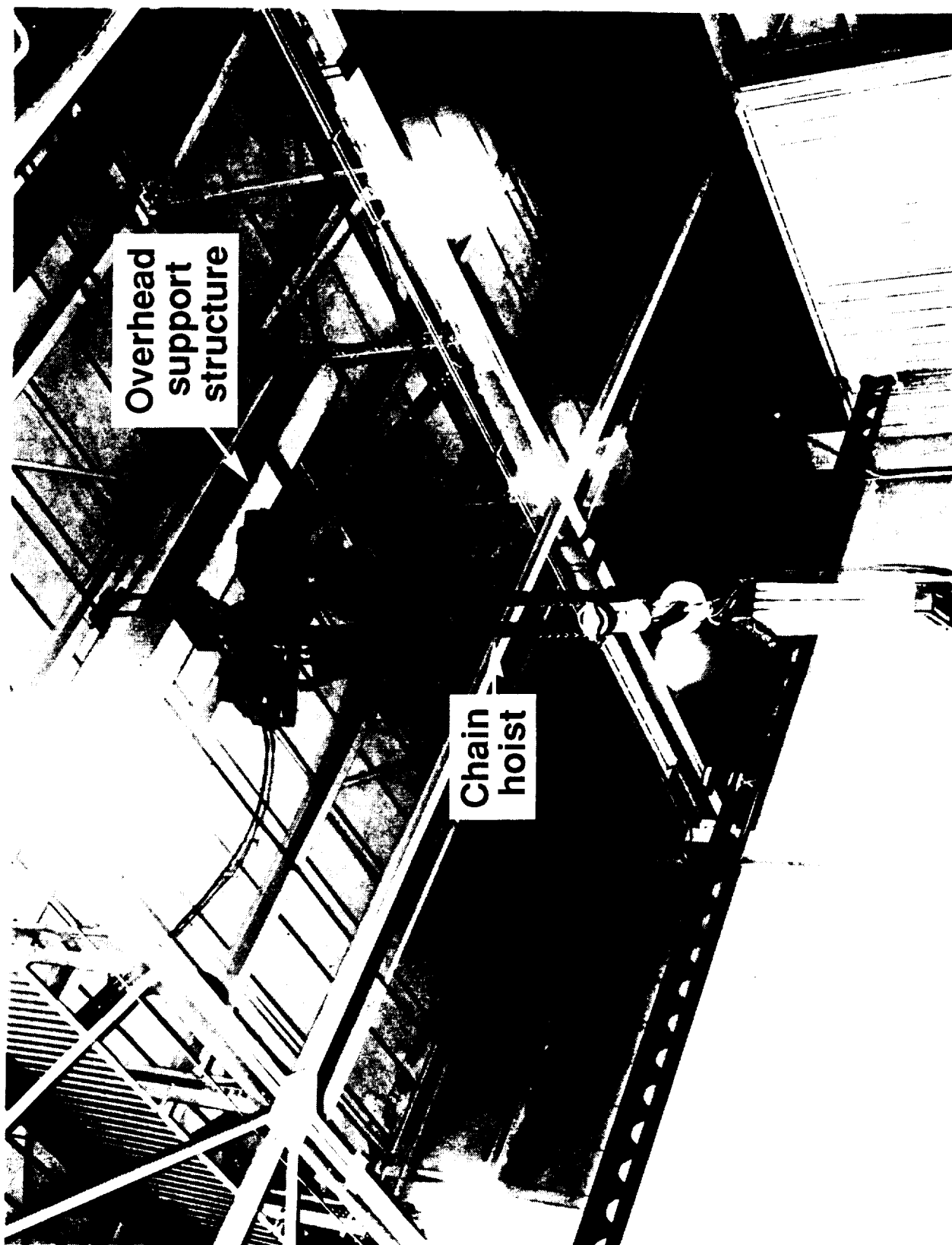
ORIGINAL PAGE IS  
OF POOR QUALITY

#### AIRCRAFT SUSPENSION (CONCLUDED)

The photograph below shows the overhead support structure for the main rotor head suspension. Acceleration measurements on the overhead roof beams showed that the supports made little or no contribution to the measured airframe response.



## AIRCRAFT SUSPENSION (CONC.)





## SECTION 4.2

### AIRCRAFT EXCITATION

## AIRCRAFT EXCITATION

Vibratory loads were applied at the main rotor hub in the vertical, lateral and longitudinal directions. The magnitude of the applied load was held constant over the frequency range of excitation. This frequency range was from 3 hz to 40 hz (0.17 to 2.3 times the blade passage frequency) for lateral and longitudinal excitation, but was extended to 45 hz in the vertical direction to include measurement of a vertical response mode at 39 hz.

The initial plans contained in the "test plan" specified a second excitation location at the tail rotor hub. This testing was deleted due to test schedule constraints. However, a second excitation investigation was performed which did provide much of the information which was required from the tail rotor location. The location for this excitation was at the bottom of the tail pylon, and the aircraft was excited in the vertical and lateral directions. Examination of the aircraft response to this tail excitation did assure that all the measurable aircraft response modes were adequately defined from main rotor head excitation.

<u>Excitation Location</u>	<u>Frequency Range</u>
Main Rotor Hub Vertical	3.0 - 45.0 Hz
Main Rotor Hub Lateral	3.0 - 40.0 Hz
Main Rotor Hub Longitudinal	3.0 - 40.0 Hz
Tail Pylon Vertical	3.0 - 40.0 Hz
Tail Pylon Lateral	3.0 - 40.0 Hz

# AIRCRAFT EXCITATION

## Main Rotor Excitation

**Vertical**  
**Lateral**  
**Longitudinal**

**Frequency range**  
**Force level**

## Tail Pylon Excitation

**Vertical**  
**Lateral**

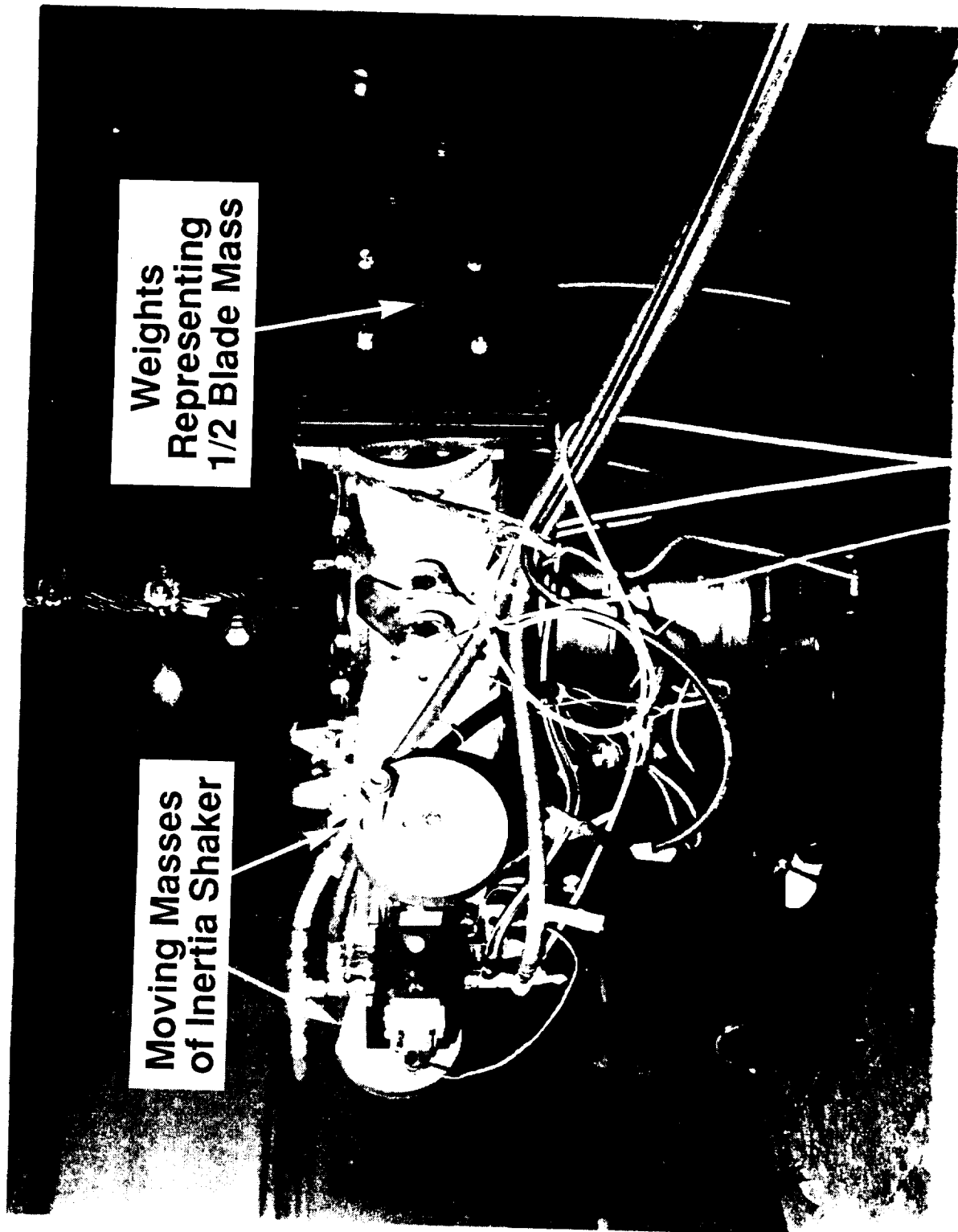
**3 Hz to 40 Hz**  
**100-200 pounds**

## METHOD OF EXCITATION

Airframe excitation was provided by two electrohydraulic inertia shakers which were mounted directly on opposing arms of the modified main rotor hub as shown in the figure. The shakers consisted of high performance servo-controlled actuators, with closed-loop displacement feedback, which provided sinusoidal acceleration of external weights. The two shakers were identical in configuration with matched servo controllers which maintained equal acceleration magnitude of the individual moving masses. Phase relationship between shakers was maintained at or close to zero throughout the frequency range of operation. The force exerted on the hub was equal and opposite to the total shaker moving mass (100 lbs) multiplied by the moving mass acceleration. This acceleration was measured on only one shaker for data processing but the relative amplitude and phase relationship between shakers was verified prior to the start of testing and checked periodically throughout the test program.

Because the hub excitation force was generated by the inertia effects of the shaker moving masses, there was no requirement for isolation of the shaker, and there were no secondary load paths to the airframe or to ground. Shaker force direction was controlled by alignment of the shakers relative to the hub arms and rotation of hub arms relative to the airframe. Inplane shaker forces (lateral and, longitudinal excitation) were applied at the shear center of the main rotor hub arms and the resultant vertical input force was applied along the axis of the main rotor shaft.

# METHOD OF EXCITATION



ORIGINAL PAGE  
BLACK AND WHITE PHOTOGRAPH

ORIGINAL PAGE IS  
OF POOR QUALITY

## ALTERNATE EXCITATION METHOD

Prior to main rotor hub excitation, some initial measurements were acquired with airframe excitation at the tail. A servo-controlled hydraulic actuator was attached to an aluminum fitting at the centerline of the stabilator attachment lugs. Two vertical excitation sweeps were performed to provide an initial checkout of the measurement system and to characterize the airframe response.

The input force was measured with a proving ring load cell and reacted by a large reaction mass at rest on the floor. Shaker control was provided by a displacement feed-back system which resulted in a shaker force that varied over the frequency range of excitation. Lateral excitation was performed in the same fashion with the shaker attachment location at the tail tiedown fitting located at the base of the tail pylon.

Although this was intended as a preliminary checkout of the measurement system and of various test techniques, the data was of good quality and provided a combination of reciprocity plots with main rotor hub excitation. These tests also served as a check that main rotor hub excitation provided adequate excitation of all modes and provided support information for the investigation of nonlinear response with force level and excitation location.



## **ALTERNATE EXCITATION METHOD**

- **Tail pylon excitation in vertical and lateral directions**
- **Displacement feed-back controlled hydraulic actuator**
- **Verified that all modes were measured from main rotor head excitation**
- **Additional assessment of nonlinear response**



## **SECTION 4.3**

# **INSTRUMENTATION AND MEASUREMENT PROCEDURES**

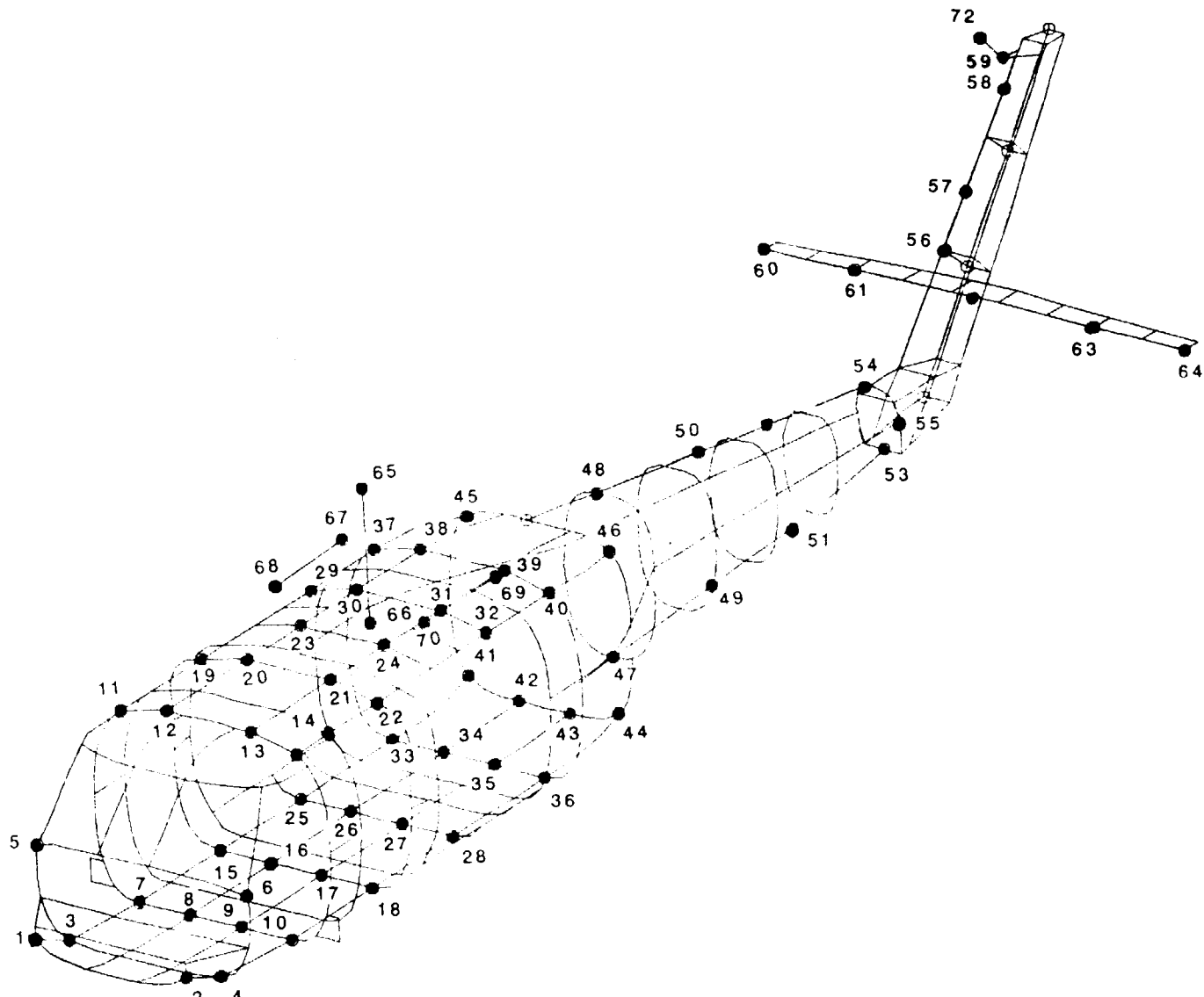
## MEASUREMENT LOCATIONS

The induced vibration response was measured at locations selected to correspond as closely as possible with NASTRAN grid points and in sufficient number to fully define the fundamental mode shapes of the airframe and major components. Emphasis was placed on primary fuselage structure, selecting measurement locations at major frame, stringer and beam intersections.

Accelerometer mounting blocks were bonded at each location, allowing quick installation and removal of accelerometers which attached to the blocks with threaded studs. The actual measurement locations were ultimately determined by the availability of suitable mounting surfaces and clearances. The associated NASTRAN grid points were modified, if necessary, to reflect the true measurement locations for correlation.

The installed accelerometers were oriented in the direction of the principal aircraft axes, with positive acceleration measured in the up, right and aft directions. In order to increase the total number of locations measured, primarily in the vertical (Z) response direction, triaxial measurements were not made at all locations.

# MEASUREMENT LOCATIONS



## MEASUREMENT LOCATIONS AND NASTRAN GRID POINTS

The station, waterline and buttline location of actual measurement points are tabulated below. Included are the revised NASTRAN grid points and test article identification numbers for reference purposes.

# MEASUREMENT LOCATIONS AND NASTRAN GRID POINTS

LOCATION	GRID POINT	STA.	B.L.	W.L.	DIRECTION	LOCATION	GRID POINT	STA.	B.L.	W.L.	DIRECTION
1	362	177.5	21	215	X, Y, Z	37	4214	399	34	260.7	Y, Z
2	351	177.5	-21	215	Y, Z	38	4210	399	15.5	260.7	Z
3	962	203.5	31	215	Y, Z	39	4204	399	-15.5	260.7	Z
4	950	203.5	-31	215	Z	40	4200	399	-34	260.7	Z
5	705	201.5	28	237	X, Y, Z	41	5317	443.5	30	206.7	Y, Z
6	744	201.5	-28	237	Z	42	5467	445	10	205	Z
7	2195	253	31	206.7	Y, Z	43	5463	445	-10	205	Z
8	2191	253	10	206.7	Z	44	5333	443.5	-30	206.7	Z
9	2186	253	-10	206.7	Z	45	5306	443.5	28	261	Y, Z
10	2182	253	-31	206.7	Y, Z	46	5344	443.5	-28	261	Z
11	2107	247	36	260	Y, Z	47	5725	485	0	203	Y, Z
12	2103	250	14	269	Z	48	5701	485	0	273	Y, Z
13	2147	250	-14	269	Z	49	6325	545	0	206	Y, Z
14	2143	247	-36	260	Y, Z	50	6301	545	0	250	Y, Z
15	2797	295	-10	206.7	Y, Z	51	6725	585	0	208	Y, Z
16	2791	295	10	206.7	Z	52	6749	585	0	245	Y, Z
17	2786	295	-35.5	206.7	Z	53	7580	643	0	215	Y, Z
18	2780	295	-35.5	206.7	Z	54	7592	643	0	237	Y, Z
19	2707	292	39	260.7	Y, Z	55	7800	658	0	239	X, Y, Z
20	2803	297	17.5	260.7	Z	56	8501	696	6.5	267	X, Y
21	2847	297	-17.5	260.7	Z	57	8601	709	5.8	282	X, Y
22	2743	292	-39	260.7	Z	58	8801	724	5.5	287	X, Y, Z
23	3203	327	16.5	260.7	Y, Z	59	60015	732	0	325	X, Y, Z
24	3247	327	-16.5	260.7	Z	60	9204	702	83.4	247	X, Z
25	3396	350	31	206.7	Y, Z	61	9244	702	47.5	247	X, Z
26	3391	350	10	206.7	Z	62	9124	702	0	247	X, Z
27	3427	350	-10	206.7	Z	63	9044	702	-47.5	247	X, Z
28	3431	350	-31	206.7	Z	64	9004	702	-83.5	247	X, Z
29	3806	360	32.5	260.7	Y, Z	65	9800	341	0	315	X, Y, Z
30	3803	360	15	260.7	Z	66	9803	340	0	260.7	X, Y, Z
31	3847	360	-15	260.7	Z	67	60008	390	31	281	X, Y, Z
32	3844	360	-32.5	260.7	Z	68	95003	356	32	285	X, Y, Z
33	4194	398	35	206.7	Y, Z	69	60009	390	-31	281	X, Y, Z
34	4190	398	11	206.7	Z	70	95002	356	-32	285	X, Y, Z
35	4184	398	-10	206.7	Z	71	8205	679	6	220	Y, Z
36	4180	398	-35	206.7	Z	72	60016	732	13	325	X, Y, Z

## MEASUREMENT PROCEDURE

Each frequency sweep was made up of two parts: an initial broad-band sweep followed by a series of detailed narrow-band sweeps around the resonance peaks as shown in the figure.

### Broad-Band Sweep

Each broad-band sweep was done over the entire frequency range with a relatively coarse frequency resolution. In addition, the "short integration" time feature of the Solartron analyser was used, which means that the measurement at each frequency was continued until the running average result became consistent within a maximum deviation of 10%. Details of the broad-band sweeps are as follows:

Start Frequency 3 Hz  
Finish Frequency 40 Hz (45 Hz for Vertical Excitation)  
Linear Sweep  
Frequency Increment 0.25 Hz  
Constant Force = 100 lbs  
Measurement Delay = 0 seconds  
Auto Integration = 10% on channel 2  
Frequency Response = Channel  $i$ /Channel 1 (where  $i = 2$  to 18)  
Display - Bode Plot

This sweep establishes the general character of each Frequency Response Function (FRF), including the location of its resonance regions.

### Narrow-Band Sweeps

Each broad-band sweep was followed by a series of narrow-band sweeps over selected frequency bands, usually resonant regions. In these regions response curves exhibit much more rapid changes and it was usually necessary to take measurements there with an increased frequency resolution. In addition, the "long integration" time feature was used, which means that the measurement at each frequency was continued until the deviations did not exceed 1%. Details for these sweeps are as follows:



# MEASUREMENT PROCEDURE

<u>Ref No.</u>	<u>Start Freq.</u>	<u>End Freq</u>	<u>Type</u>	<u>No of Points</u>
<u>VERTICAL EXCITATION</u>				
1	3.0	45.0	BROAD	168
2	6.6	7.0	NARROW	20
3	12.1	12.9	NARROW	20
4	13.5	14.5	NARROW	20
5	18.9	20.1	NARROW	20
6	24.4	25.7	NARROW	20
7	25.9	27.1	NARROW	20
8	31.5	32.8	NARROW	20
9	33.6	34.8	NARROW	20
10	35.5	37.2	NARROW	20
11	38.7	40.2	NARROW	20
<u>LATERAL EXCITATION</u>				
1	3.0	40.0	BROAD	148
2	4.85	5.15	NARROW	20
3	5.35	5.65	NARROW	20
4	9.5	10.7	NARROW	20
5	13.2	14.4	NARROW	20
6	14.9	15.8	NARROW	20
7	26.2	27.5	NARROW	20
8	30.0	31.0	NARROW	20
9	31.9	33.2	NARROW	20
10	34.0	36.0	NARROW	30
<u>LONGITUDINAL EXCITATION</u>				
1	3.0	40.0	BROAD	148
2	6.6	7.0	NARROW	20
3	11.8	12.7	NARROW	20
4	13.4	14.4	NARROW	20
5	18.8	20.1	NARROW	20
6	24.5	25.8	NARROW	20
7	26.2	27.5	NARROW	20
8	30.3	31.5	NARROW	20
9	28.8	29.8	NARROW	20
10	31.5	33.0	NARROW	20

## MEASUREMENT PROCEDURE (CONT.)

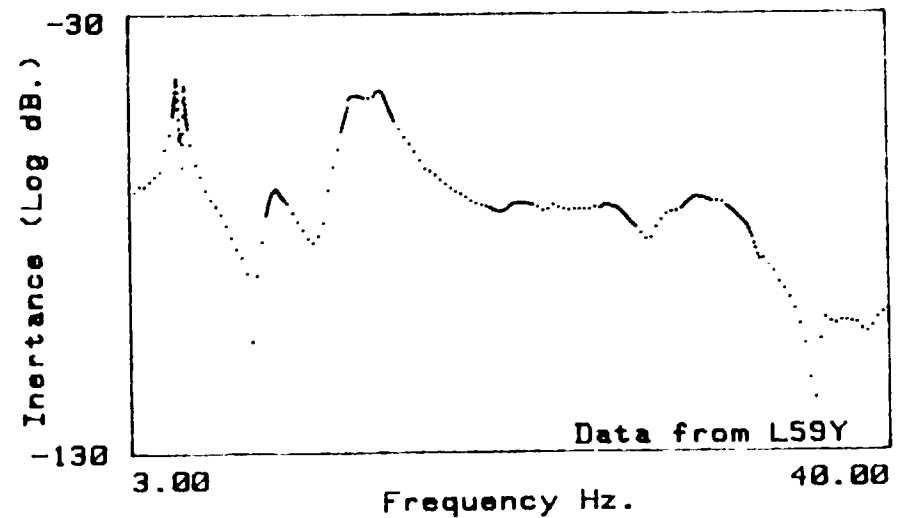
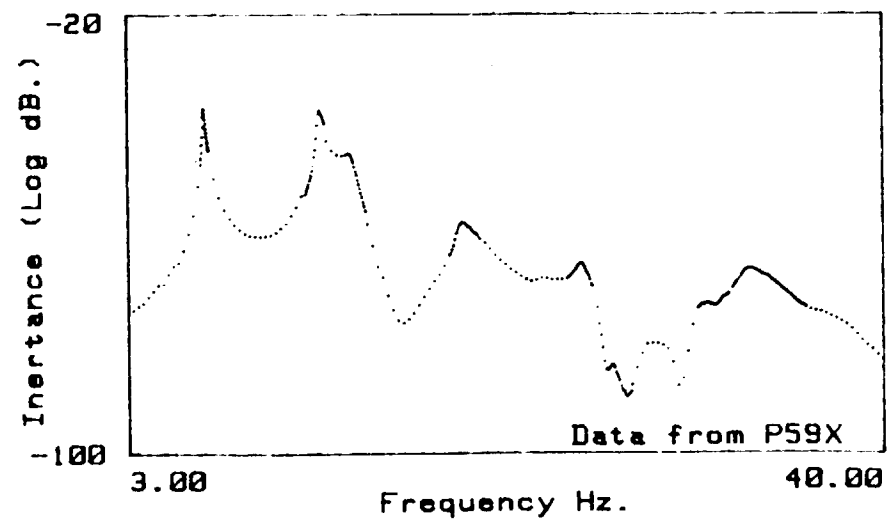
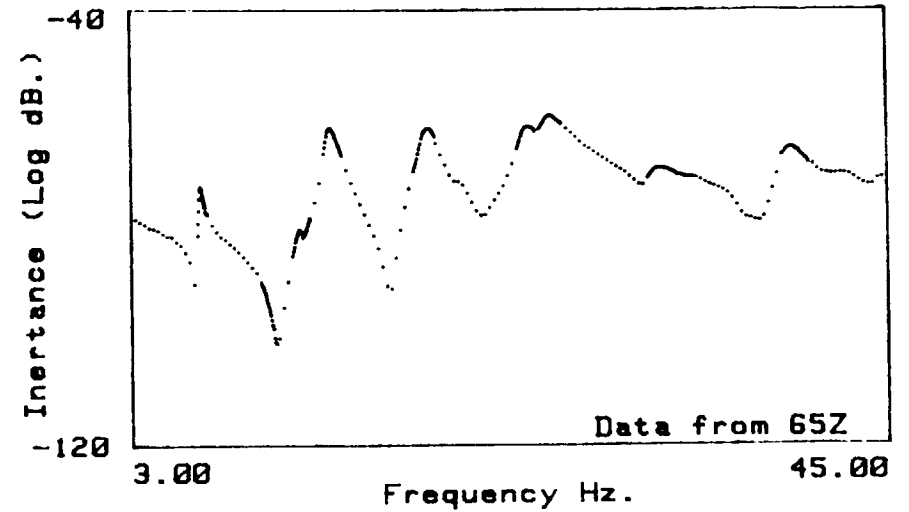
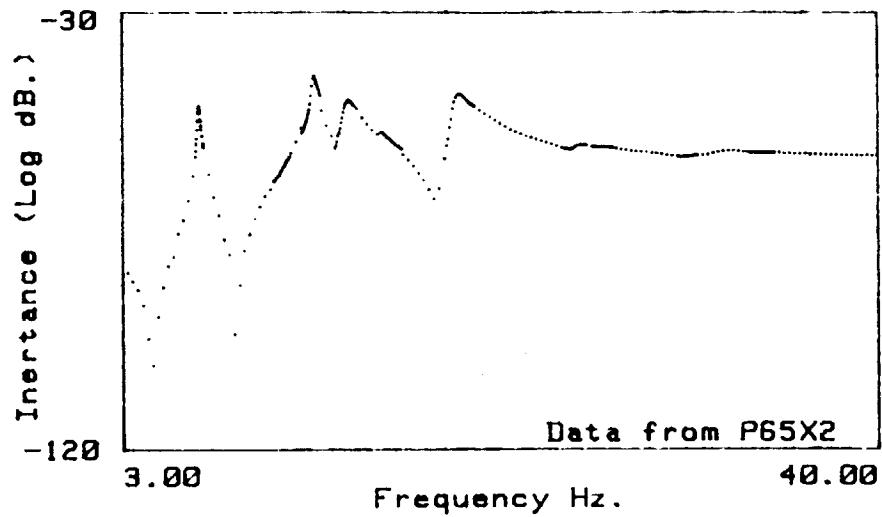
Frequency Range  $\pm 3\%$  of Peak Frequency  
Linear Sweep of 20 equally spaced points  
Constant Force = 100 lbs  
Measurement Delay = 1 second  
Auto Integration = 1% on Channel 2  
Frequency Response = Channel  $i$ /Channel 1 (where  $i = 2$  to 18)  
Display - Nyquist Plot

These narrow-band sweeps furnished a more accurate definition of the FRF in the regions of the resonance peaks.

### Final Frequency Response Functions

Each final FRF was formed by combining the between-resonance response points, which were measured in the broad-band sweep, with the near-resonance response points measured in the narrow-band sweeps. The figure shows the resulting final appearance of four of the FRF's.

## MEASUREMENT PROCEDURE (CONT.)





**SECTION 5.0**  
**SHAKE TEST RESULTS**



## SECTION 5.1

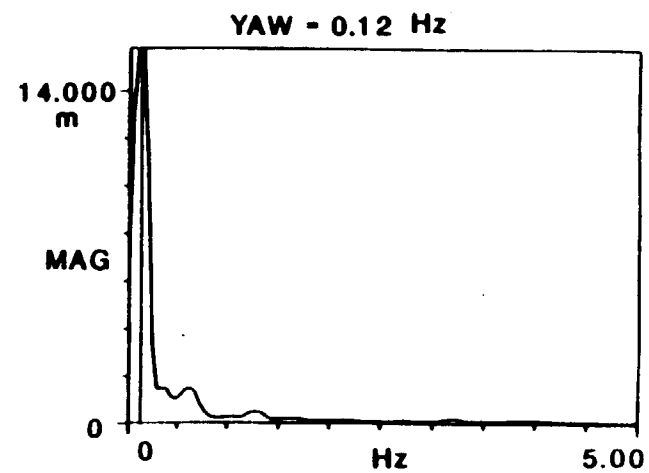
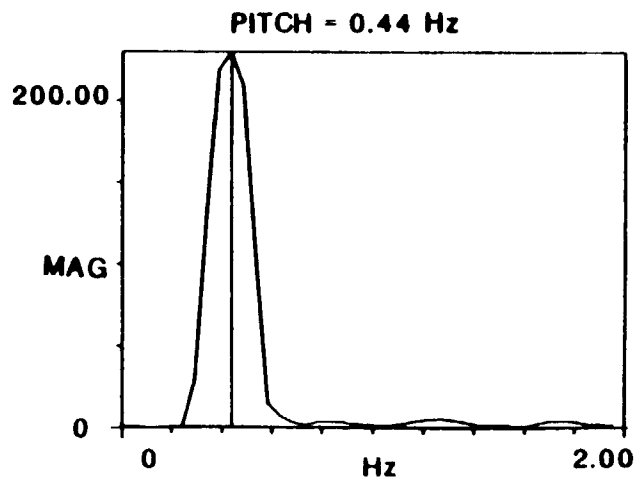
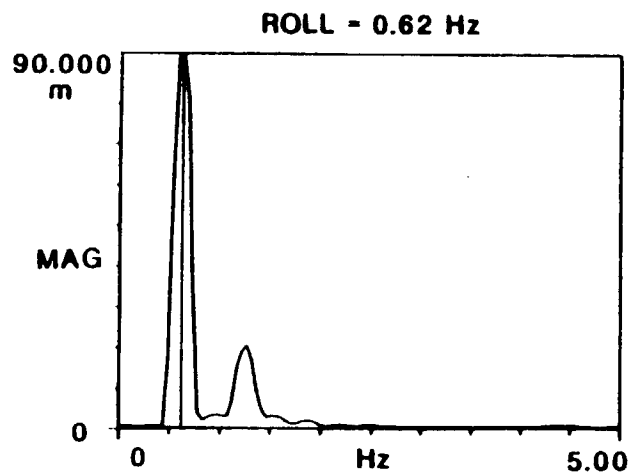
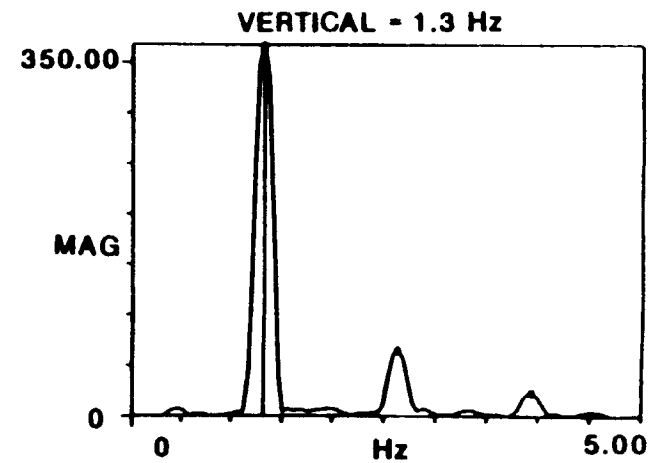
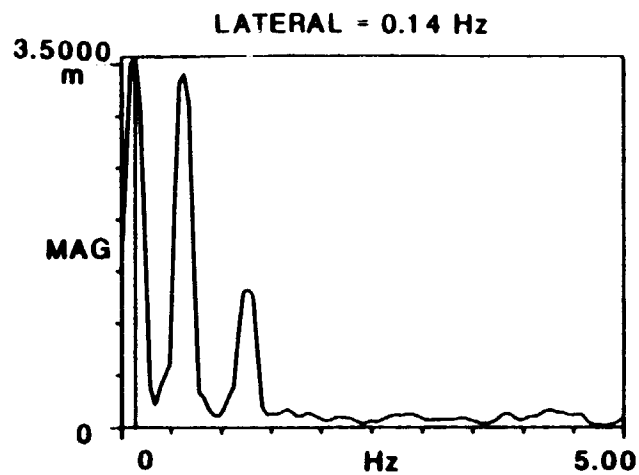
# RIGID BODY MODES

## SUSPENDED UH-60A RIGID BODY MODES MEASURED BEFORE TEST

The rigid body modes of the suspended aircraft were excited manually prior to the start of the frequency sweeps and were measured using an FFT analyzer. The figure below shows that the rigid body modes are low, with only the vertical mode being above 1 Hz. This mode is at approximately 17% of the first elastic mode in the vertical direction which is within the objective of 20%. The responses that show harmonics are the modes that had to be periodically excited by hand in order to maintain the oscillations. This excitation was not a pure sine wave and therefore excited the harmonics also.



# SUSPENDED UH-60A RIGID BODY MODES MEASURED BEFORE TEST

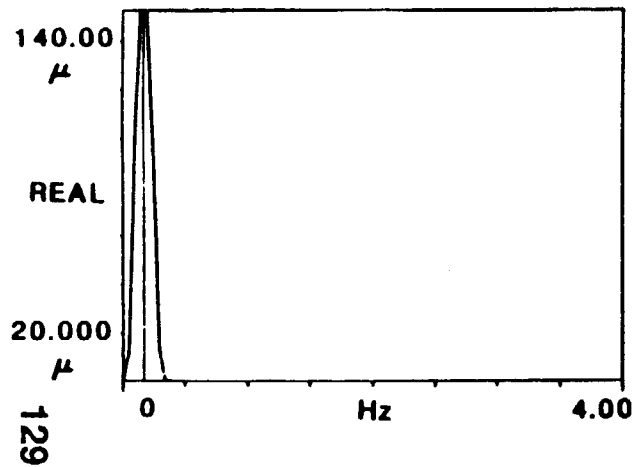


## SUSPENDED UH-60A RIGID BODY MODES MEASURED AFTER TEST

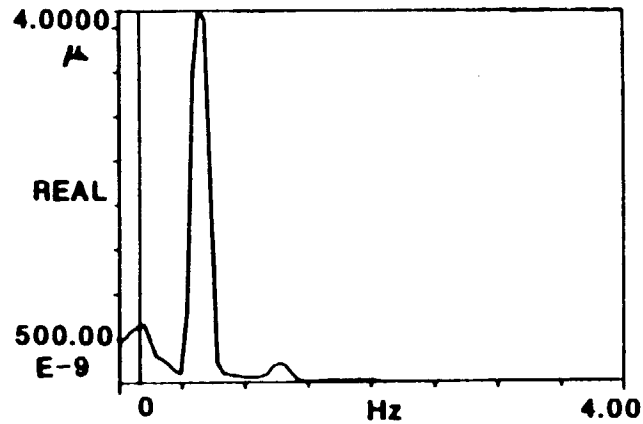
The figure below shows the rigid body modes measured following the lateral excitation sweeps. Very little change is noted indicating that little change has occurred in the support system during the test.

# SUSPENDED UH-60A RIGID BODY MODES MEASURED AFTER TEST

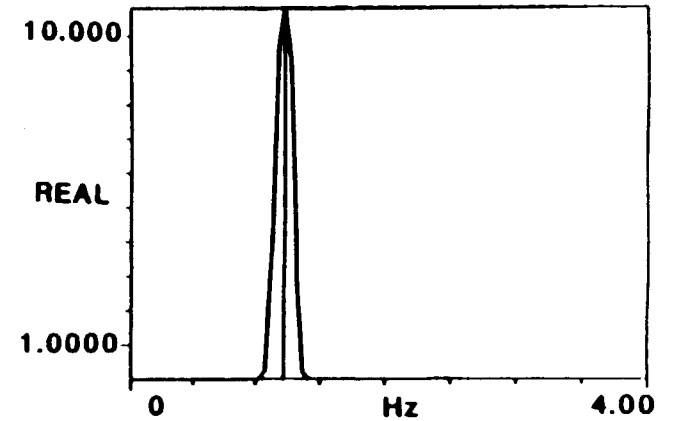
LONGITUDINAL - 0.17 Hz



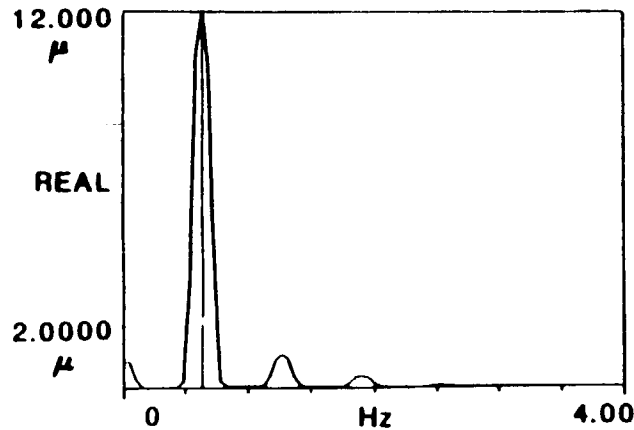
LATERAL - 0.16 Hz



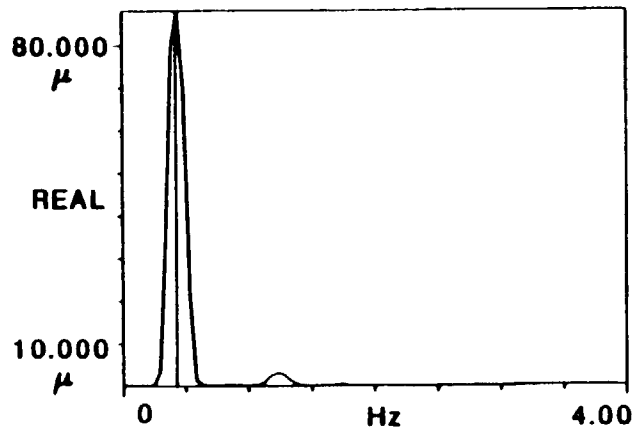
VERTICAL - 1.2 Hz



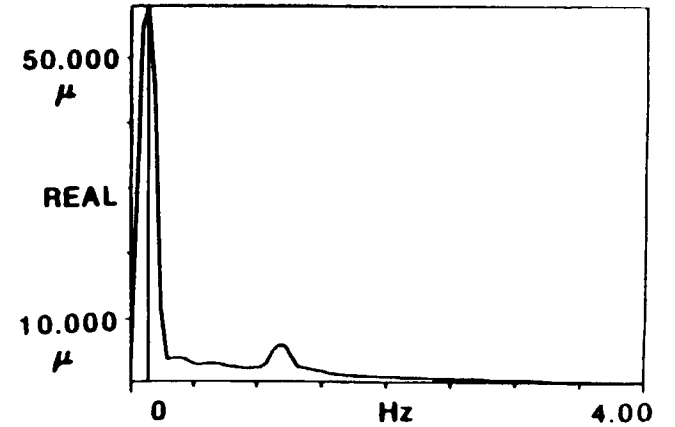
ROLL - 0.63 Hz



PITCH - 0.43Hz



YAW - 0.14 Hz





## **SECTION 5.2**

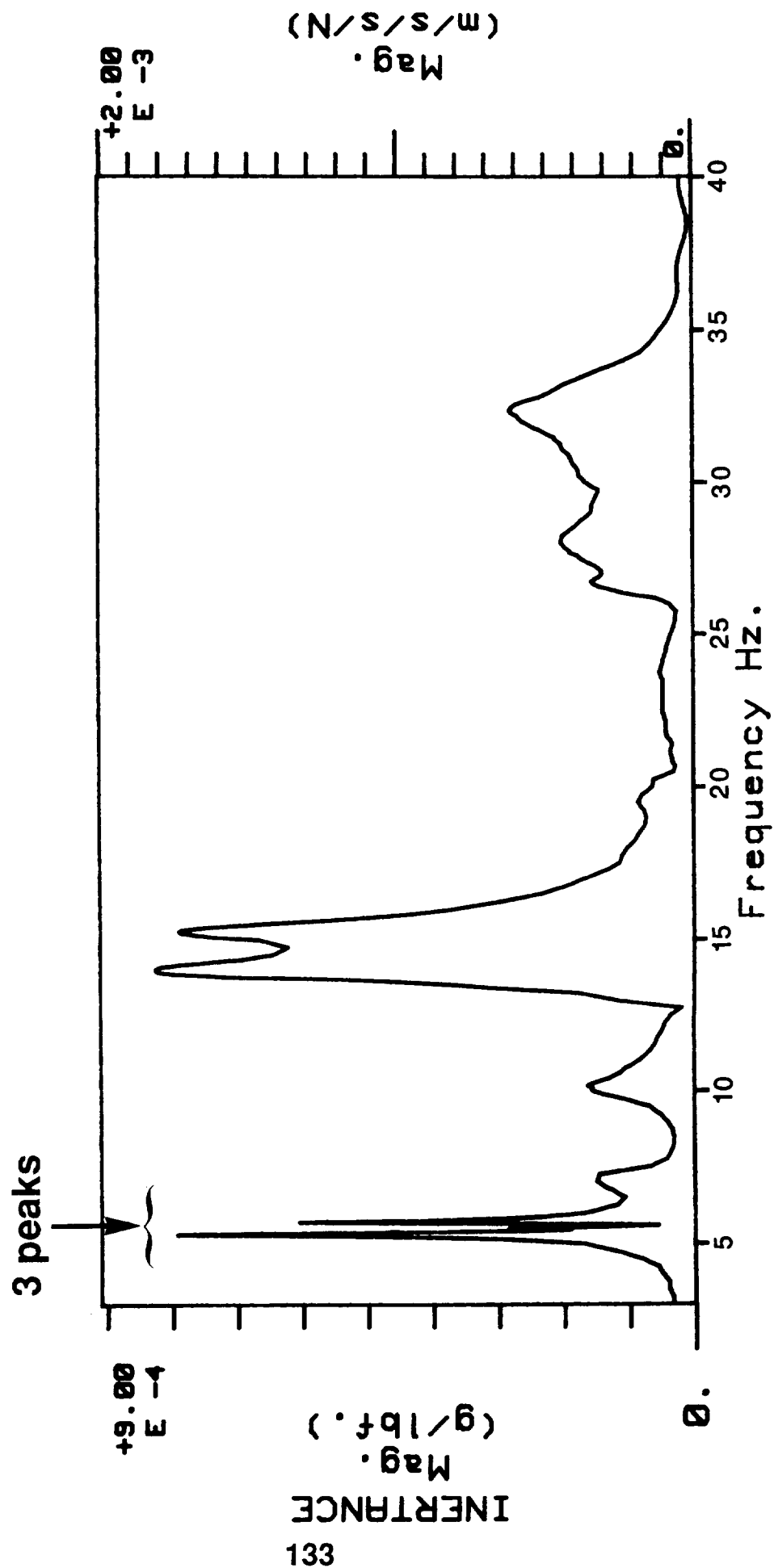
# **SUSPENSION SYSTEM MODES**

## ADDITIONAL MODES INTRODUCED BY SUSPENSION SYSTEM

When exciting the aircraft laterally, two and sometimes three closely-spaced resonance peaks were observed in the vicinity of the fuselage first lateral bending mode. This can be seen in this figure, which shows the frequency response of the tail rotor gearbox in the vertical direction (Location 502) due to main rotor hub excitation in the lateral (Y) direction. The close peaks here are at 5.3, 5.5, and 5.7 Hz. Without the presence of the suspension system it is expected that only one peak would occur in this region, namely that of the fuselage 1st lateral bending mode. Physical observation of the bungee system response in this frequency range indicated that local lateral "cable" (or "guitar string") modes of both the fore and aft cable/bungee systems were being excited and were coupling with the first fuselage bending mode to produce three coupled fuselage/bungee modes.

A brief attempt was made to lower the frequencies of the cable modes by adding weights and by removing bungee strands. Shifting these frequencies proved difficult to do and the effort was abandoned due to lack of time. No evidence of the cable modes was observed at higher frequencies.

# ADDITIONAL MODES INTRODUCED BY SUSPENSION SYSTEM

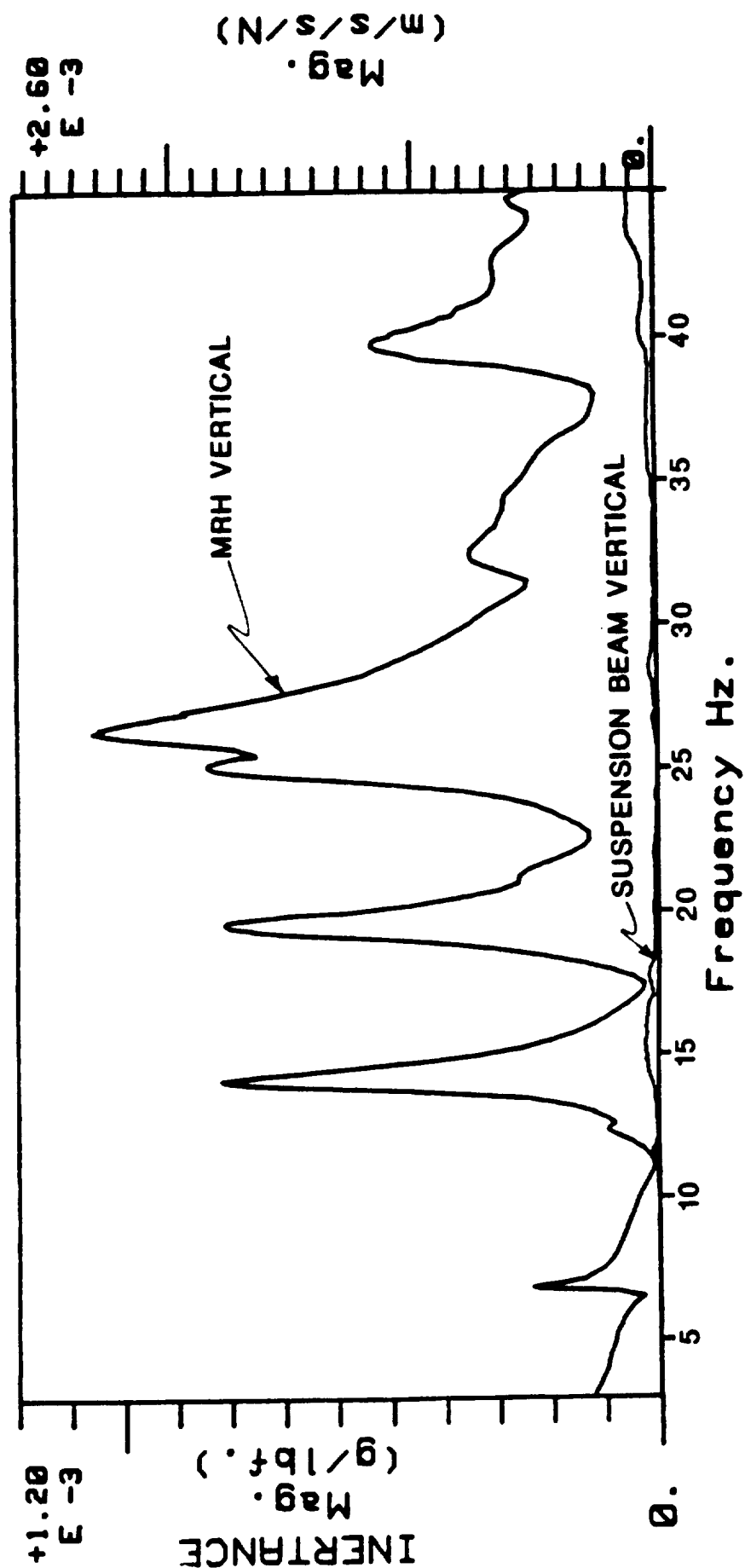


## COMPARISON OF RESPONSES OF MRH VERTICAL AND FORWARD SUSPENSION BEAM VERTICAL

Response of the test facility ceiling near the attachment points of the suspension system was measured during vertical excitation. The figure below illustrates the vertical response of the ceiling compared to the main rotor head. This plot shows that the response of the ceiling is almost negligible compared to the main rotor head. The only significant response is in the range of approximately 14 to 18 Hz. This support motion did not appear to influence any of the structural modes of the fuselage.



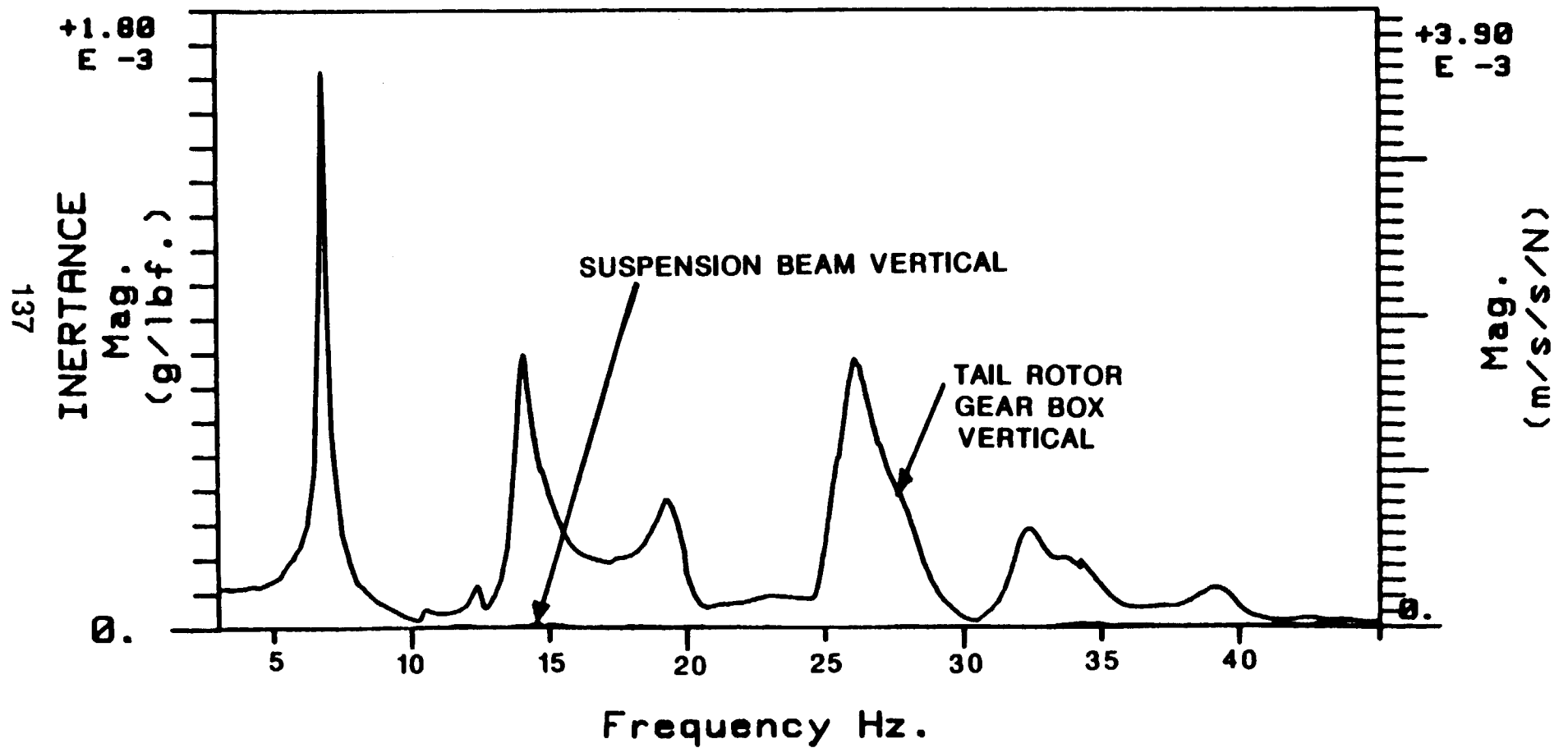
# COMPARISON OF RESPONSES OF MRH VERTICAL AND FWD SUSPENSION BEAM VERTICAL



#### COMPARISON OF RESPONSES OF TRGB VERTICAL AND AFT SUSPENSION BEAM VERTICAL

The figure below illustrates the vertical response of the ceiling compared to the tail rotor head. This plot shows that the response at the tail rotor suspension beam support attachment point is less than the main rotor support attachment point and is not considered to be significant.

# COMPARISON OF RESPONSES OF TRGB VERTICAL AND AFT SUSPENSION BEAM VERTICAL





## SECTION 5.3

# NON LINEAR RESPONSE INVESTIGATION

## NONLINEAR RESPONSE INVESTIGATION

To investigate in detail the extent of nonlinear behavior in the measured airframe response, a series of measurements were recorded for various excitation control methods, locations and amplitudes.

### Tail Vertical - Constant Displacement (CD)

Vertical excitation at the stabilator attachment lugs was performed with a displacement feedback control system. Hydraulic actuator motion was held constant throughout the frequency range, allowing the force level to vary with airframe response through resonances, as shown in the figure.

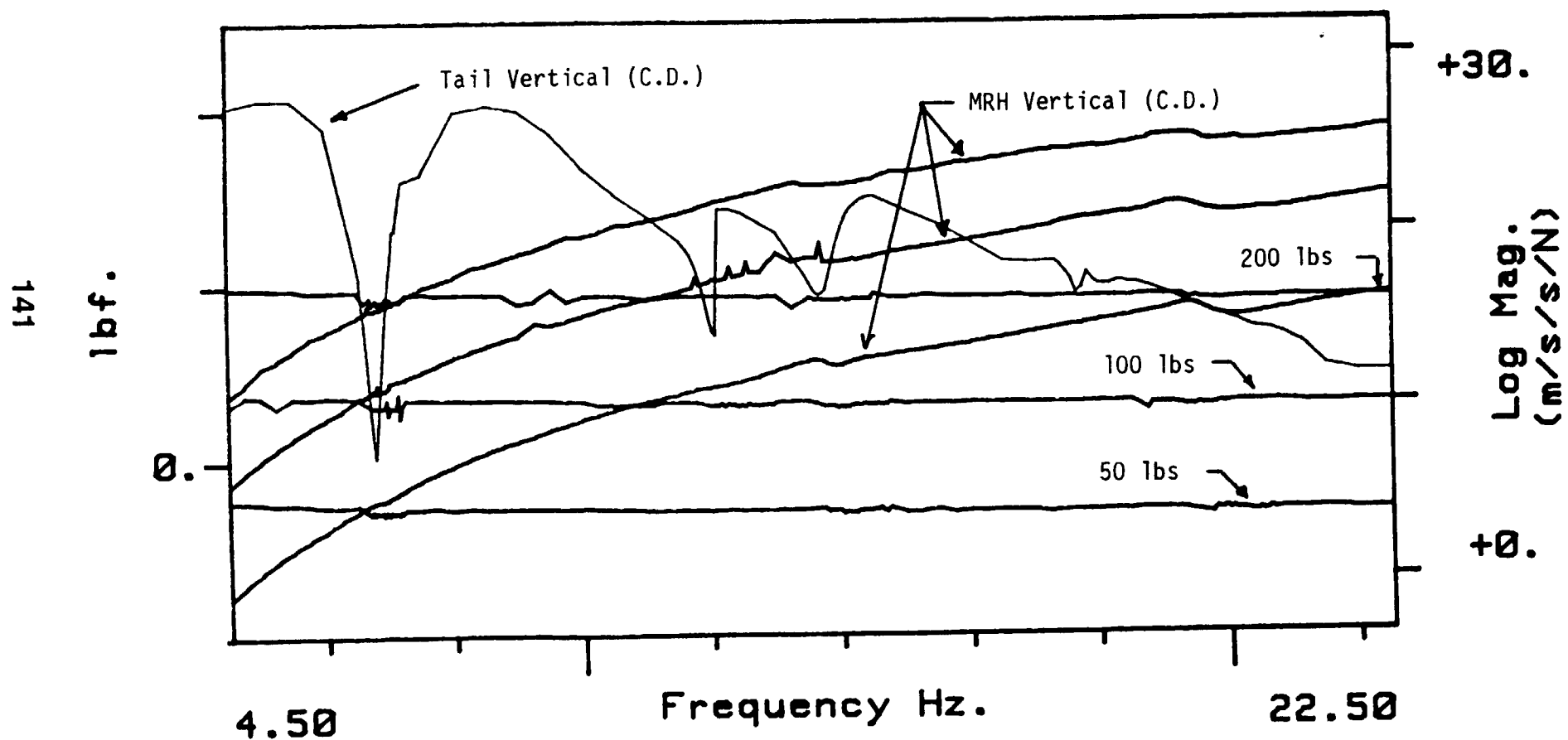
### Main Rotor Hub Vertical - Constant Displacement (CD) (3 Levels)

The primary control for the main rotor inertial shakers is displacement feedback, maintaining constant shaker moving mass displacement relative to the hub over the frequency range of excitation. This method results in a force level which increases in proportion to the frequency squared, as shown in the figure.

### Main Rotor Hub Vertical - Constant Force (CD) (3 Levels)

This method, which was used for the measurement phase of the program, uses the measurement system as part of the control loop to maintain constant force. Prior to each measurement, inertial shaker mass acceleration is measured and compared to a preset level. The generator output is automatically adjusted until the correct level is set, at which time the measurements are recorded. This process is repeated throughout the frequency range, resulting in a true constant force excitation. The method was repeated at force levels of 50, 100 and 200 pounds.

# NONLINEAR RESPONSE INVESTIGATION

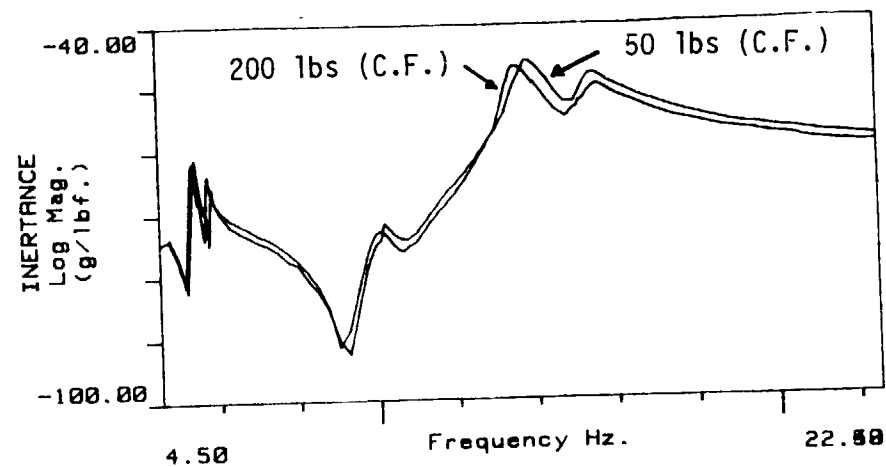
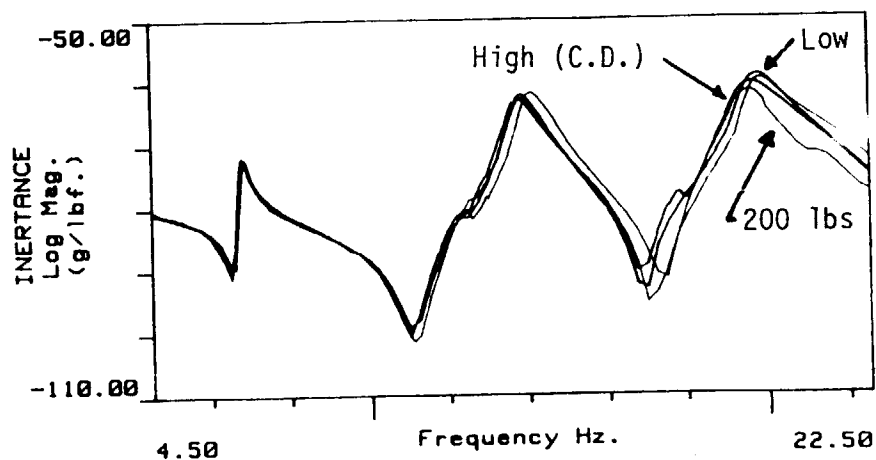


## NONLINEAR RESPONSE INVESTIGATION (CONTINUED)

The figures below show the effect of force level on the measured frequency response functions for three airframe locations. The three locations are vertical responses to main rotor hub vertical excitation of various amplitudes and control techniques. The primary factor resulting in variation of response is force level. A secondary factor affecting amount of variation is the amplitude of response at each location for each individual mode. Tail gearbox vertical response for the mode in the 19.5 Hz range exhibits a much greater variation with force level as compared with the nose and main rotor hub responses. This mode is a predominantly tail pylon response mode, with much higher levels of response at the tail gearbox than at the other locations.

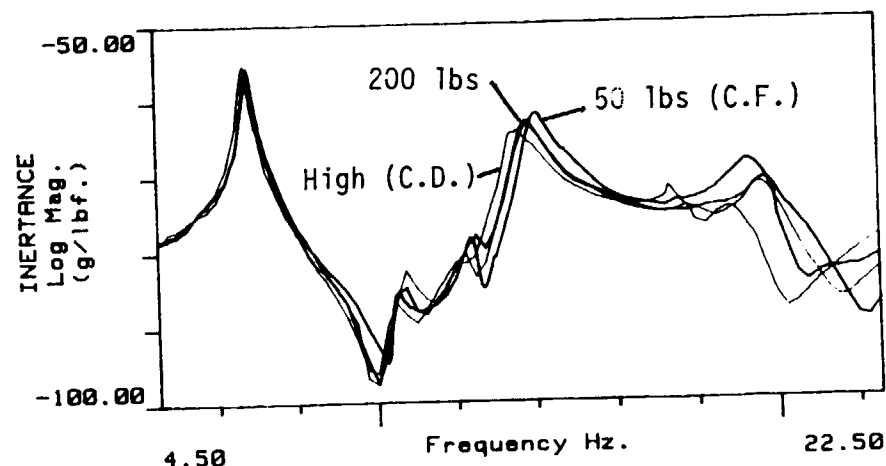
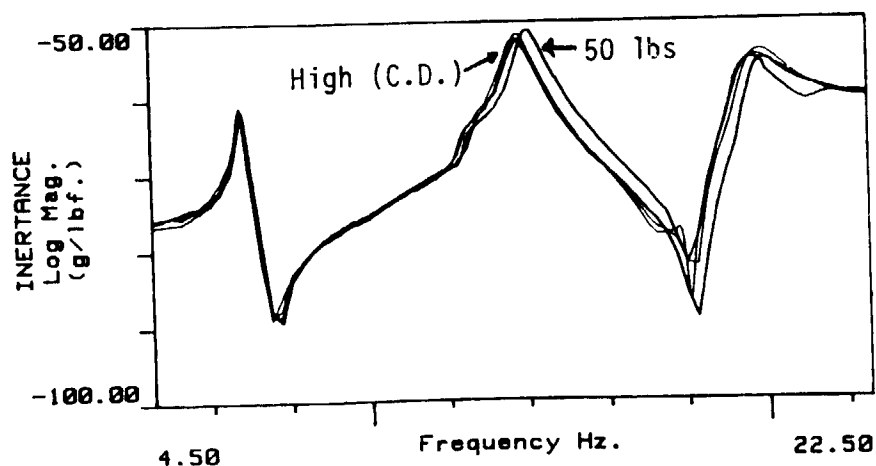


# NONLINEAR RESPONSE INVESTIGATION (CONT.)



143 MR HUB VERTICAL RESPONSE COMPARISON

MRH LATERAL RESPONSE COMPARISON



NOSE VERTICAL - RESPONSE COMPARISON

TAIL GEARBOX VERT. RESPONSE COMPARISON

# NONLINEAR RESPONSE INVESTIGATION (CONTINUED)

The table below presents the results of a single degree-of-freedom analysis on each of the first three response modes for all combinations of excitation technique, amplitude and location. The values are arranged in order of increasing force level of excitation through each individual mode. With few exceptions, the table indicates a decrease in apparent natural frequency together with increased estimates of damping as the force level is increased over the resonant region.

# NONLINEAR RESPONSE INVESTIGATION (CONT.)

MODE 1

Excitation Type	Force Level	Nose		MR Hub		TRGB	
		Freq	Damp	Freq	Damp	Freq	Damp
50# CF	50 lbs	6.92	.029	6.93	.028	6.92	.029
Low CD	50 lbs	6.80	.027	6.80	.027	6.80	.029
100# CF	100 lbs	6.79	.027	6.80	.027	6.79	.029
Med CD	100 lbs	6.75	.028	6.76	.027	6.75	.028
Tail CD	150 lbs	6.70	.029	6.74	.028	6.73	.027
200# CF	200 lbs	6.77	.034	6.74	.032	6.77	.033
High CD	200 lbs	6.73	.034	6.73	.032	6.74	.033

MODE 2

Excitation Type	Force Level	Nose		MR Hub		TRGB	
		Freq	Damp	Freq	Damp	Freq	Damp
50# CF	50 lbs	14.08	.038	14.05	.035	14.09	.033
100# CF	100 lbs	13.99	.040	14.03	.042	13.98	.040
Low CD	125 lbs	13.76	.042	13.76	.044	13.76	.044
200# CF	200 lbs	13.77	.047	13.77	.047	13.78	.048
Med CD	250 lbs	13.66	.049	13.65	.049	13.67	.049
Tail CD	350 lbs	13.42	.051	13.45	.055	13.40	.052
High CD	425 lbs	13.36	.050	13.35	.045	13.35	.046

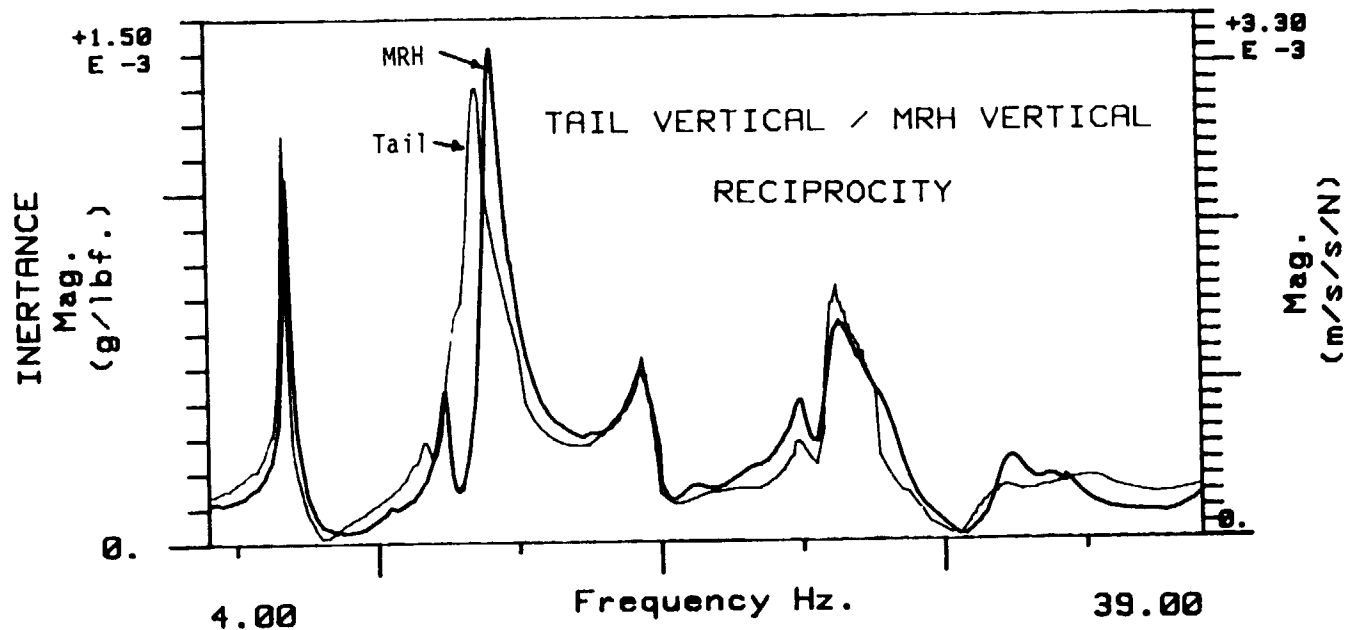
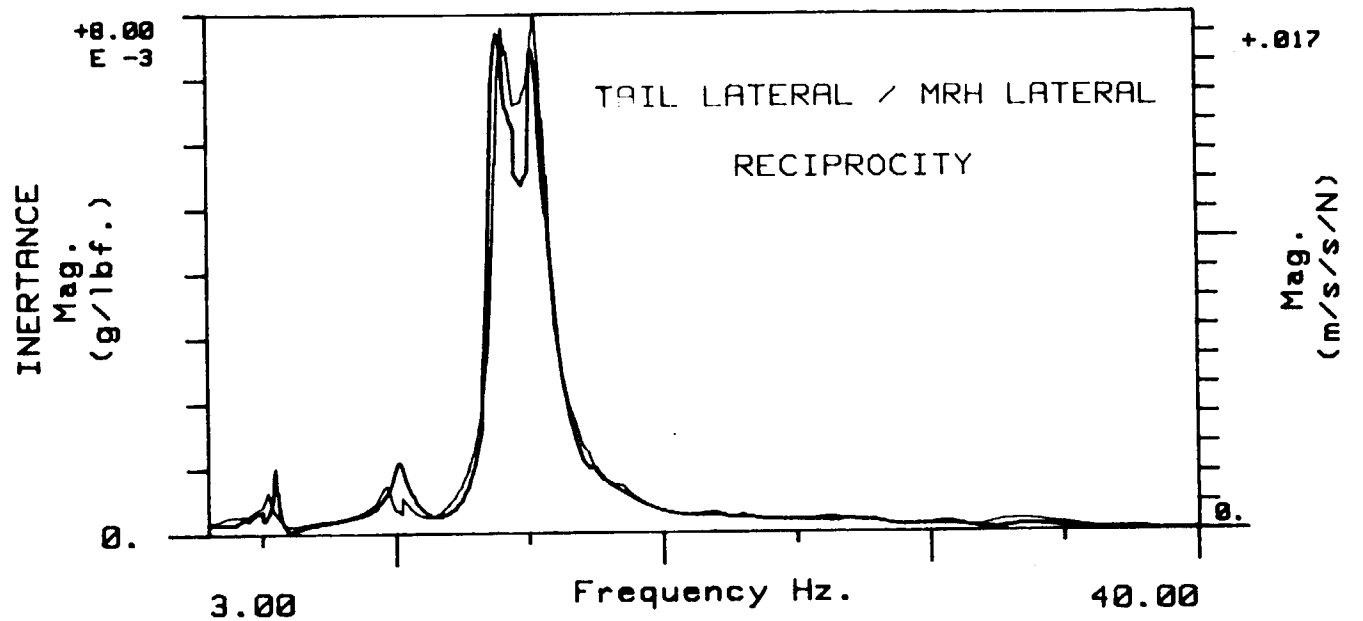
MODE 3

Excitation Type	Force Level	Nose		MR Hub		TRGB	
		Freq	Damp	Freq	Damp	Freq	Damp
50# CF	50 lbs	20.38	.040	20.37	.038	20.37	.038
100# CF	100 lbs	19.40	.042	19.52	.039	19.30	.053
200# CF	200 lbs	19.71	.042	19.69	.039	19.68	.047
Low CD	200 lbs	19.60	.048	19.57	.044	19.52	.047
Med CD	350 lbs	19.51	.053	19.50	.056	19.28	.067
Tail CD	425 lbs	19.34	.052	19.42	.045	19.35	.044
High CD	550 lbs	19.54	.041	19.54	.038	19.08	.061

## NONLINEAR RESPONSE INVESTIGATION (CONTINUED)

The figures below show the results of reciprocity checks made between main rotor hub response to tail excitation and tail response to main rotor hub excitation. For a linear system, these response plots would be identical. Differences which are apparent can be attributed to different levels of excitation used for the main and tail rotor hubs. The main rotor hub force was held constant at 100 lbs. while the tail rotor force varied (see figure on page 141).

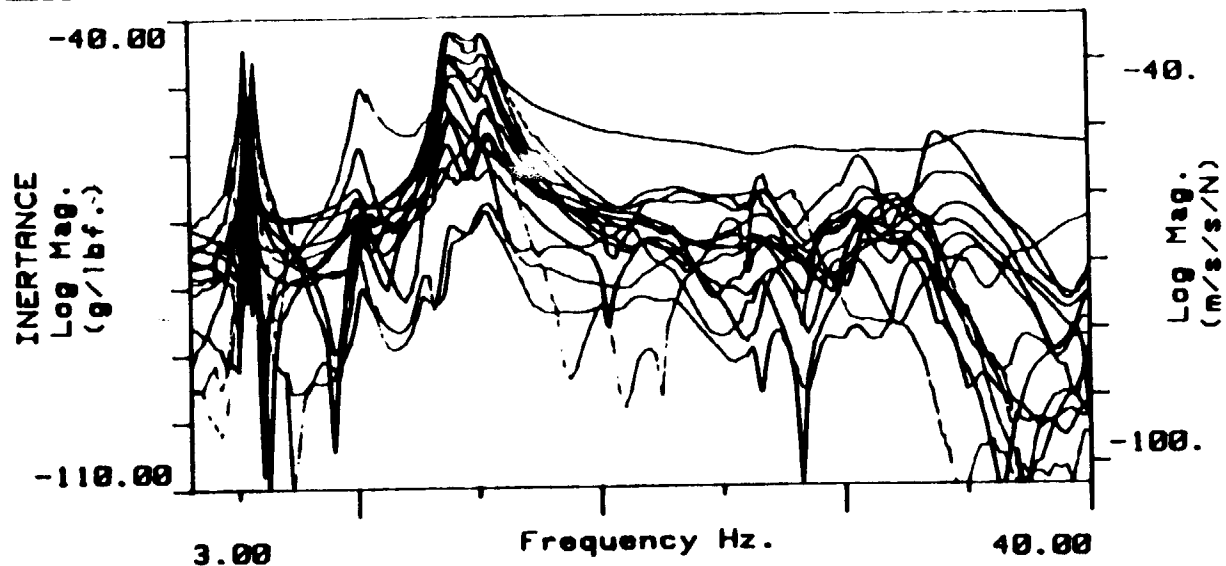
# NONLINEAR RESPONSE INVESTIGATION (CONT.)



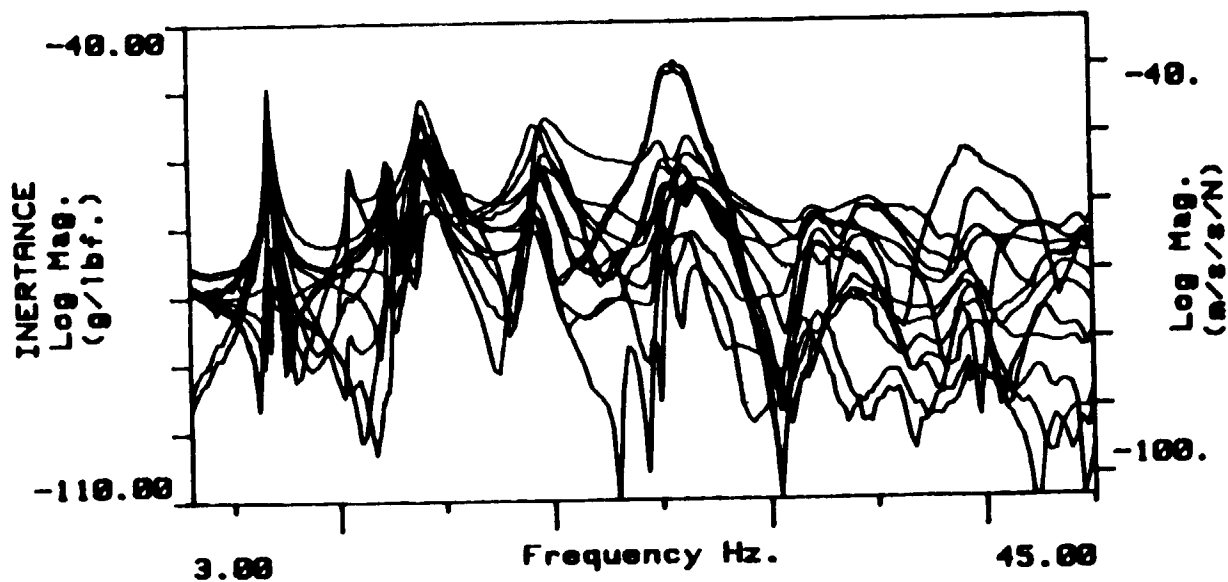
## NONLINEAR RESPONSE INVESTIGATION (CONCLUDED)

The figures below present superimposed response characteristics at various locations on the airframe to main rotor hub vertical and lateral excitations of 100 pounds constant force. The amount of variability in apparent frequencies of peak response increases with frequency of excitation as response modes become more complex.

# NONLINEAR RESPONSE INVESTIGATION (CONC.)



COMPOSITE RESPONSE / LATERAL EXCITATION



COMPOSITE RESPONSE / VERTICAL EXCITATION





## SECTION 5.4

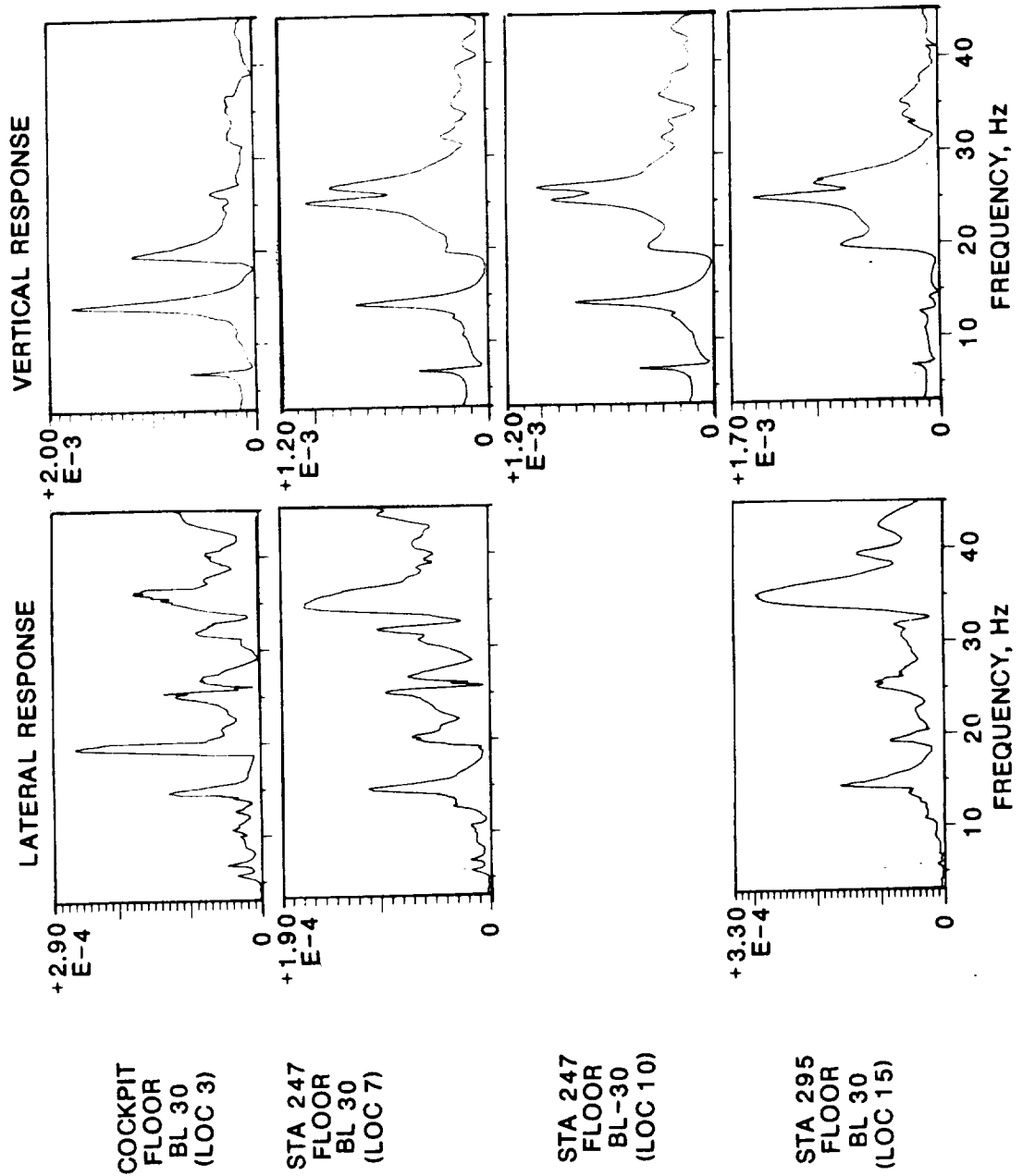
# SUMMARY OF TEST RESULTS

SHAKE TEST RESULTS - FREQUENCY RESPONSE  
MRH VERTICAL EXCITATION

For each of the 3 excitation directions at the main rotor head, approximately 50 responses were selected for presentation here. The remaining 80 responses are saved on tape and are available for plotting. The transfer functions are presented in a linear magnitude (g's/lbf) format.

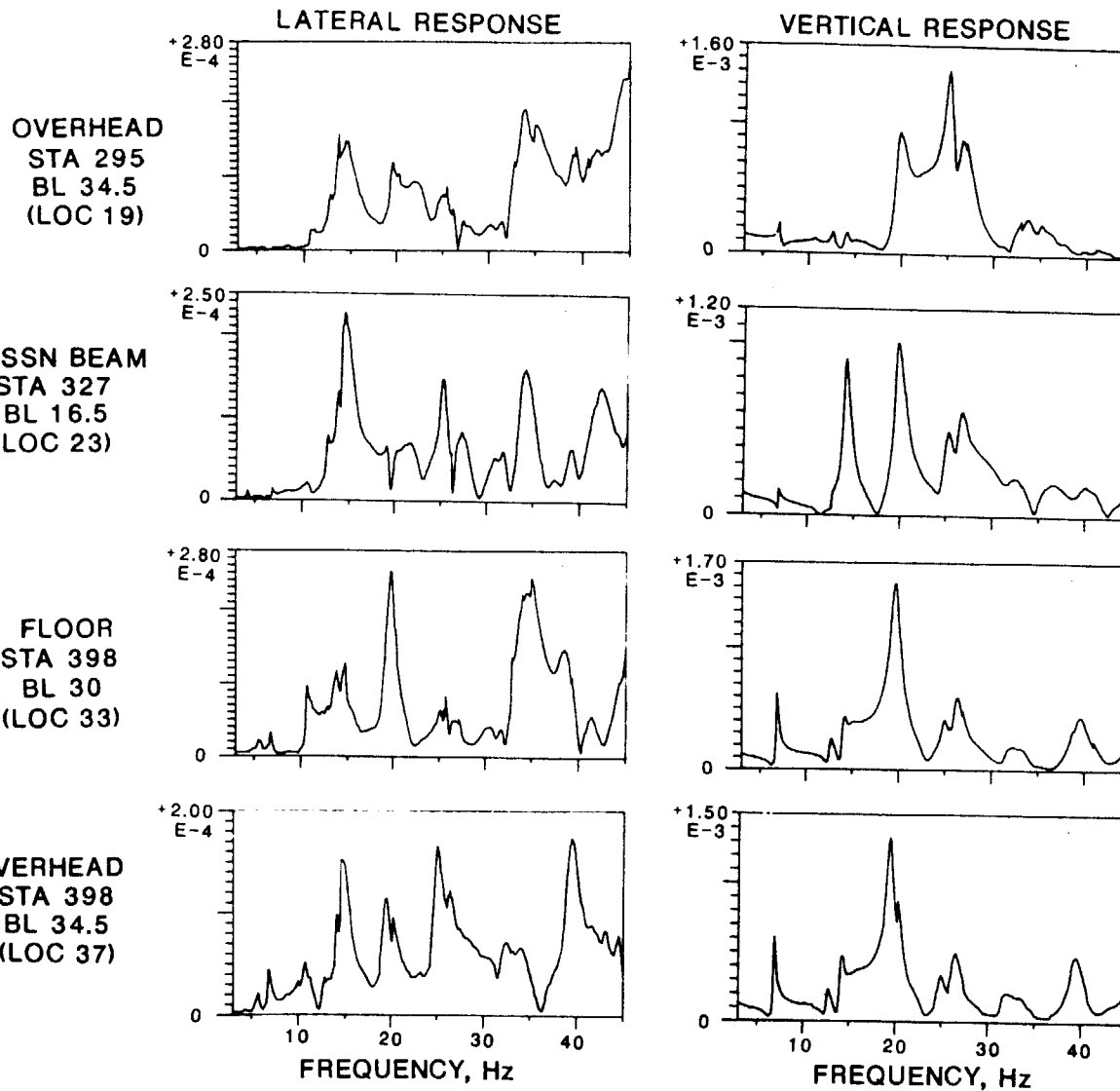
For the vertical excitation, the vertical and longitudinal components of the responses are generally of the same order of magnitude, while lateral components of the responses are usually one order smaller. This is not surprising considering the near symmetry of the UH-60A fuselage. The major peaks in the vertical response are at 6.8 Hz, 14.1 Hz, 19.4 Hz and 25.1 Hz.

# SHAKE TEST RESULTS - FREQUENCY RESPONSE (g/ibf) MRH VERTICAL EXCITATION

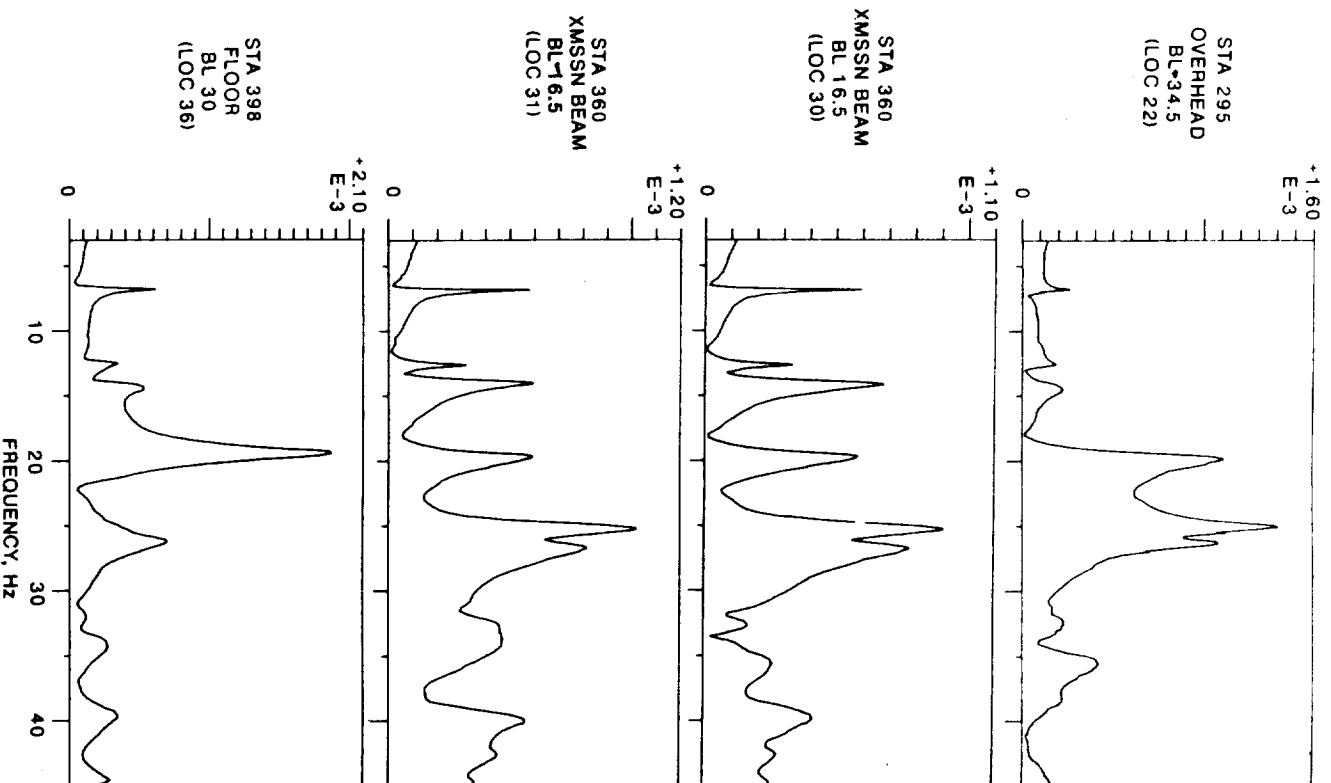


# SHAKE TEST RESULTS - FREQUENCY RESPONSE (g/lbf)

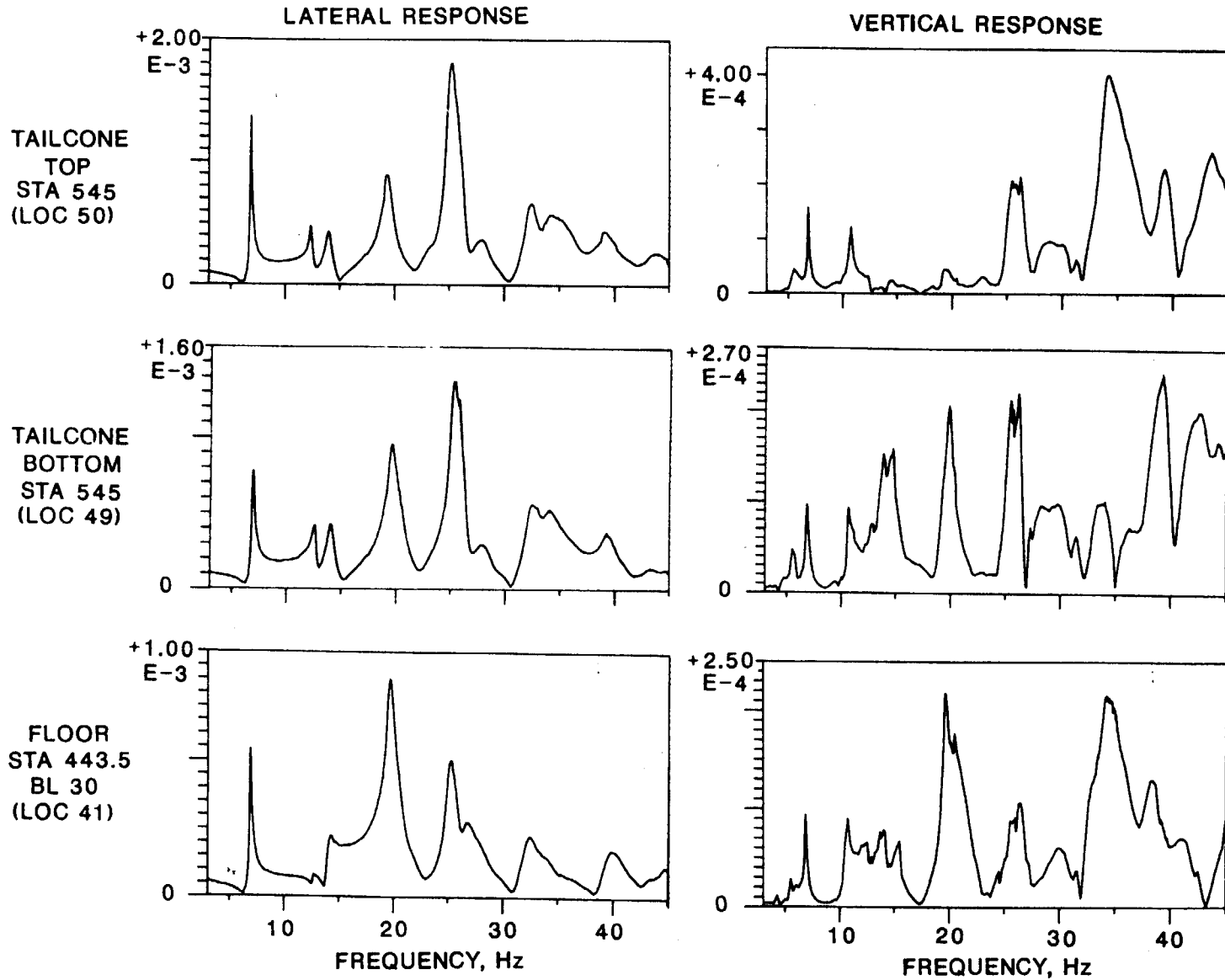
## MRH VERTICAL EXCITATION



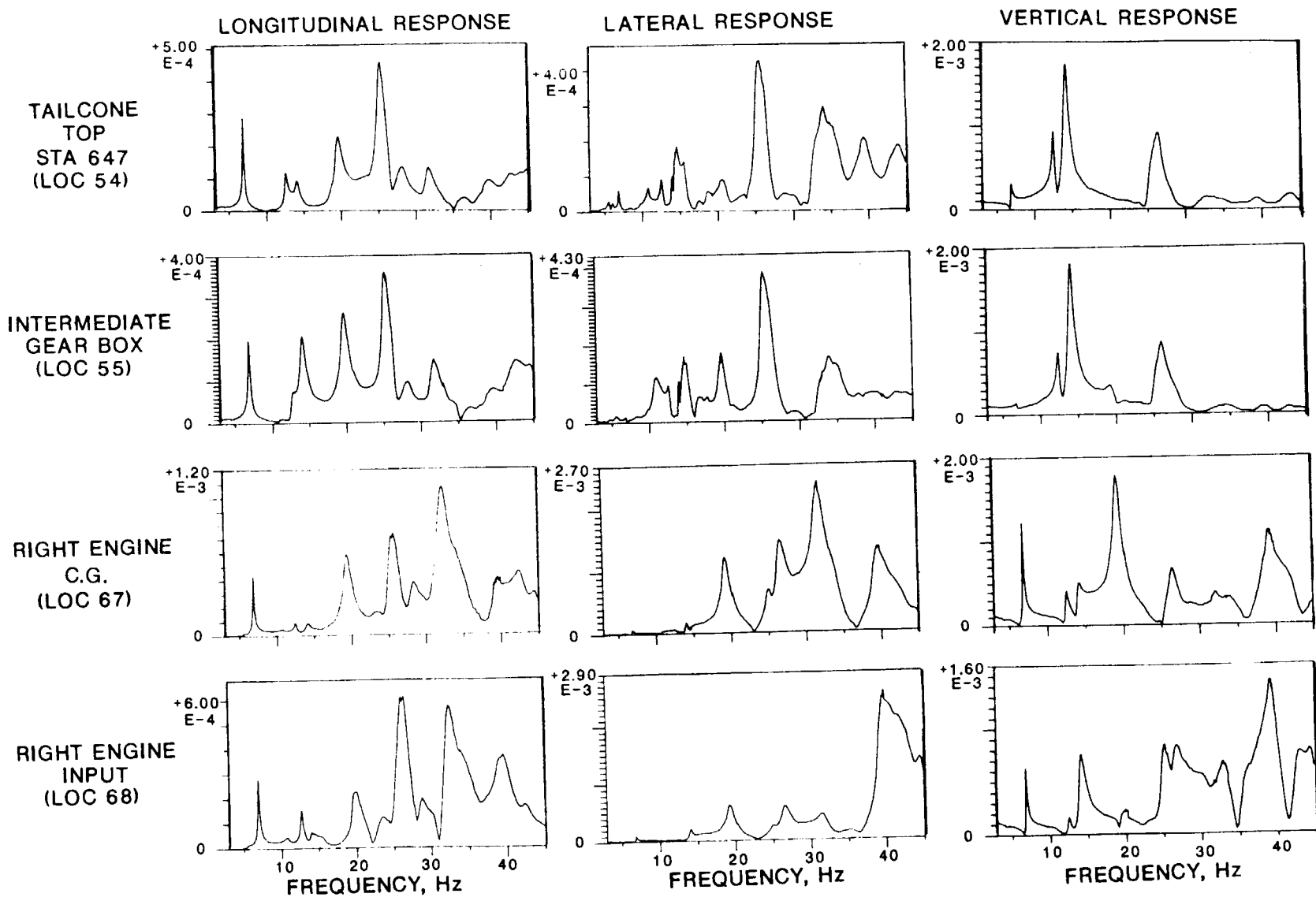
# SHAKE TEST RESULTS - FREQUENCY RESPONSE (g/ibf) MRH VERTICAL EXCITATION



# SHAKE TEST RESULTS - FREQUENCY RESPONSE (g/lbf) MRH VERTICAL EXCITATION

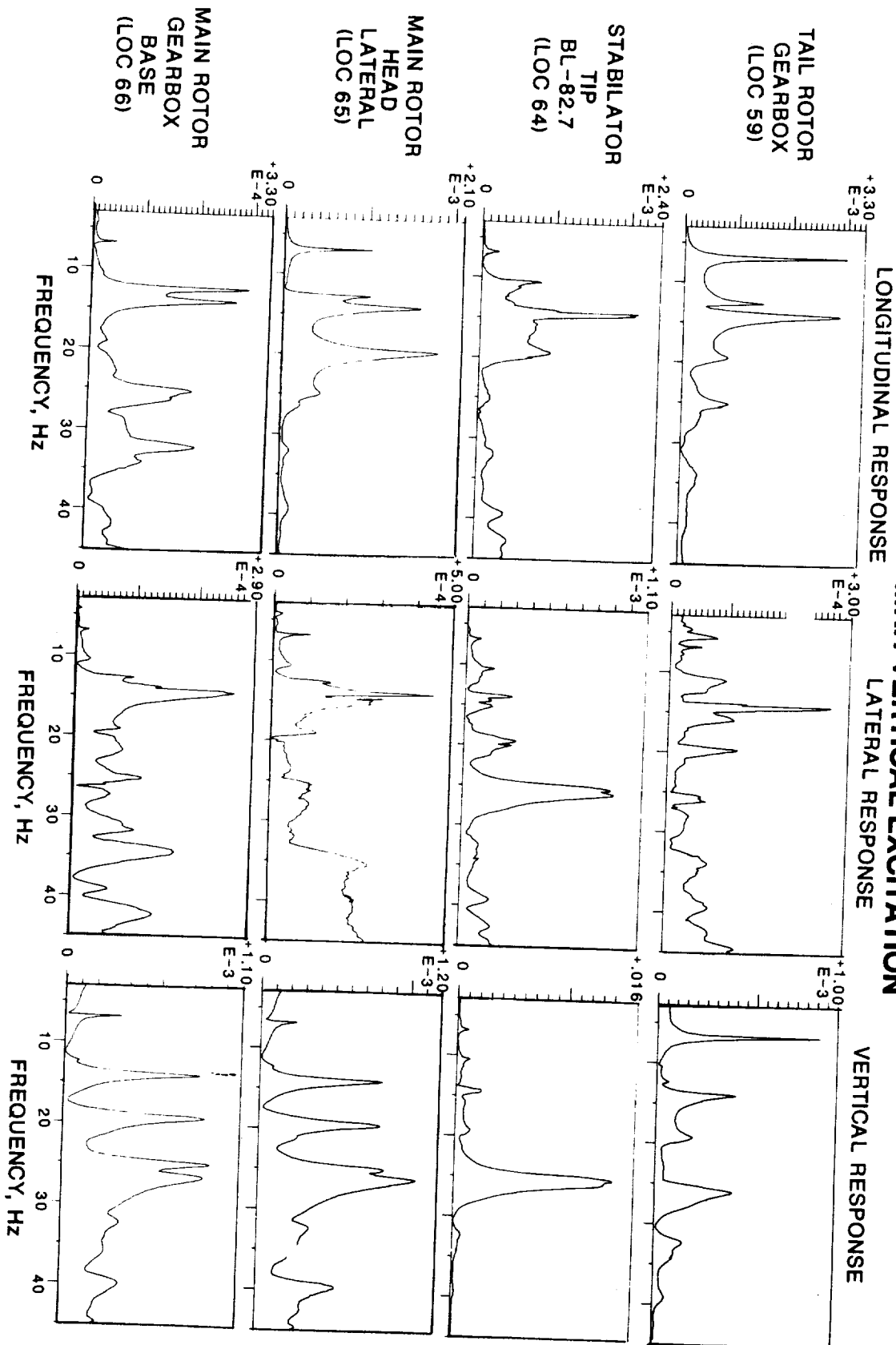


# SHAKE TEST RESULTS - FREQUENCY RESPONSE (g/lbf) MRH VERTICAL EXCITATION



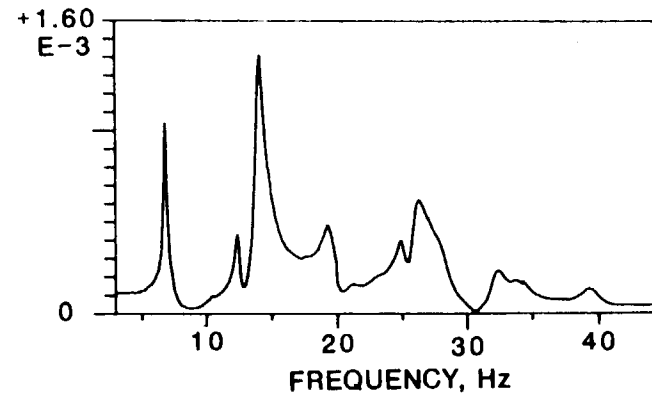
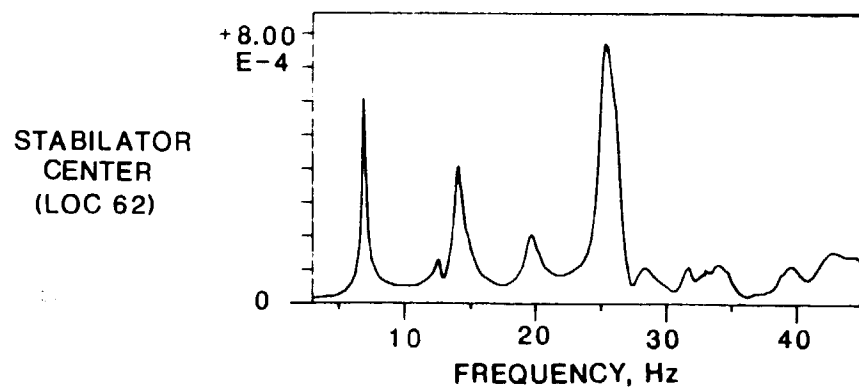
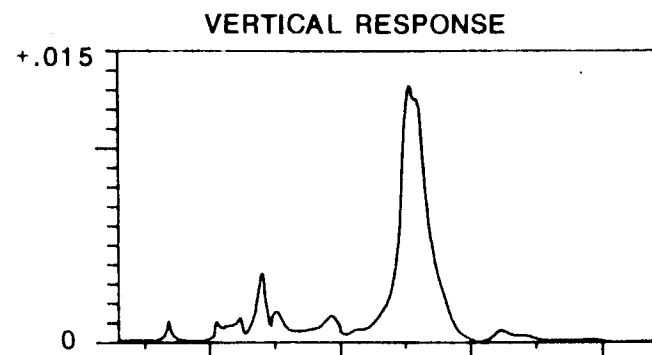
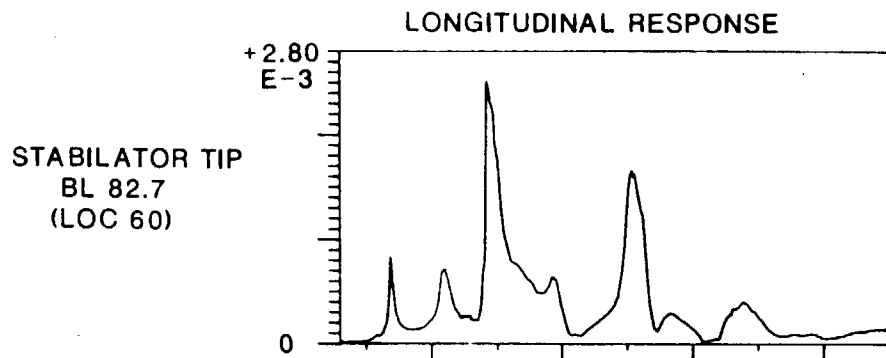
# SHAKE TEST RESULTS - FREQUENCY RESPONSE (g/ibf)

## MRH VERTICAL EXCITATION





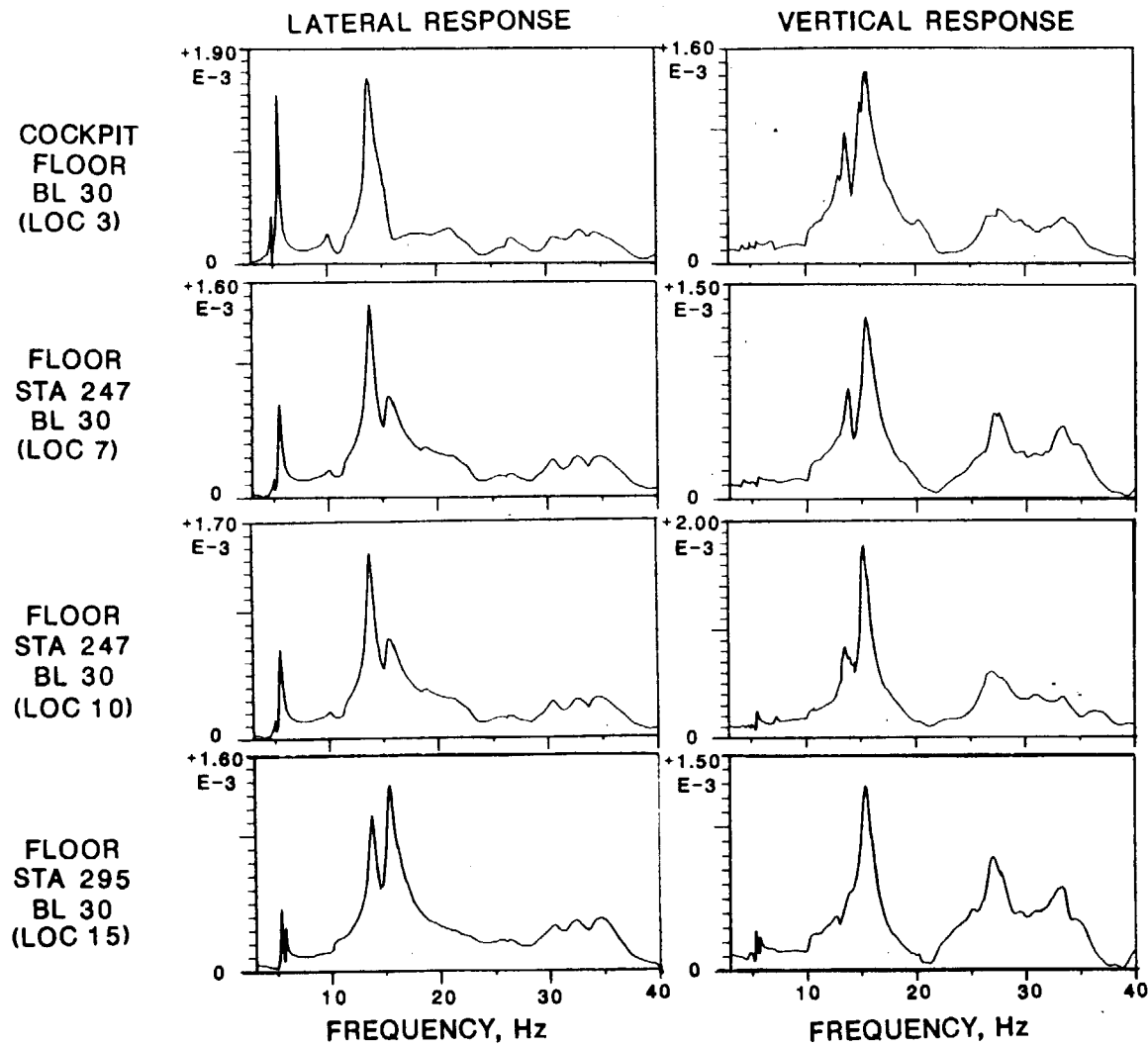
## SHAKE TEST RESULTS - FREQUENCY RESPONSE (g/lbf) MRH VERTICAL EXCITATION



SHAKE TEST RESULTS - FREQUENCY RESPONSE  
MRH LATERAL EXCITATION

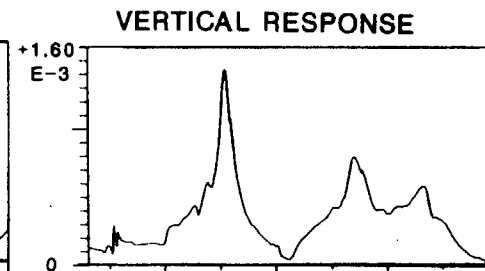
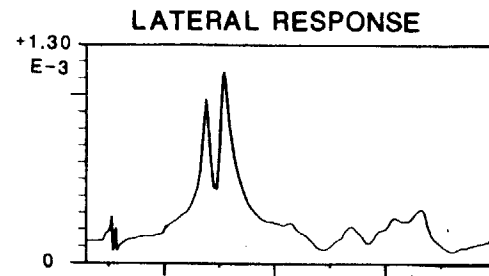
The lateral components of the responses to lateral excitation are generally an order of magnitude greater than the vertical and longitudinal components of response, again due to the near symmetry of the UH-60A fuselage. The major peaks in the lateral response are usually at 5.0/5.4 Hz, 10.6 Hz, 14.0 Hz and 15.3 Hz.

# SHAKE TEST RESULTS - FREQUENCY RESPONSE (g/lbf) MRH LATERAL EXCITATION

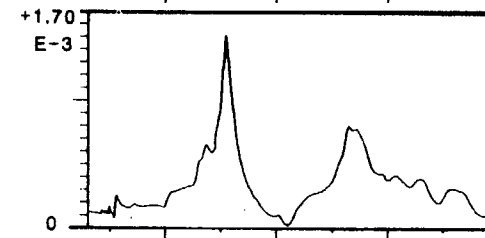


# SHAKE TEST RESULTS - FREQUENCY RESPONSE (g/lbf) MRH LATERAL EXCITATION

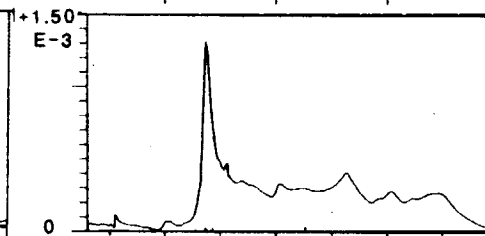
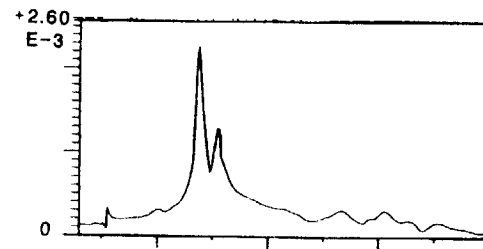
OVERHEAD  
STA 295  
BL 34.5  
(LOC 19)



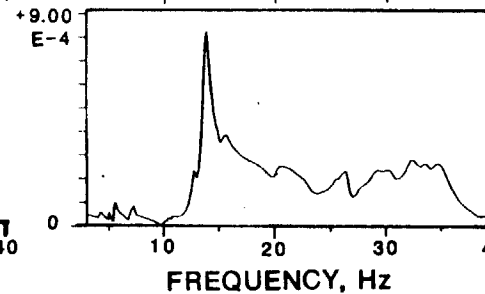
OVERHEAD  
STA 295  
BL 34.5  
(LOC 22)



XMSSN BEAM  
STA 327  
BL 16.5  
(LOC 23)



XMSSN BEAM  
STA 360  
BL 16.5  
(LOC 30)



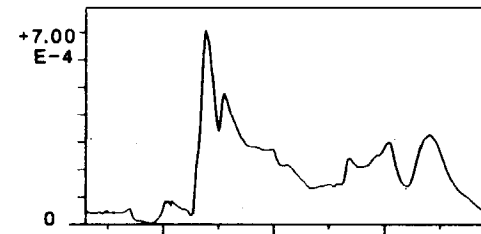
# SHAKE TEST RESULTS - FREQUENCY RESPONSE (g/lbf)

## MRH LATERAL EXCITATION

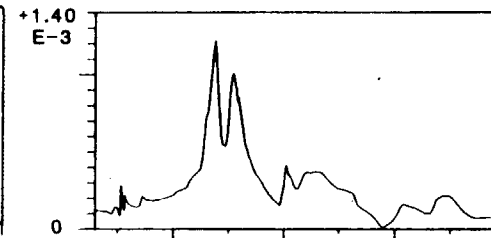
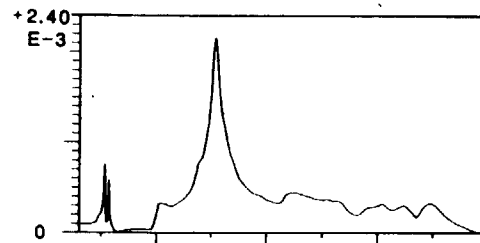
LATERAL RESPONSE

VERTICAL RESPONSE

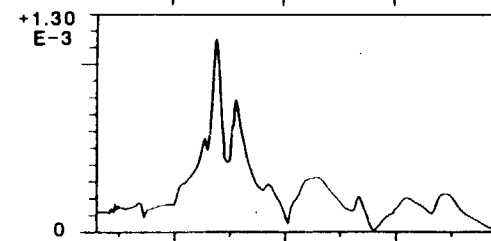
XMSSN BEAM  
STA 360  
BL 16.5  
(LOC 31)



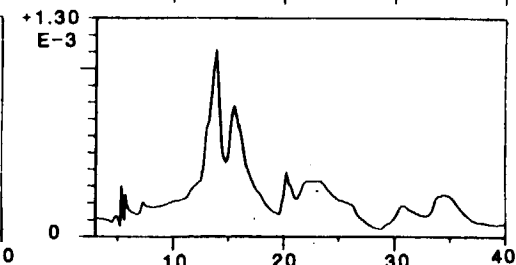
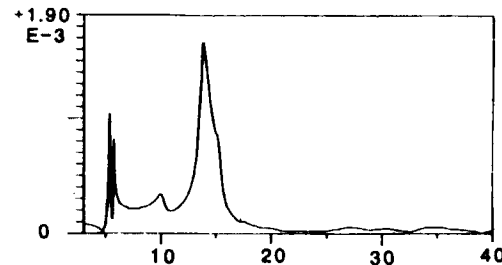
FLOOR  
STA 398  
BL 30  
(LOC 33)



FLOOR  
STA 398  
BL 30  
(LOC 36)



OVERHEAD  
STA 398  
BL 34.5  
(LOC 37)

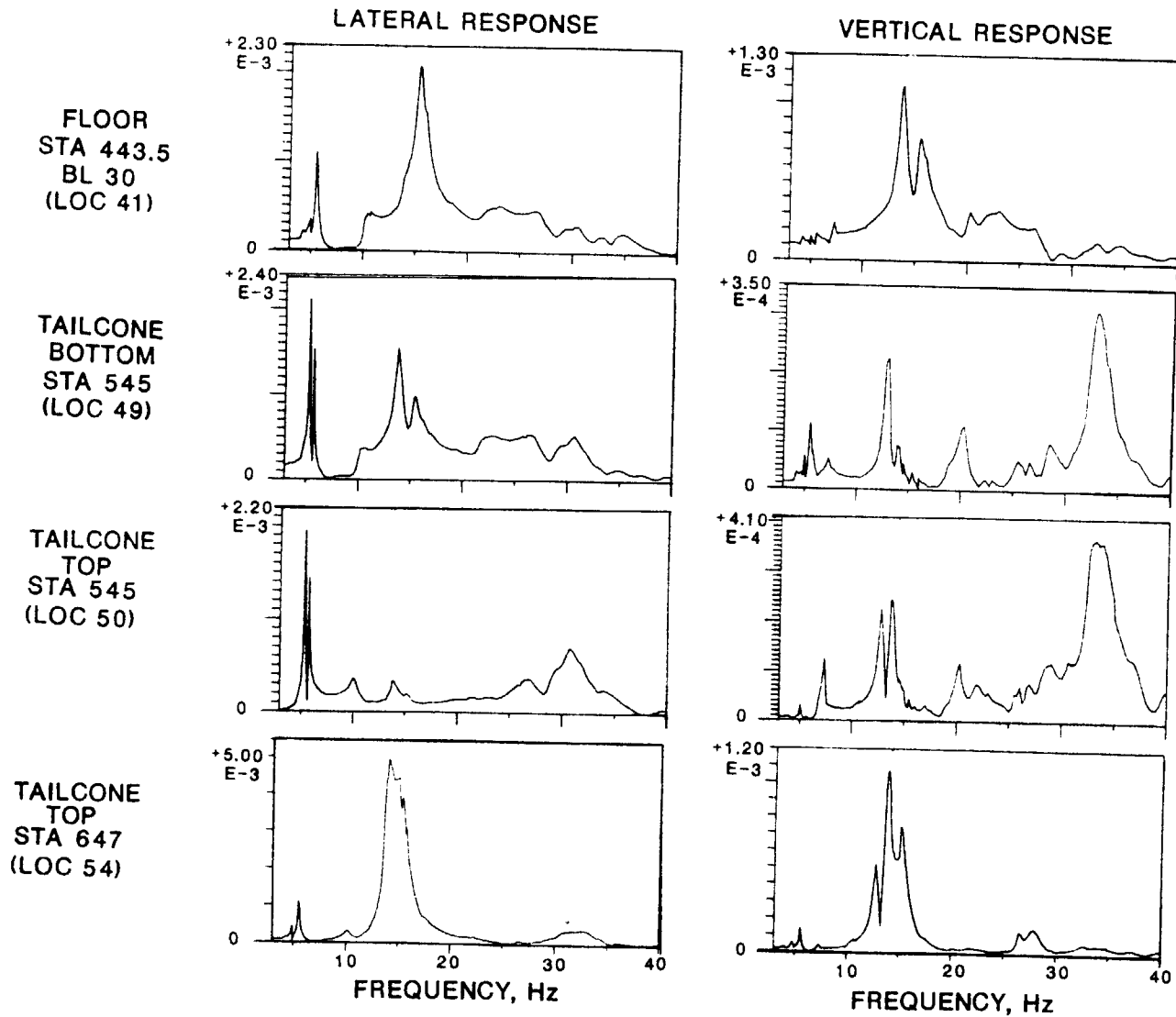


FREQUENCY, Hz

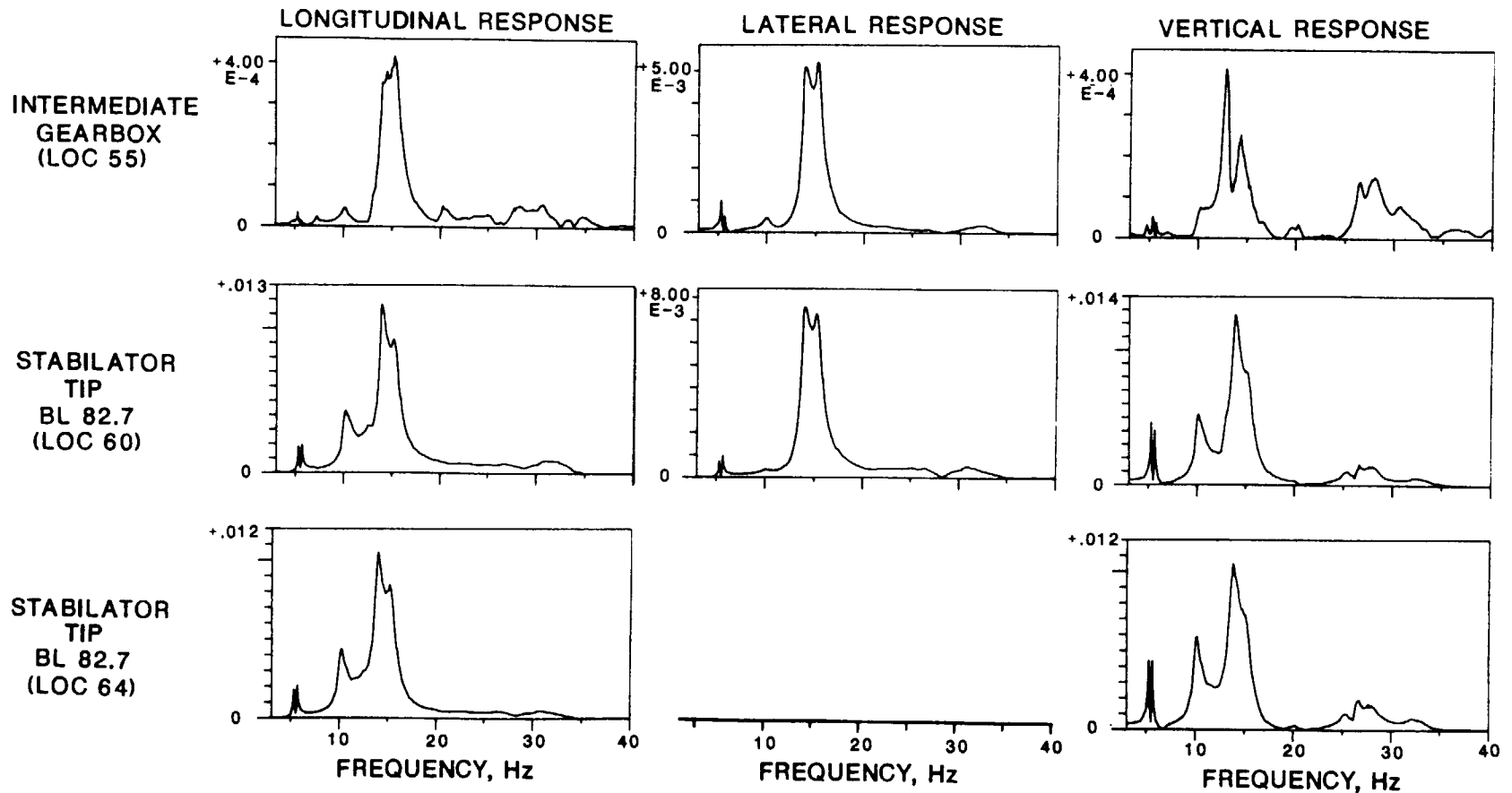
FREQUENCY, Hz

# SHAKE TEST RESULTS - FREQUENCY RESPONSE (g/lbf)

## MRH LATERAL EXCITATION

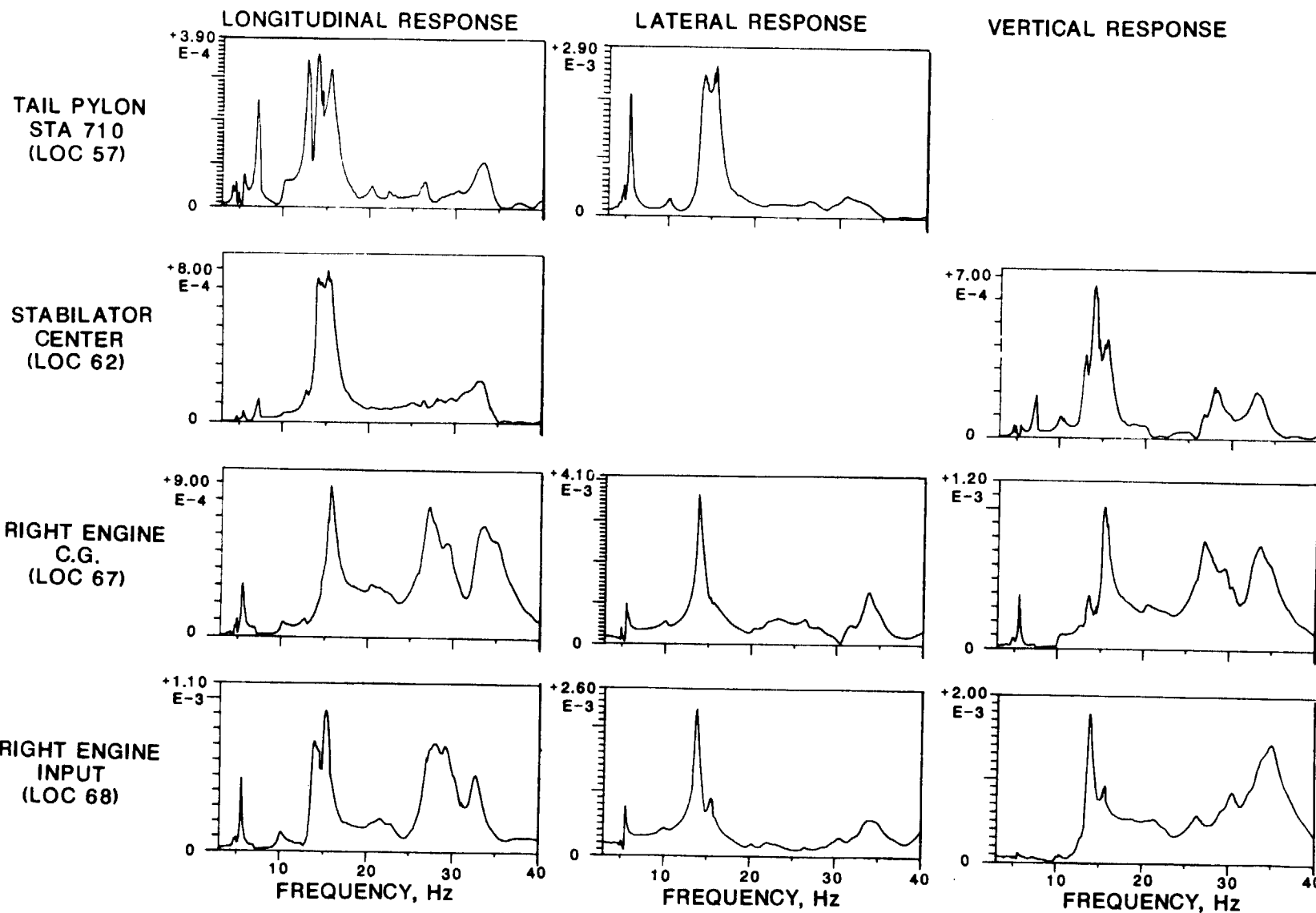


# SHAKE TEST RESULTS - FREQUENCY RESPONSE (g/lbf) MRH LATERAL EXCITATION



# SHAKE TEST RESULTS - FREQUENCY RESPONSE (g/lbf)

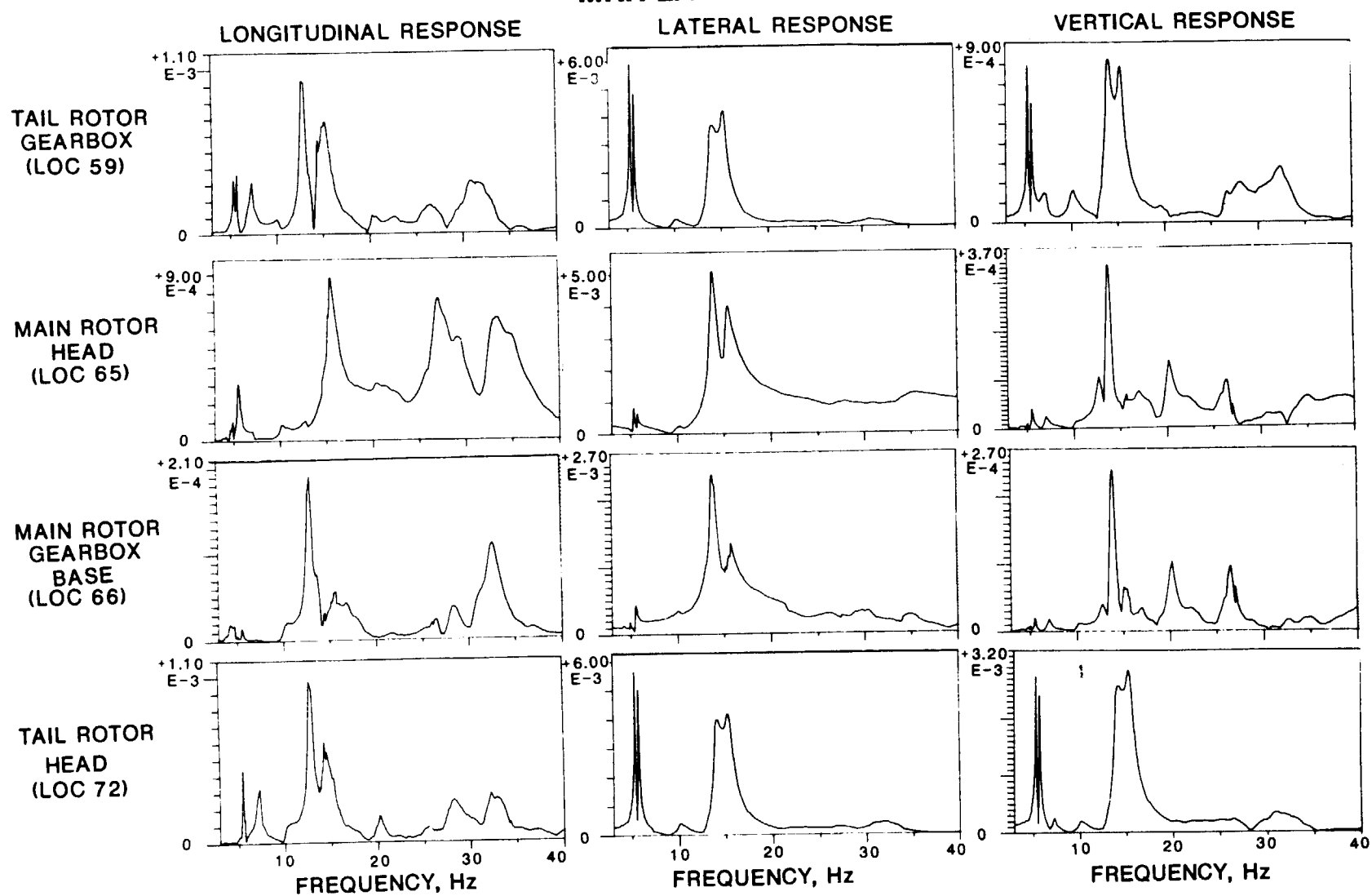
## MRH LATERAL EXCITATION





# SHAKE TEST RESULTS - FREQUENCY RESPONSE (g/lbf)

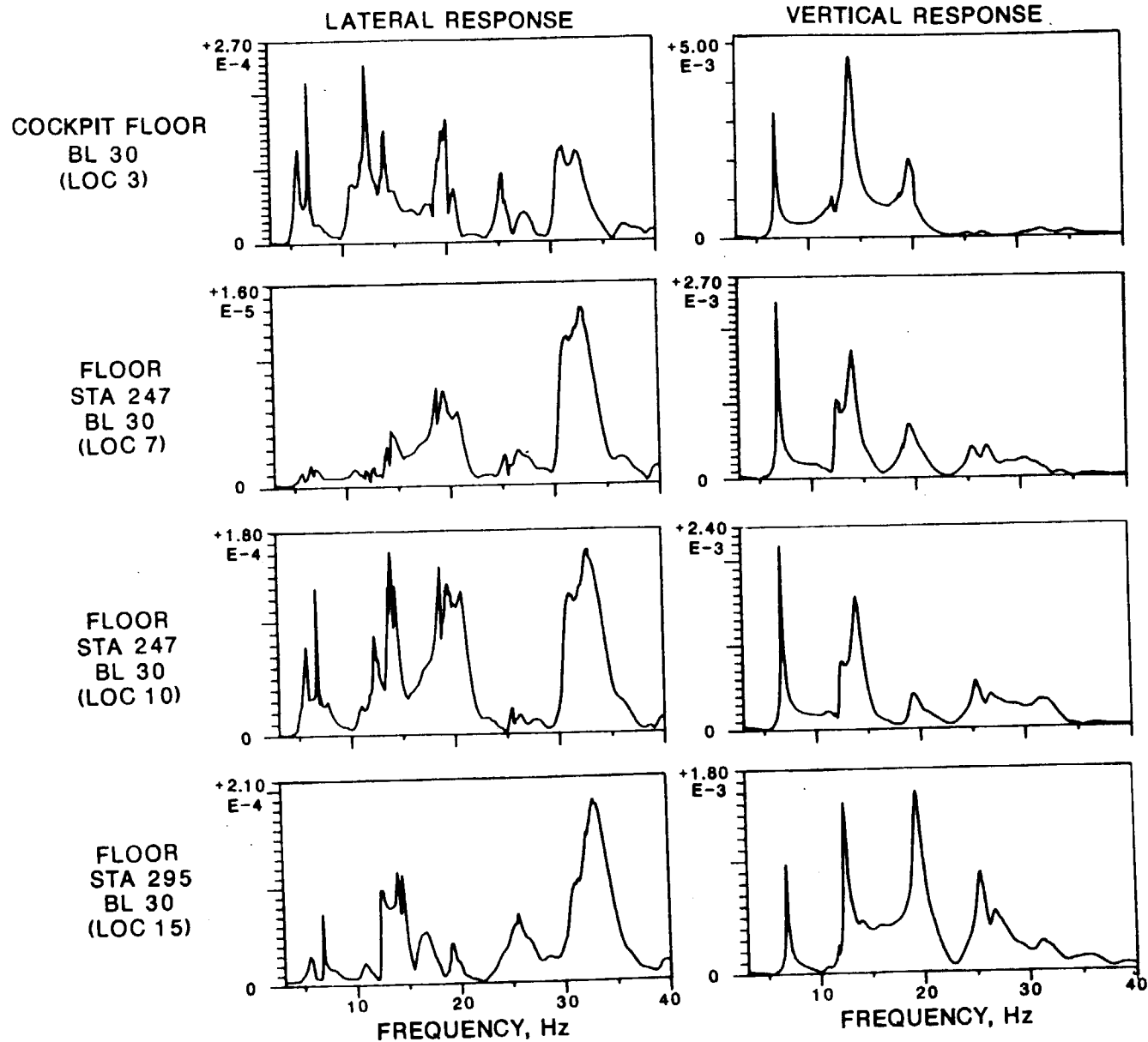
## MRH LATERAL EXCITATION



SHAKE TEST RESULTS - FREQUENCY RESPONSE  
MRH LONGITUDINAL EXCITATION

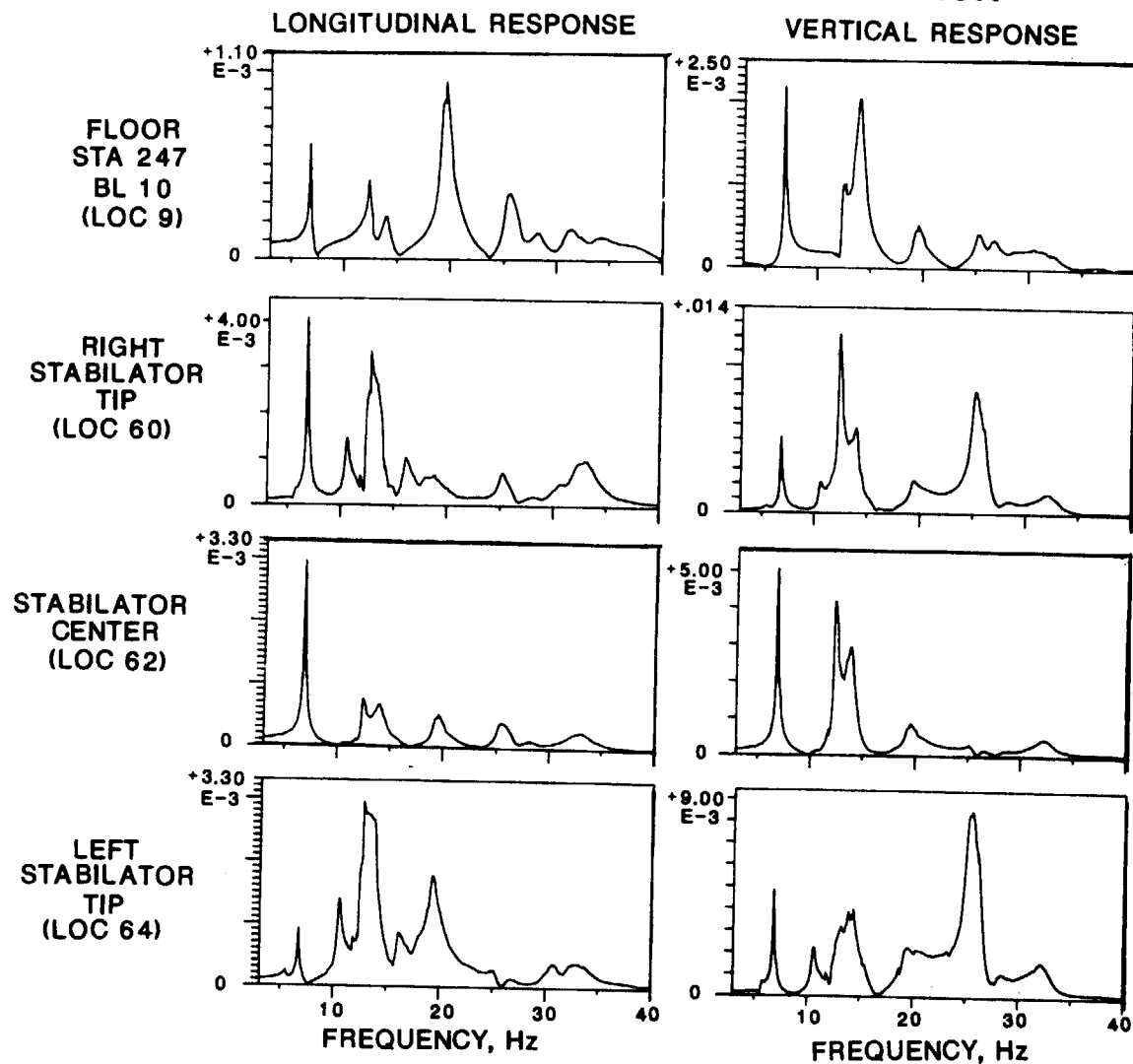
Excitation in the longitudinal direction resulted in frequency response plots similar to those obtained for vertical excitation. Some modes responded at higher levels but generally the same resonances were excited.

# SHAKE TEST RESULTS - FREQUENCY RESPONSE (g/lbf) MRH LONGITUDINAL EXCITATION

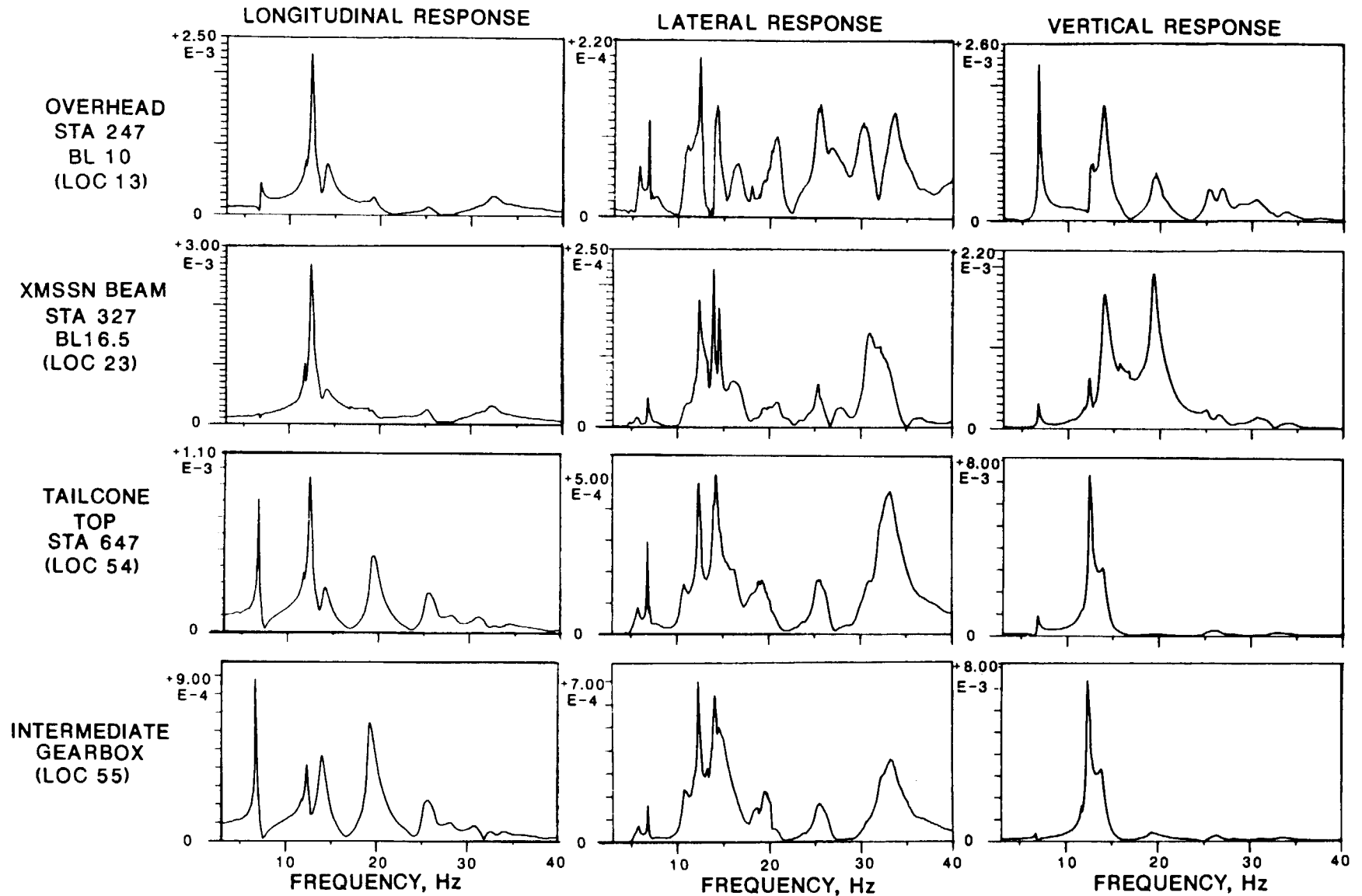


# SHAKE TEST RESULTS - FREQUENCY RESPONSE (g/lbf)

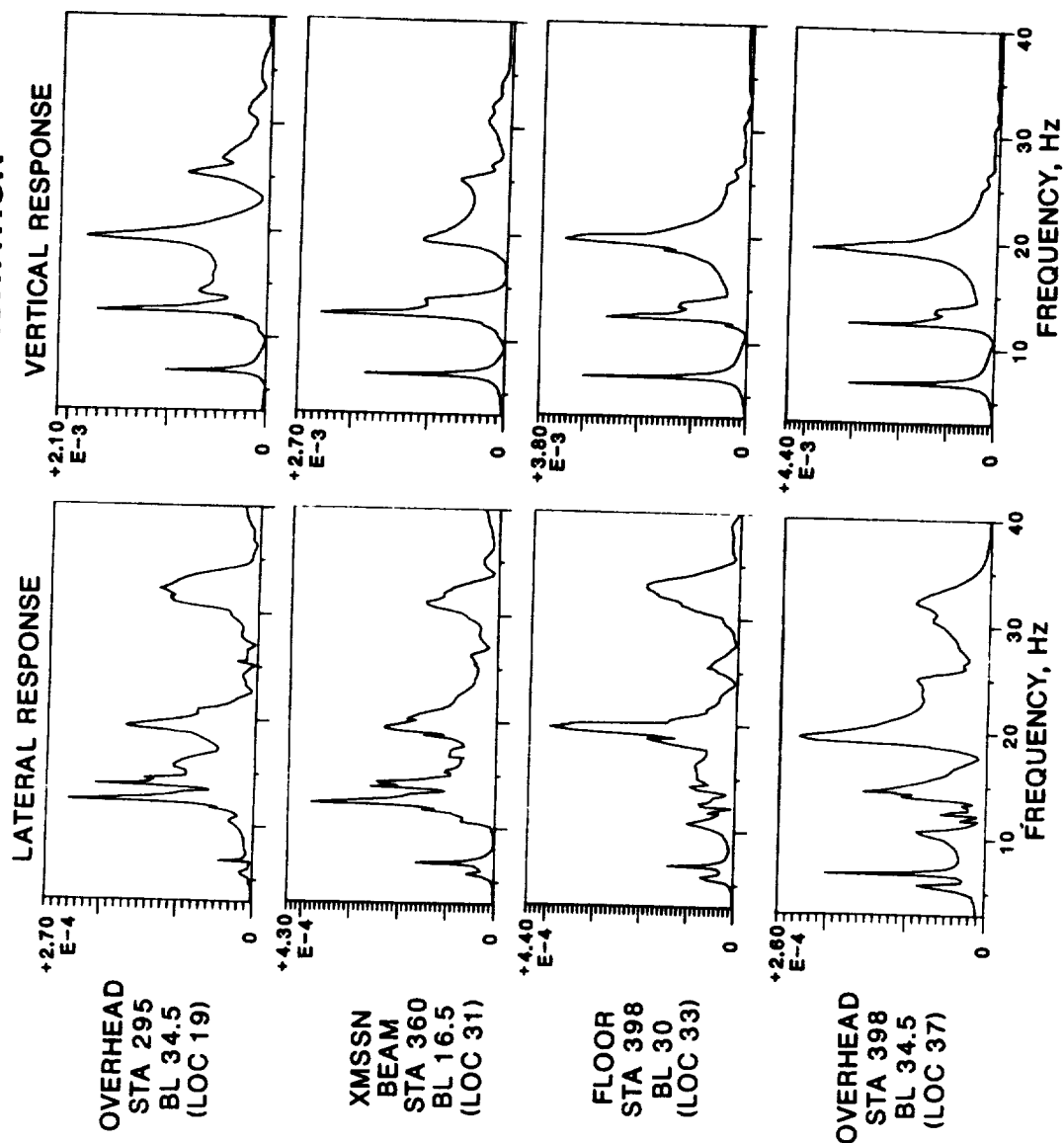
## MRH LONGITUDINAL EXCITATION



# SHAKE TEST RESULTS - FREQUENCY RESPONSE (g/lbf) MRH LONGITUDINAL EXCITATION

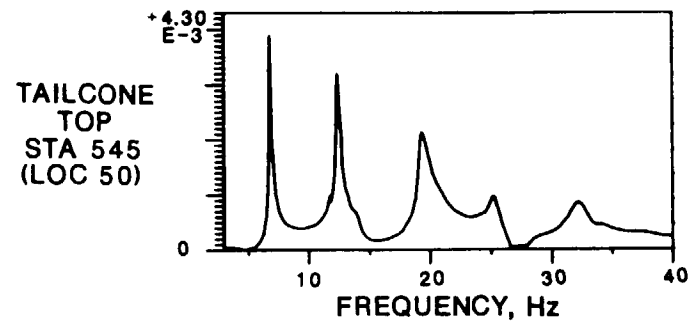
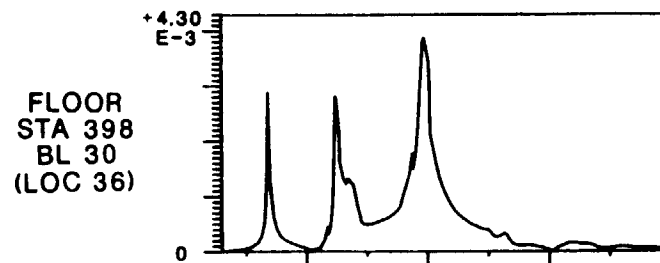
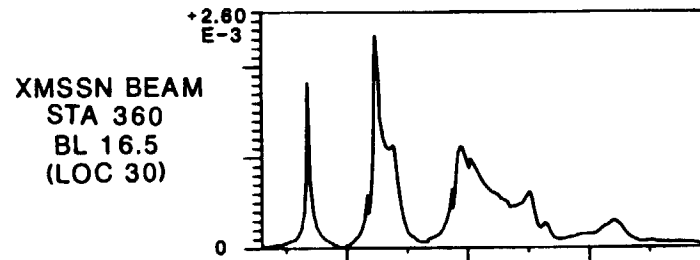
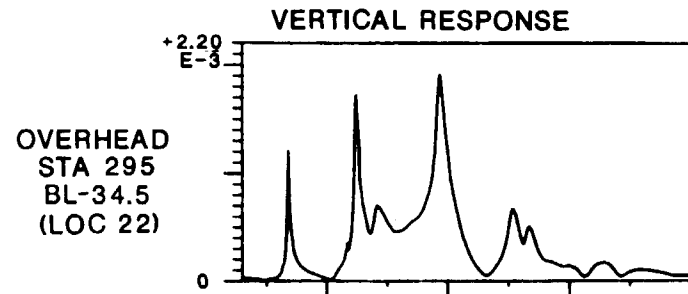


# SHAKE TEST RESULTS - FREQUENCY RESPONSE (g/lbf) MRH LONGITUDINAL EXCITATION



# SHAKE TEST RESULTS - FREQUENCY RESPONSE (g/lbf)

## MRH LONGITUDINAL EXCITATION



# SHAKE TEST RESULTS - FREQUENCY RESPONSE (g/lbf)

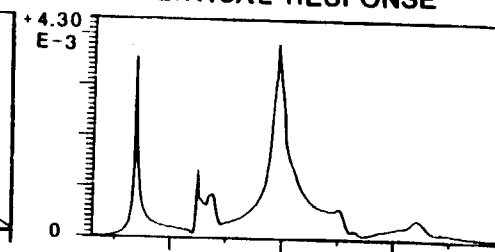
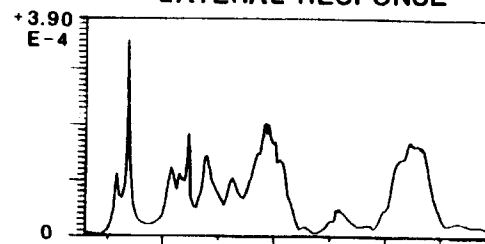
## MRH LONGITUDINAL EXCITATION

LONGITUDINAL RESPONSE

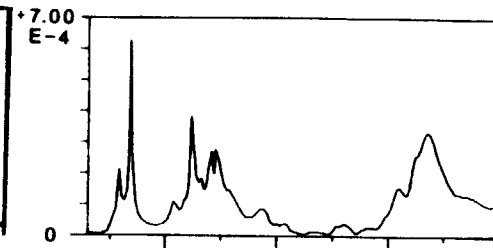
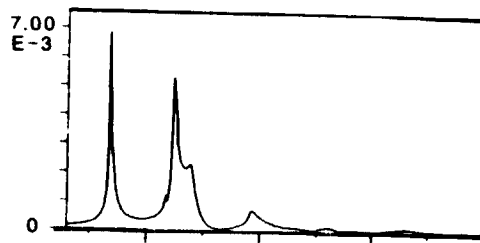
LATERAL RESPONSE

VERTICAL RESPONSE

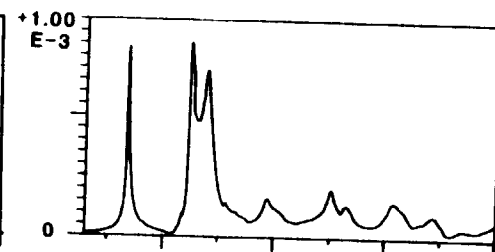
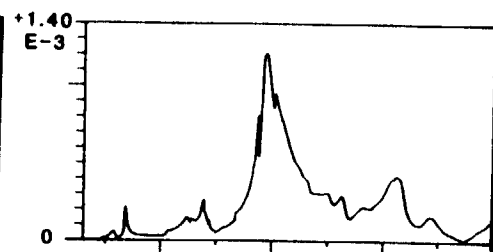
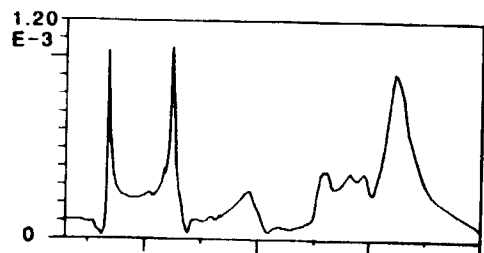
FLOOR  
STA 343.5  
BL 30  
(LOC 41)



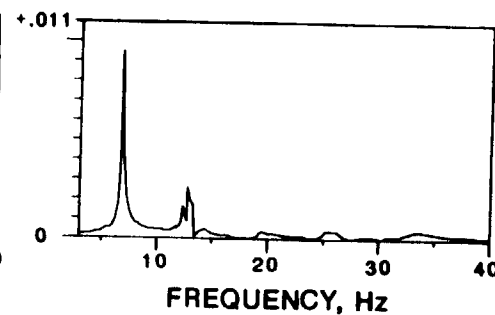
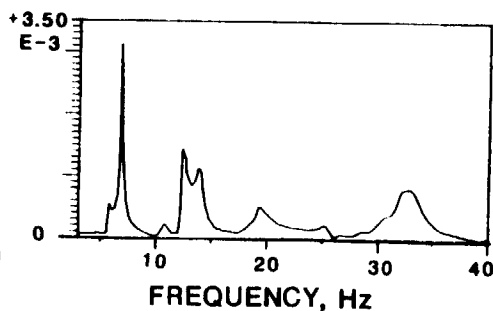
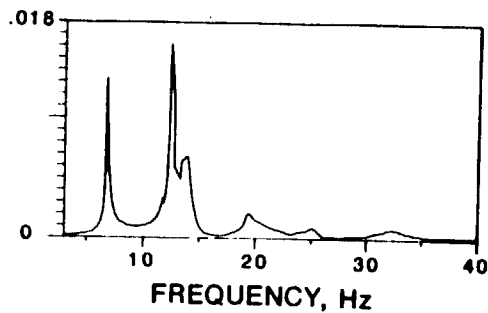
TAIL PYLON  
STA 710  
(LOC 57)



RIGHT ENGINE  
INPUT  
(LOC 68)

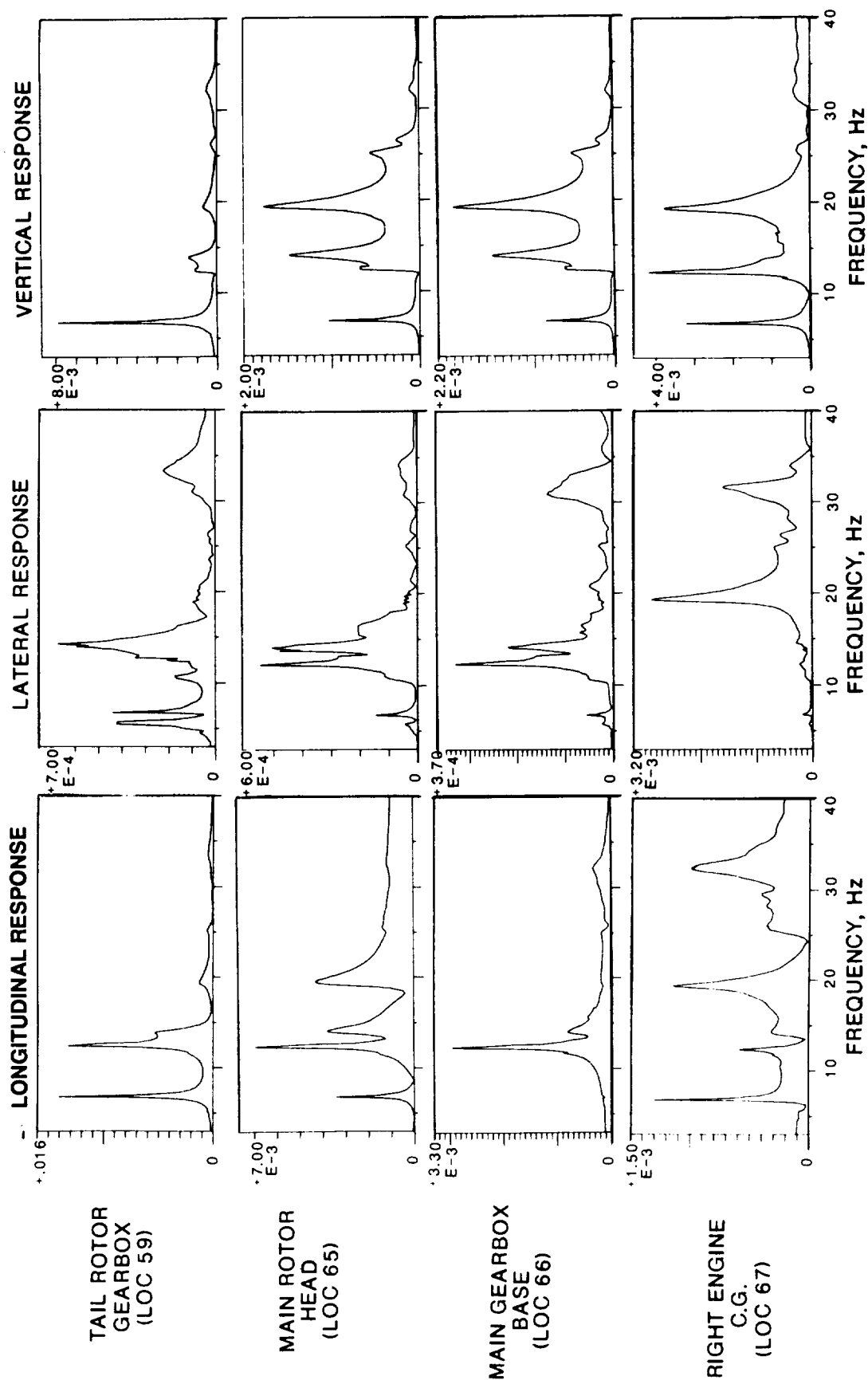


TAIL  
ROTOR HEAD  
(LOC 72)





# SHAKE TEST RESULTS - FREQUENCY RESPONSE (g/lbf) MRH LONGITUDINAL EXCITATION





# **SECTION 6.0**

## **NASTRAN ANALYSIS**

PRECEDING PAGE BLANK NOT FILMED

177

~~177~~ 176 INTENTIONALLY BLANK

## UH-60A NASTRAN MODEL

The NASTRAN finite element model of the UH-6A, which was developed in a different task under this program and is described in Reference 2, was expressly formulated for the aircraft configuration which was tested. It represents a production aircraft in an empty-weight configuration. The empty weight and center of gravity of the NASTRAN model were: 4501 kg (9923 lb.) and Station 9.14 m (360 in.) respectively. These compared well with the corresponding measured values of the test article, which were: 4599 kg (10,140 lb.) and Station 9.12m (359 in). Thus, the FEM of Ref. 2 was used without adjustment for the analytical predictions of the forced vibration response of the present test configuration.

## UH-60A NASTRAN MODEL

	<u>NASTRAN Model</u>	<u>Test Article</u> <u>(Measured Values)</u>
Empty weight	4501 Kg (9923 Lb)	4599 Kg (10,140 Lb)
Horizontal C.G.	STA 360	STA 359
Lateral C.G.	B.L. 0.09	NA
Vertical C.G.	W.L. 261	NA
Roll Inertia	4989 Kg-m <sup>2</sup>	NA
Pitch Inertia	45,573 Kg-m <sup>2</sup>	NA
Yaw Inertia	43,486 Kg-m <sup>2</sup>	NA

NASTRAN FORCED VIBRATION ANALYSIS  
DEGREES OF FREEDOM AND DAMPING USED

The NASTRAN-calculated modes of the free-free aircraft were used as degrees of freedom for the forced vibration analyses which were performed using NASTRAN Rigid Format SOL 30 (Model Forced Response). Forced vibration analyses were done using successively the first 60, 100, and 150 modes as d.o.f. Using 100 and 150 modes showed no difference. Thus the analyses were done using the first 100 modes. The modal damping values used were those obtained from the shake test, where available.

# **NASTRAN FORCED VIBRATION ANALYSIS**

## **DEGREES OF FREEDOM AND DAMPING USED**

181

- **First 100 NASTRAN-generated modes used as degrees of freedom**
- **Shake-test modal damping values used, where available**

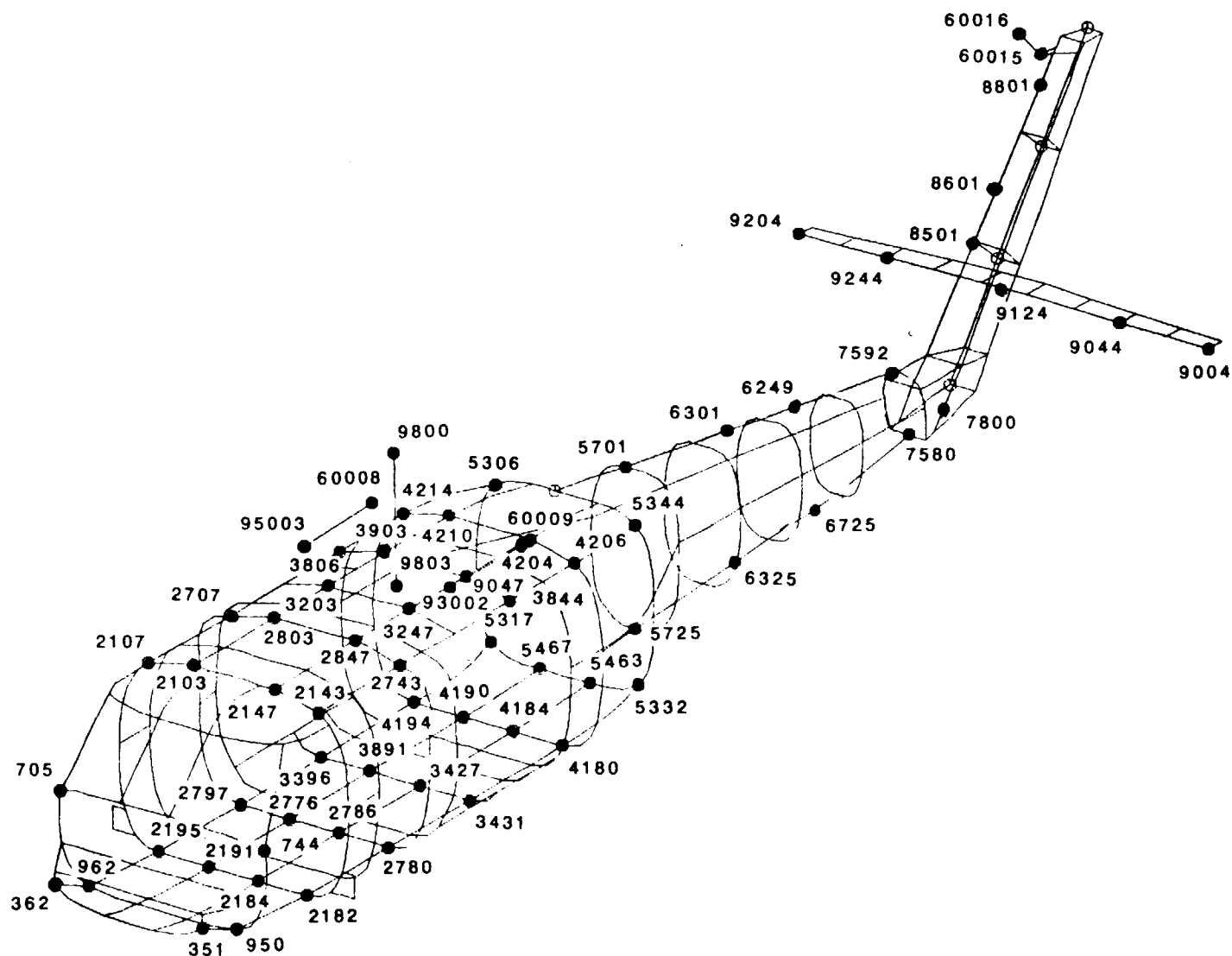
## NASTRAN FORCED VIBRATION ANALYSIS

### RESPONSE GRID POINT LOCATIONS

The frequency response was calculated by NASTRAN at GRID point locations which corresponded as closely as possible to the measured response locations. The GRID point numbers of these points are shown in the figure. The corresponding measurement point numbers are shown on page 227.



## 183





## **SECTION 7.0**

# **NASTRAN VS. SHAKE TEST: FREQUENCY RESPONSE**

## FREQUENCY RESPONSE: NASTRAN VERSUS SHAKE TEST

The following figures show a representative comparison between the UH-60A frequency response functions measured in shake test and the corresponding functions as predicted by NASTRAN. Data are presented for three excitation directions, and response comparisons are given at the main rotor head (MRH), cockpit right hand side (CPIT-RT), main rotor shaft bottom (MRSB), stabilator left tip (STAB-LT), forward cabin floor-STA 295 (295-FLR) and tail rotor gearbox (TRGB). The response comparisons are made in terms of linear amplitude and phase angle vs. forcing frequency.

## **FREQUENCY RESPONSE: NASTRAN VS. SHAKE TEST**

- Data presented for three excitation directions
- Data presented for six response locations

- Cockpit - right side	CPIT-RT
- Station 295 - floor	295-FLR
- Main rotor head	MRH
- Main rotor shaft base	MRSB
- Tail rotor gear box	TRGB
- Stabilator - left tip	STAB-LT

## UH-60A Frequency Response: NASTRAN Versus Shake Test

### Main Rotor Head Longitudinal Excitation Response at Main Rotor Head (MRH)

This plot illustrates the frequency response of the main rotor head due to a longitudinal force. The first bending vertical mode shows good agreement between the test and analysis. This plot helps to identify the transmission pitch mode vs the 2nd vertical bending mode. Transmission pitch is seen to be off in frequency (12%) and magnitude. The second vertical bending mode also has considerable error in both frequency and amplitude. The third vertical mode shows reasonable agreement considering its high frequency. NASTRAN shows a resonance region around 23 Hz that is not obvious in the test results. Examination of this region shows that the high NASTRAN response is due to the presence of three closely spaced modes that are mostly cabin torsion and vertical modes.

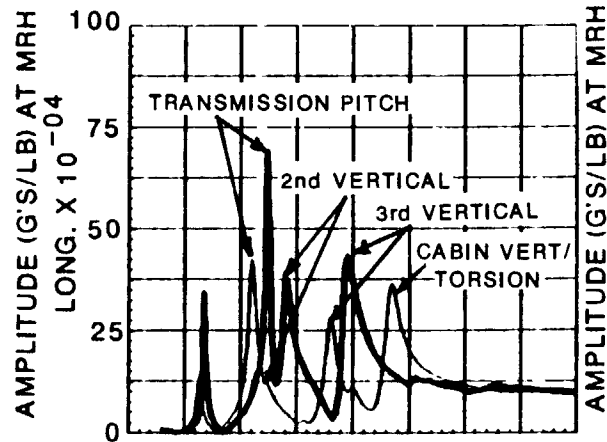
# UH-60A FREQUENCY RESPONSE: NASTRAN VERSUS SHAKE TEST

## MRH LONG. EXCITATION

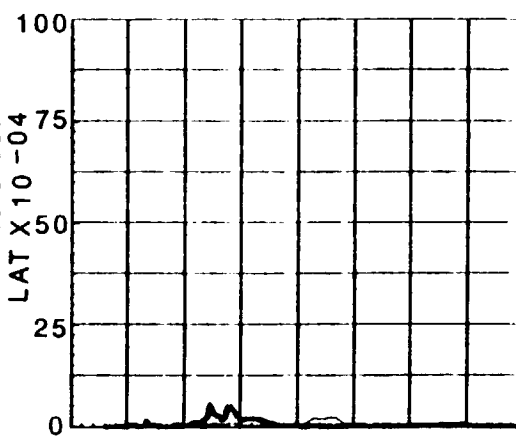
### RESPONSE AT MRH

— ANALYSIS  
— TEST

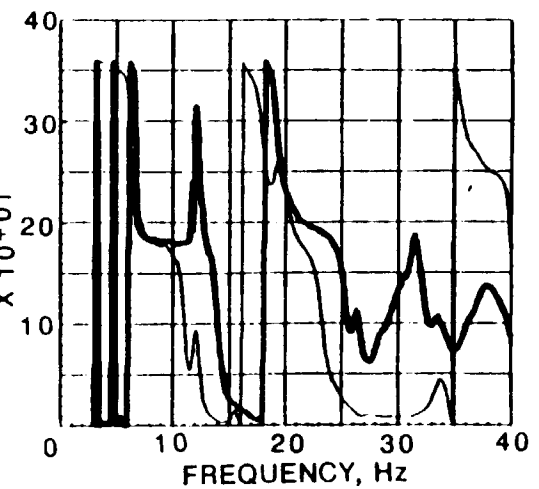
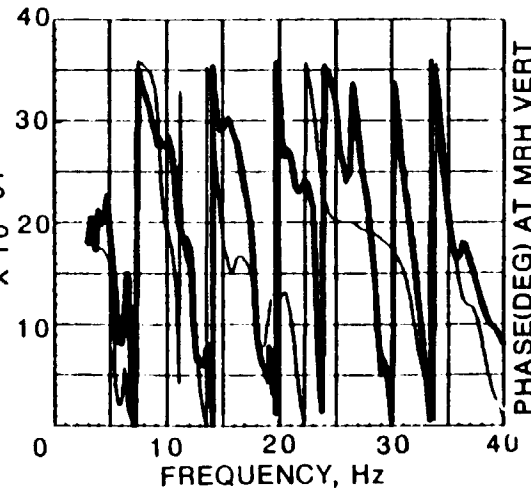
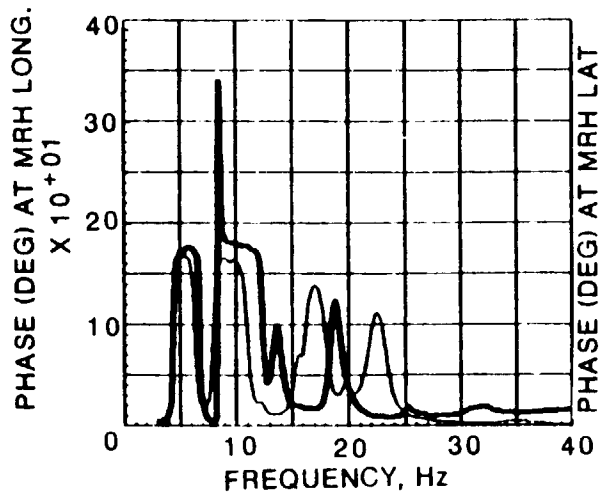
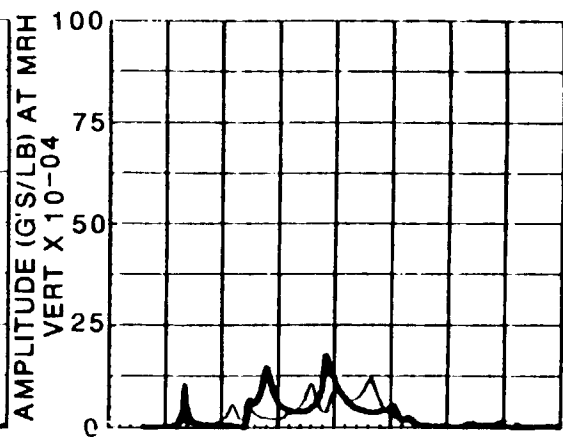
#### LONGITUDINAL RESPONSE



#### LATERAL RESPONSE



#### VERTICAL RESPONSE



## UH-60A Frequency Response: NASTRAN Versus Shake Test

### Main Rotor Head Longitudinal Excitation Response at Main Rotor Shaft Base (MRSB)

The longitudinal response of the main rotor shaft base shows the test and analysis peaks for the transmission pitch mode to be similar to the previous plot. The test transmission pitch mode response appears to dominate over the frequency spectrum so other modes are not well defined here.

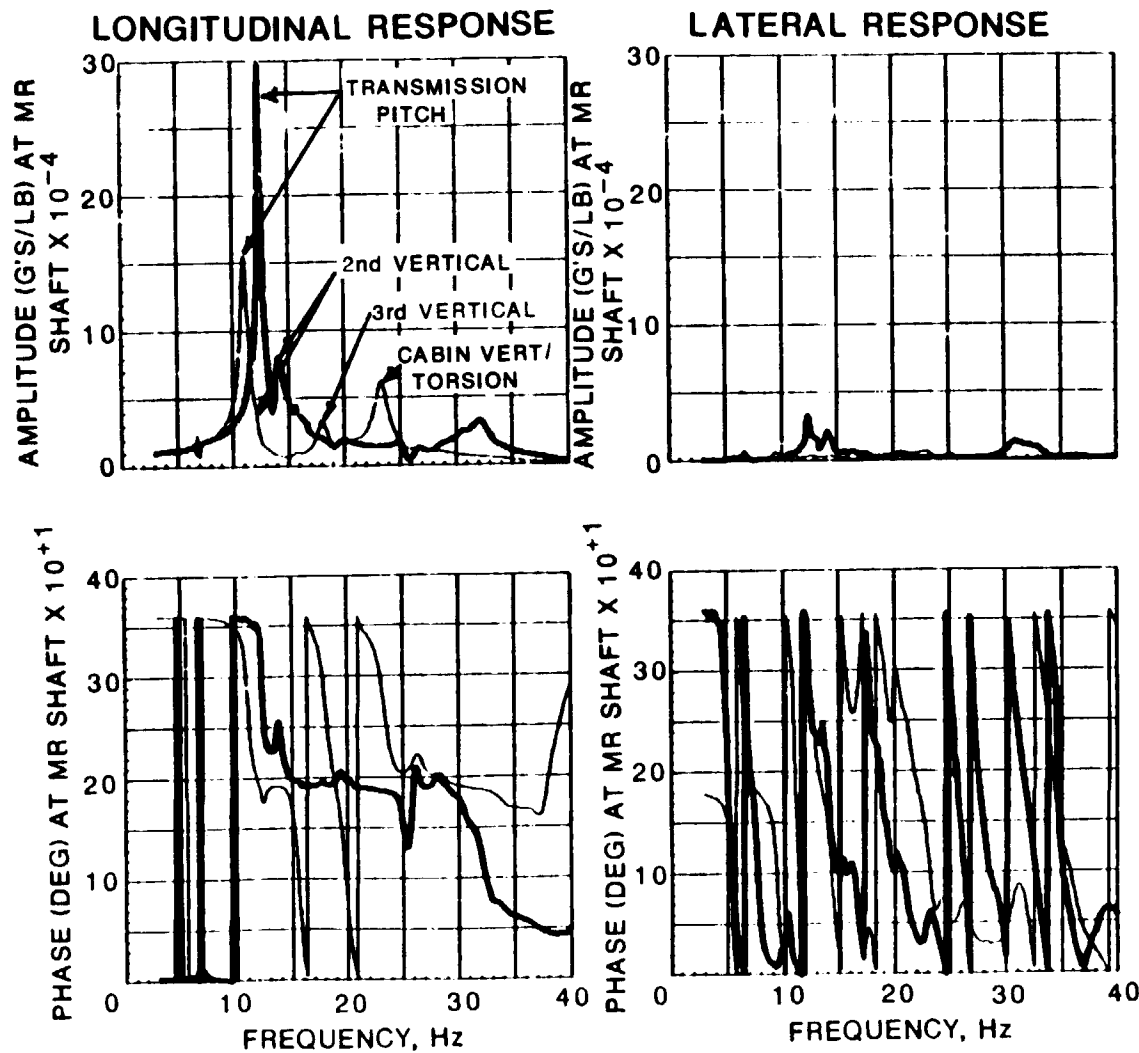


# UH-60A FREQUENCY RESPONSE: NASTRAN VERSUS SHAKE TEST

## MRH LONG. EXCITATION

### RESPONSE LOCATION: MRSB

— ANALYSIS  
— TEST



## UH-60A Frequency Response: NASTRAN Versus Shake Test

### Main Rotor Head Longitudinal Excitation Response at Cockpit Floor Right (CPIT-RT)

The plot below of the cockpit floor response to a longitudinal excitation shows poor agreement for the transmission pitch mode. The amplitude of the 2nd bending mode response is again greater from test than analysis. The 3rd vertical mode agrees quite well in amplitude at this location.

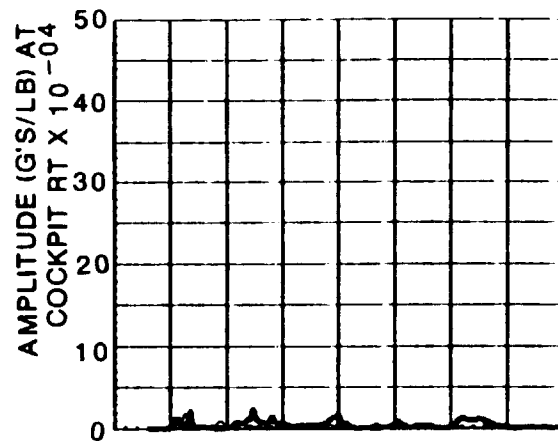
# UH-60A FREQUENCY RESPONSE: NASTRAN VERSUS SHAKE TEST

## MRH LONG. EXCITATION

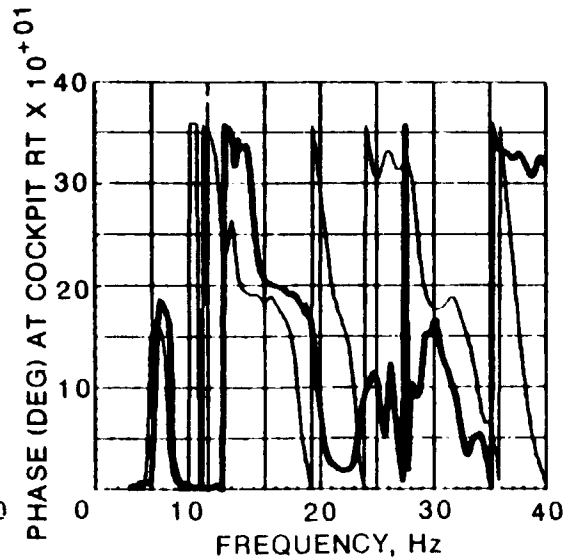
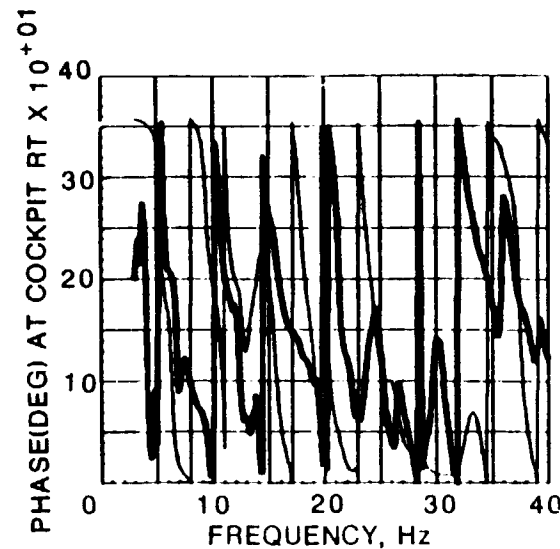
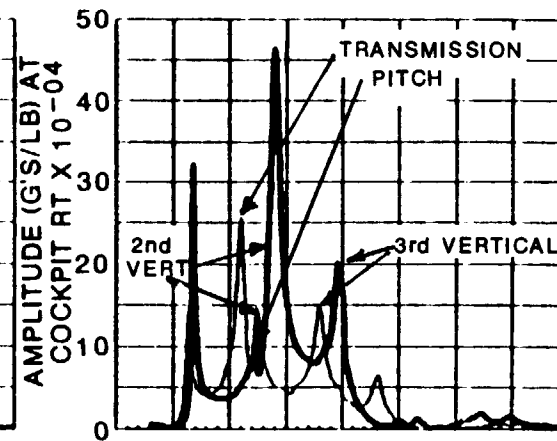
### RESPONSE LOCATION: CPIT-RT

— ANALYSIS  
— TEST

#### LATERAL RESPONSE



#### VERTICAL RESPONSE



## UH-60A Frequency Response: NASTRAN Versus Shake Test

### Main Rotor Head Longitudinal Excitation Response at Station 295 Floor Right (CPIT-RT)

The station 295 floor (mid-cabin) vertical response shown below shows better agreement than some of the previous comparisons. The amplitude of the transmission pitch and 3rd vertical mode responses agree well between test and analysis. The 2nd vertical mode is at a node point at this location in both test and analysis and shows little response. The NASTRAN cabin vertical and torsion mode at 23 Hz appears to be similar to the 25 Hz test mode but the mode shape presented later show these modes to be much different.

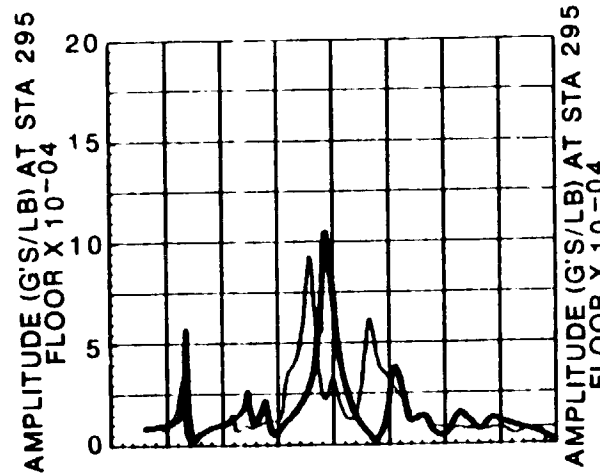
# UH-60A FREQUENCY RESPONSE: NASTRAN VERSUS SHAKE TEST

## MRH LONG. EXCITATION

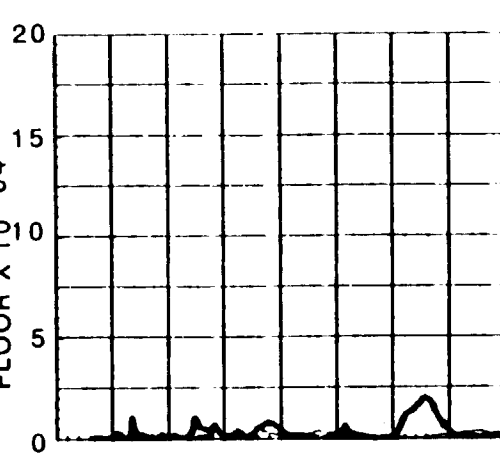
### RESPONSE LOCATION: 295-FLR

— ANALYSIS  
— TEST

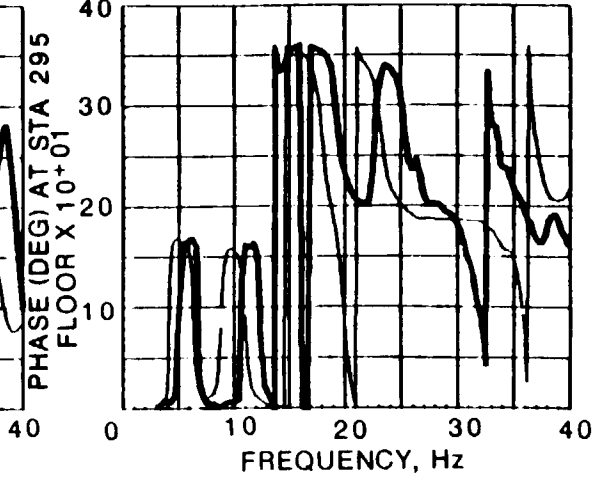
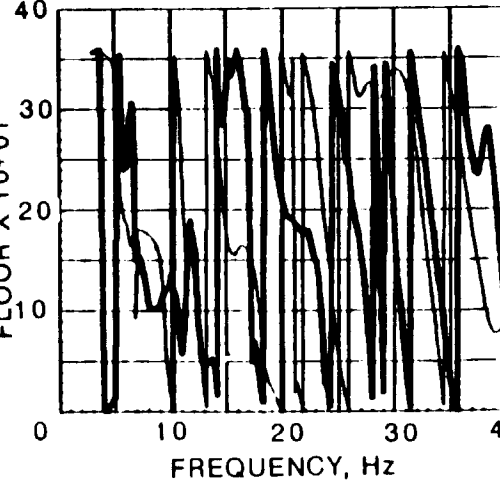
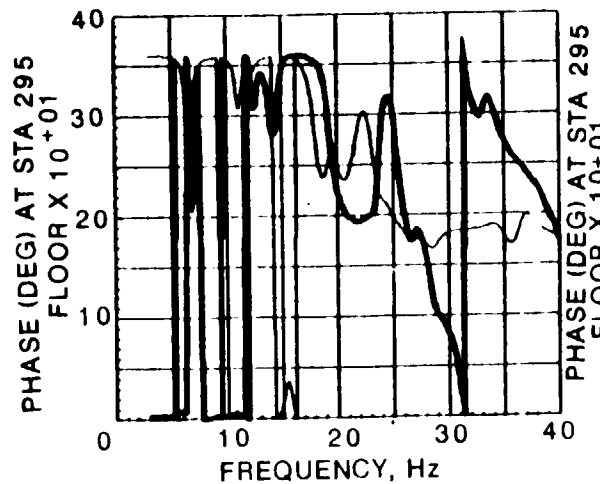
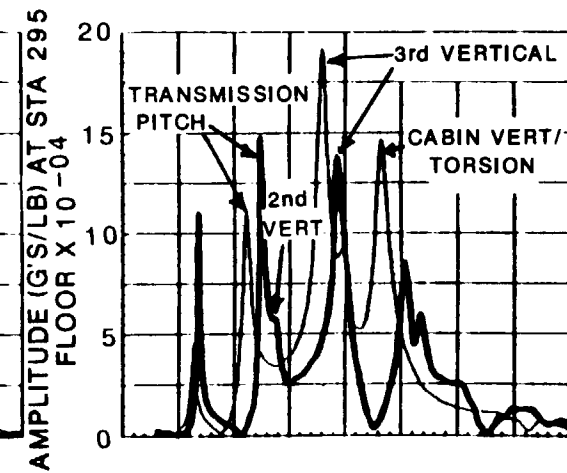
#### LONGITUDINAL RESPONSE



#### LATERAL RESPONSE



#### VERTICAL RESPONSE



## UH-60A Frequency Response: NASTRAN Versus Shake Test

### Main Rotor Head Longitudinal Excitation Response at Stabilator Tip Left (STAB-LT)

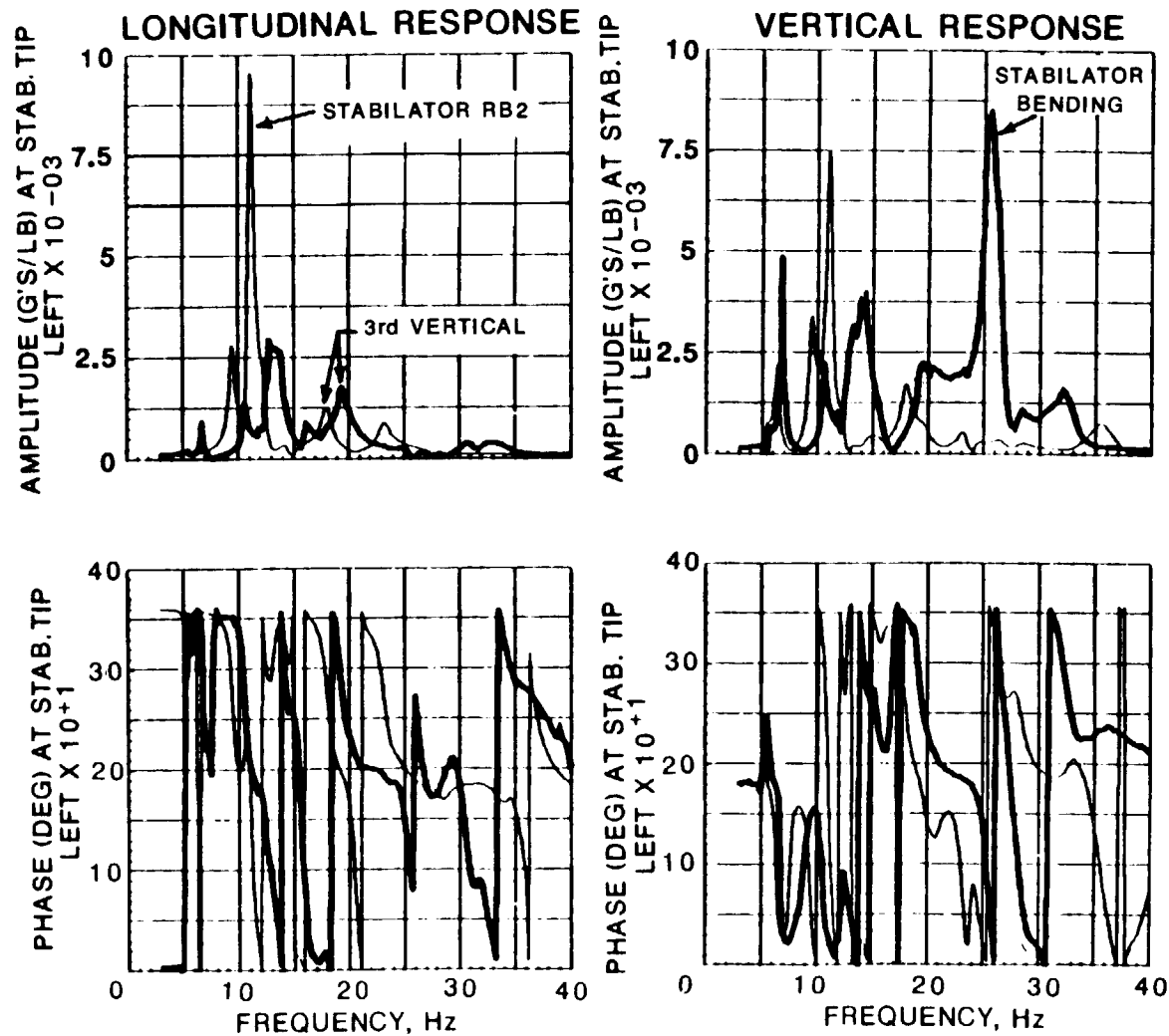
The stabilator tip response presented below shows that NASTRAN predicts higher response amplitudes than measured in test for the stabilator rigid body modes around 10 Hz. The NASTRAN model does not predict the stabilator bending mode at 25 Hz which is seen in the stabilator vertical response.

# UH-60A FREQUENCY RESPONSE: NASTRAN VERSUS SHAKE TEST

## MRH LONG. EXCITATION

### RESPONSE LOCATION: STAB.-LT

— ANALYSIS  
— TEST



## UH-60A Frequency Response: NASTRAN Versus Shake Test

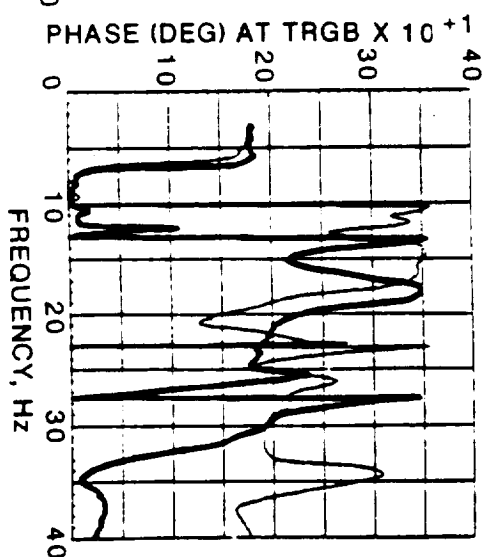
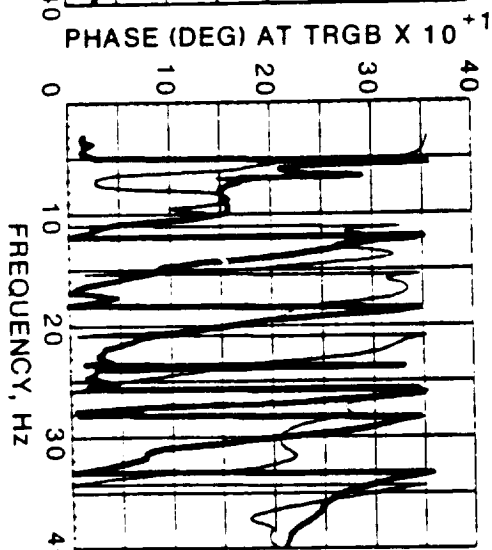
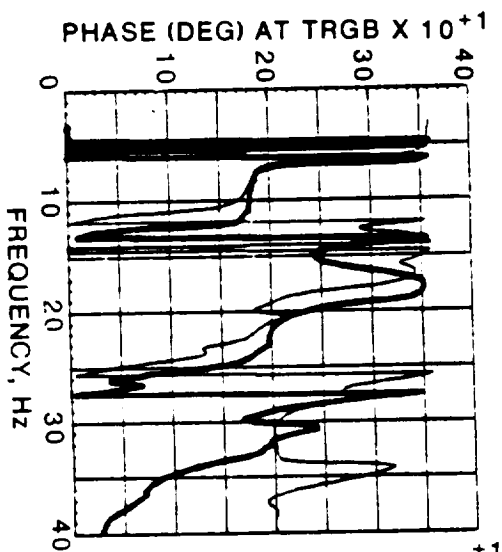
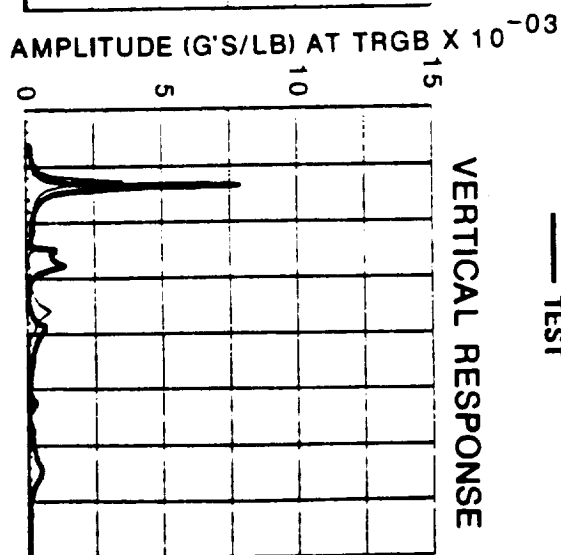
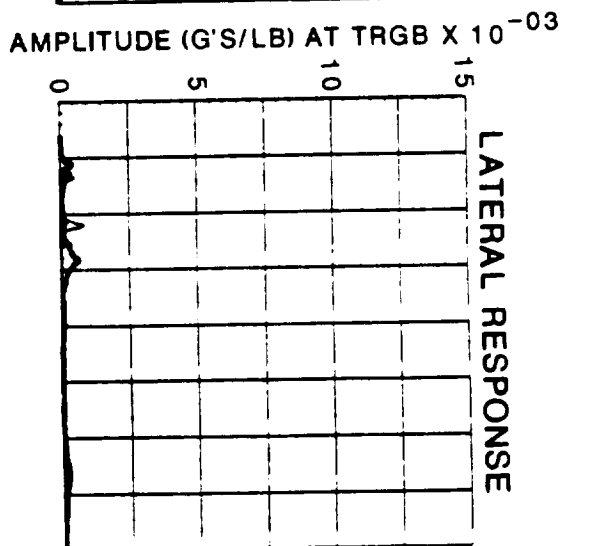
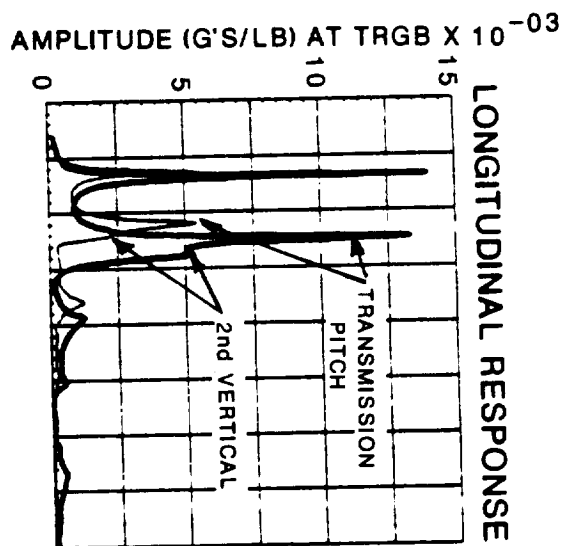
### Main Rotor Head Longitudinal Excitation Response at Tail Rotor Gearbox (TRGB)

The tail rotor gearbox frequency response comparison shows similar results to previous plots when looking at the transmission pitch, 2nd vertical and 3rd vertical bending modes.



# UH-60A FREQUENCY RESPONSE: NASTRAN VERSUS SHAKE TEST MRH LONG. EXCITATION RESPONSE LOCATION: TRGB

— ANALYSIS  
— TEST



## UH-60A Frequency Response: NASTRAN Versus Shake Test

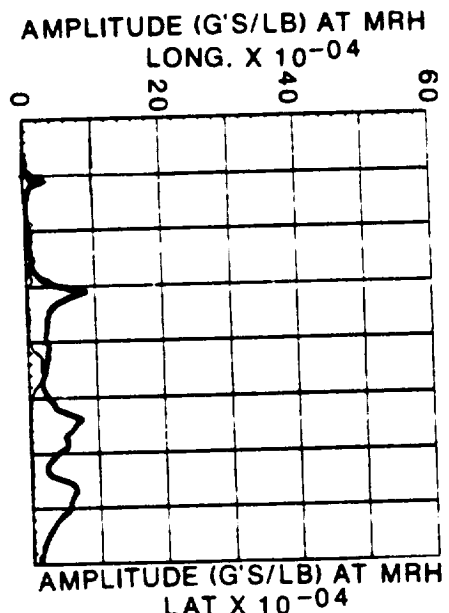
### Main Rotor Head Lateral Excitation Response at Main Rotor Head (MRH)

The main rotor hub lateral response appears to be dominated by two similar modes in both the analysis and test frequency response functions shown in this figure. With close examination of the mode shapes, the test mode at 13.8 Hz appears to be a coupled transmission roll and 2nd lateral mode. From the NASTRAN analysis, there are actually two modes, one at 12.7 Hz (transmission roll) and another at 15.3 Hz (2nd lateral). The cockpit cabin torsion mode at 15.4 Hz from test and 14.5 Hz from NASTRAN have reasonably good frequency agreement (6%) but are off in magnitude when compared to the transmission roll mode.

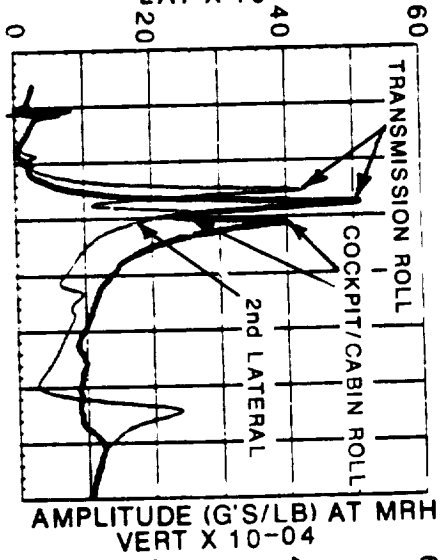
# UH-60A FREQUENCY RESPONSE: NASTRAN VERSUS SHAKE TEST MRH LAT. EXCITATION RESPONSE LOCATION: MRH

— ANALYSIS  
 — TEST

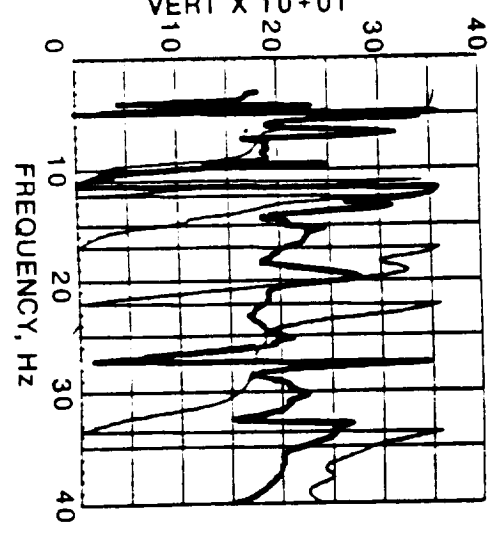
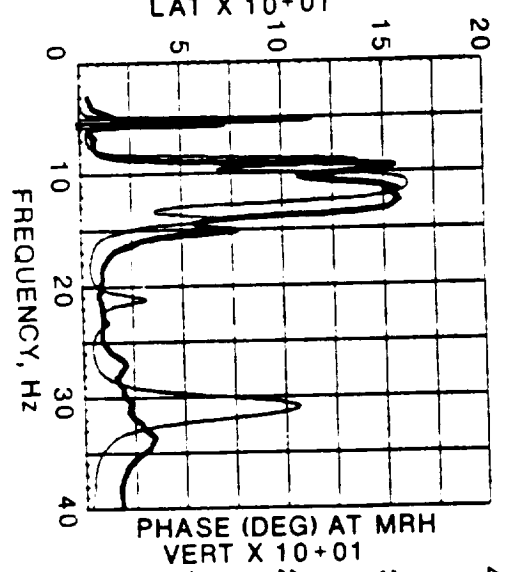
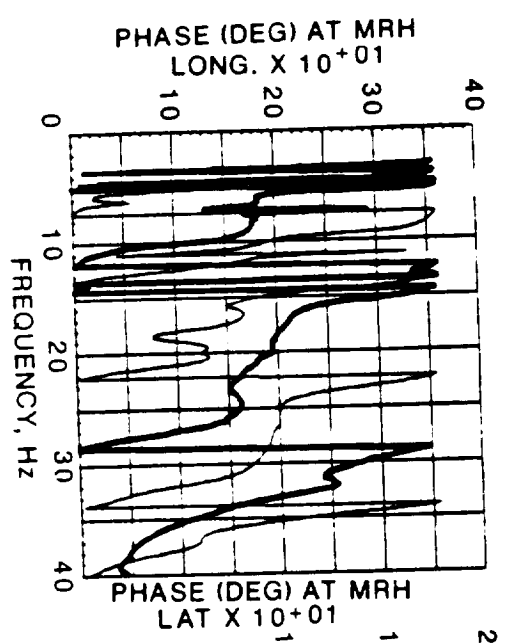
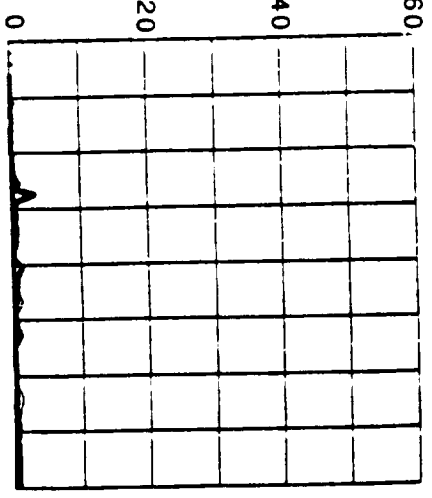
LONGITUDINAL RESPONSE



LATERAL RESPONSE



VERTICAL RESPONSE



## UH-60A Frequency Response: NASTRAN Versus Shake Test

### Main Rotor Head Lateral Excitation Response at Main Rotor Shaft Base (MRSB)

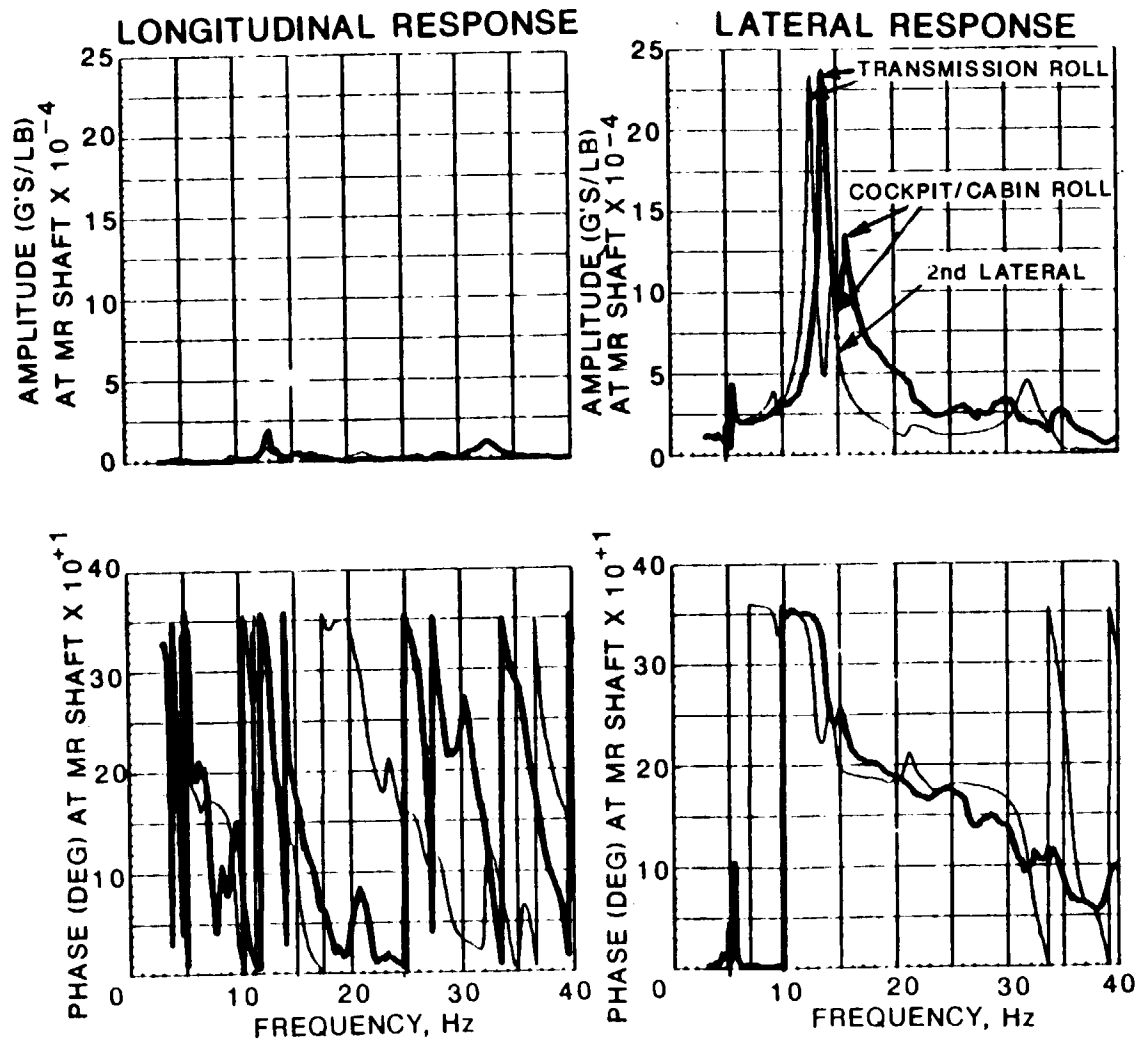
The bottom of the main rotor shaft response is very similar to the hub response although the transmission roll mode is somewhat stronger.

# UH-60A FREQUENCY RESPONSE: NASTRAN VERSUS SHAKE TEST

## MRH LAT. EXCITATION

### RESPONSE LOCATION: MRSB

— ANALYSIS  
— TEST



## UH-60A Frequency Response: NASTRAN Versus Shake Test

### Main Rotor Head Lateral Excitation Response at Cockpit Floor Right (CPIT-RT)

The cockpit floor lateral response in the accompanying figure shows the separation of the transmission roll and 2nd lateral modes in NASTRAN while only one mode appears from test. The cockpit floor vertical response shows very good agreement for the cockpit / cabin roll mode.

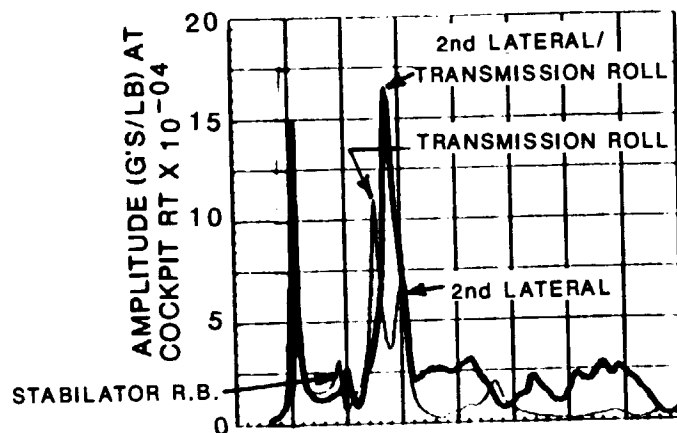
# UH-60A FREQUENCY RESPONSE: NASTRAN VERSUS SHAKE TEST

## MRH LAT. EXCITATION

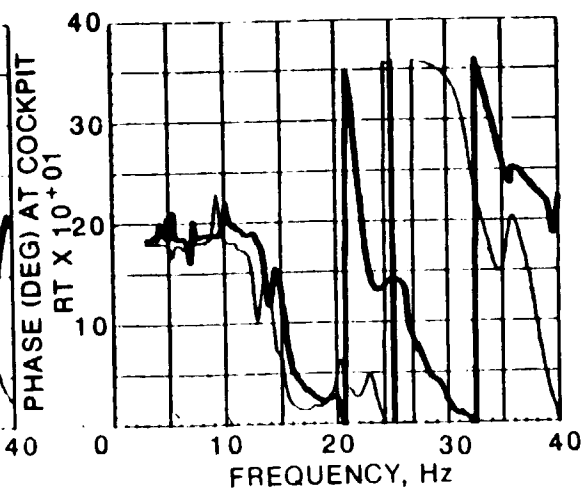
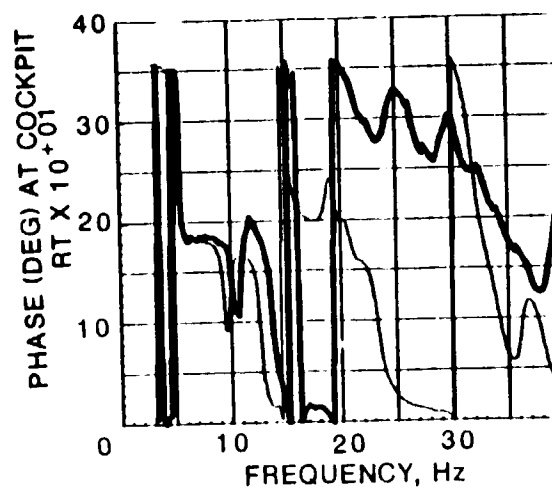
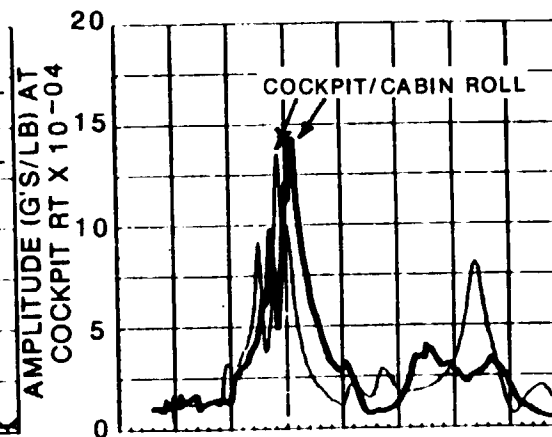
### RESPONSE LOCATION: CPIT-RT

— ANALYSIS  
— TEST

#### LATERAL RESPONSE



#### VERTICAL RESPONSE



## UH-60A Frequency Response: NASTRAN Versus Shake Test

### Main Rotor Head Lateral Excitation Response at Station 295 Floor Right (CPIT-RT)

The station 295 floor vertical response again shows good agreement for the cockpit / cabin roll mode. Some higher frequency modes are evident in both the test and analysis data. The mode shapes of these higher frequency modes are often cabin torsion and vertical and are difficult to match NASTRAN and test modes.

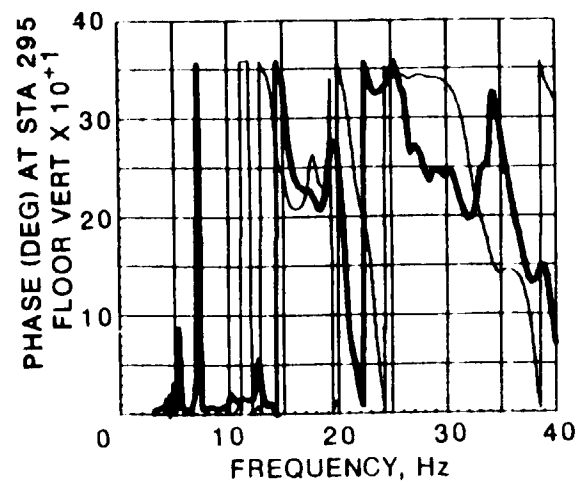
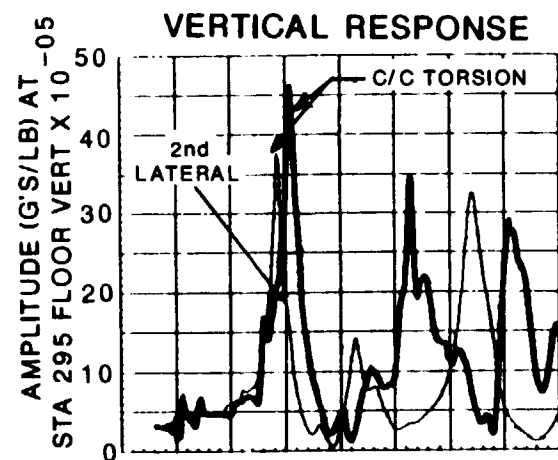


# UH-60A FREQUENCY RESPONSE: NASTRAN VERSUS SHAKE TEST

## MRH LAT. EXCITATION

### RESPONSE LOCATION: 295-FLR

— ANALYSIS  
— TEST



## UH-60A Frequency Response: NASTRAN Versus Shake Test

### Main Rotor Head Lateral Excitation Response at Stabilator Tip Left (STAB-LT)

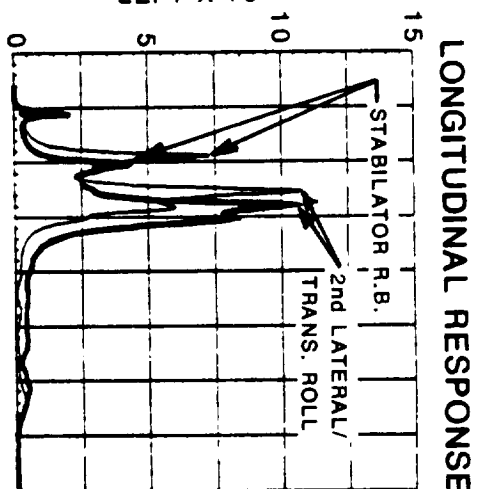
The left stabilator tip response is presented in the accompanying figure. Comparisons between test and analysis for both the stabilator rigid body and the 2nd lateral modes are illustrated. Normally, NASTRAN tends to under-predict the test in both frequency and amplitude. The amplitude of the NASTRAN response for both these modes, in both the longitudinal and vertical response directions, is greater than the test amplitude.

# UH-60A FREQUENCY RESPONSE: NASTRAN VERSUS SHAKE TEST MRH LAT. EXCITATION

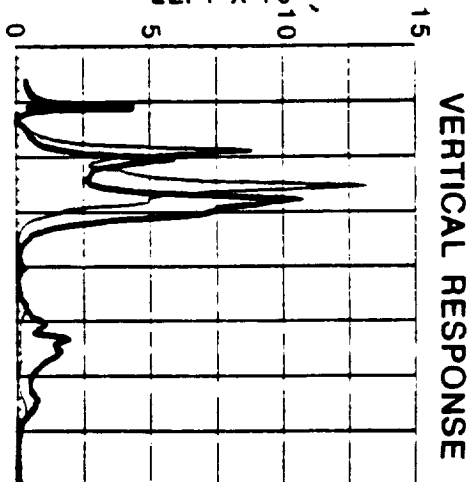
RESPONSE LOCATION: STAB.-LT

— ANALYSIS  
— TEST

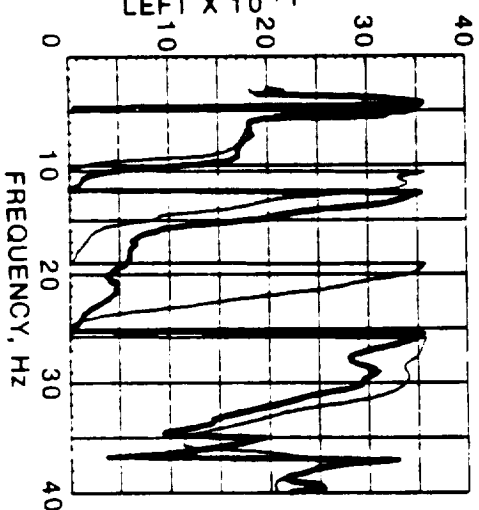
AMPLITUDE (G'S/LB) AT STAB. TIP  
LEFT X  $10^{-03}$



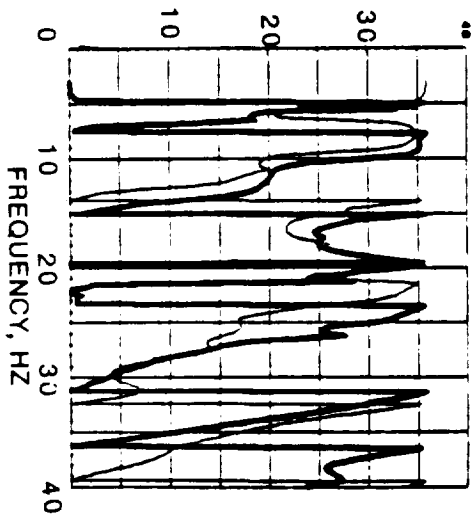
AMPLITUDE (G'S/LB) AT STAB. TIP  
LEFT X  $10^{-03}$



PHASE (DEG) AT STAB. TIP  
LEFT X  $10^{+1}$



PHASE (DEG) AT STAB. TIP  
LEFT X  $10^{+1}$



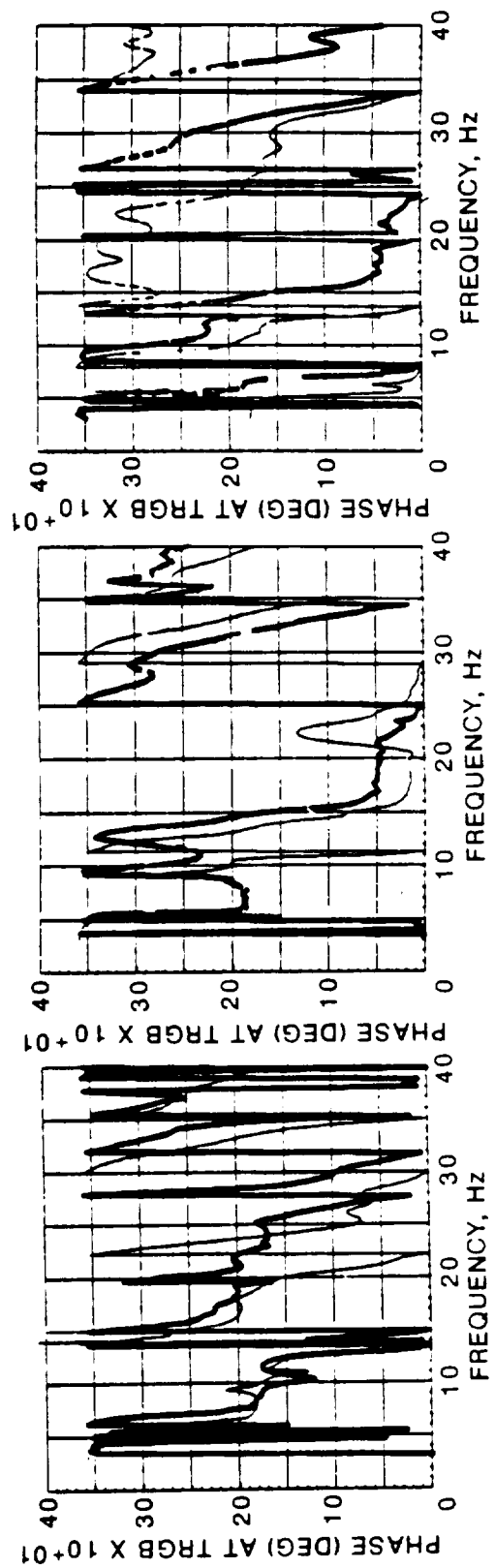
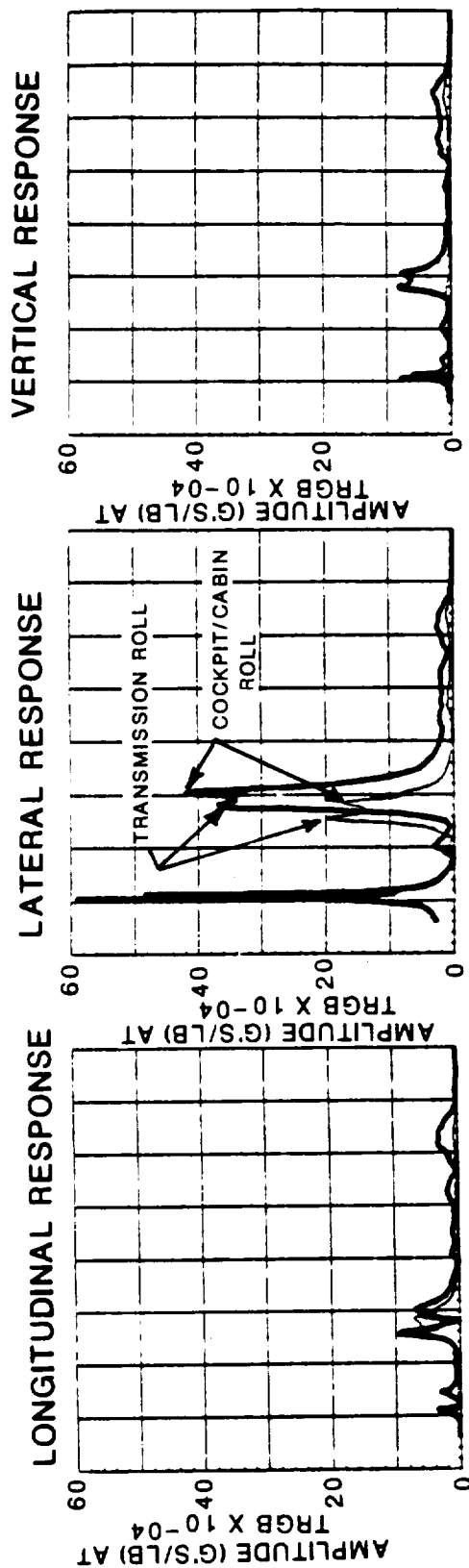
## UH-60A Frequency Response: NASTRAN Versus Shake Test

### Main Rotor Head Lateral Excitation Response at Tail Rotor Gearbox (TRGB)

The tail rotor gearbox response again illustrates the first lateral bending, transmission roll, and cockpit / cabin roll modes.

# UH-60A FREQUENCY RESPONSE: NASTRAN VERSUS SHAKE TEST MRH LAT. EXCITATION RESPONSE LOCATION: TRGB

— ANALYSIS  
— TEST



## UH-60A Frequency Response: NASTRAN Versus Shake Test

### Main Rotor Head Vertical Excitation Response at Main Rotor Head (MRH)

The modes excited by the vertical excitation are generally similar to those excited by a longitudinal force. The figure below shows the frequency response of the main rotor head in three directions. From the longitudinal response, the transmission pitch mode is under-predicted by NASTRAN in both frequency and amplitude. The same is true of the 2nd vertical bending mode. The 3rd vertical bending mode matches between test and analysis somewhat better than other modes.

The main rotor vertical response shows better amplitude prediction from the analysis data.

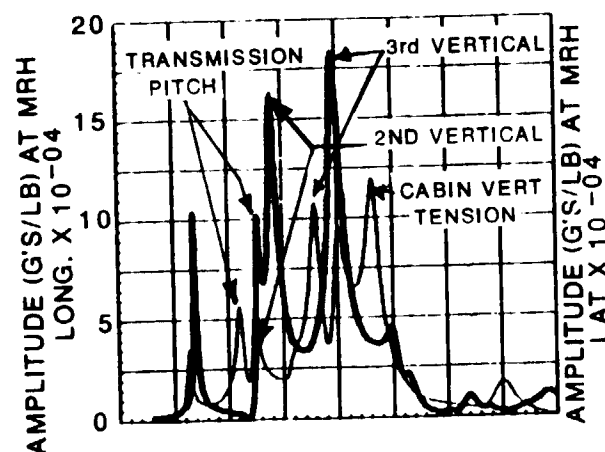
# UH-60A FREQUENCY RESPONSE: NASTRAN VERSUS SHAKE TEST

## MRH VERT. EXCITATION

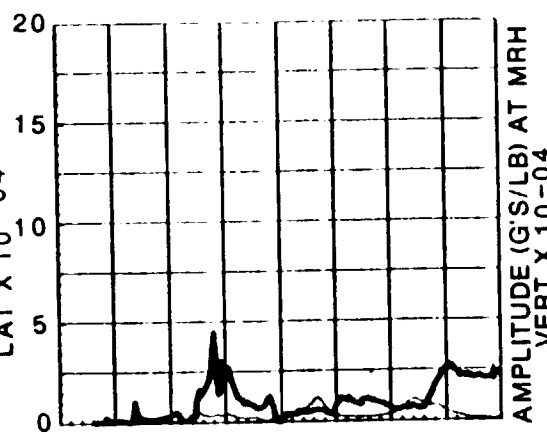
### RESPONSE LOCATION: MRH

— ANALYSIS  
— TEST

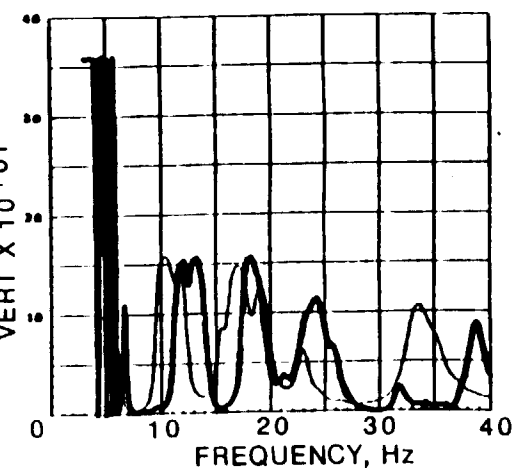
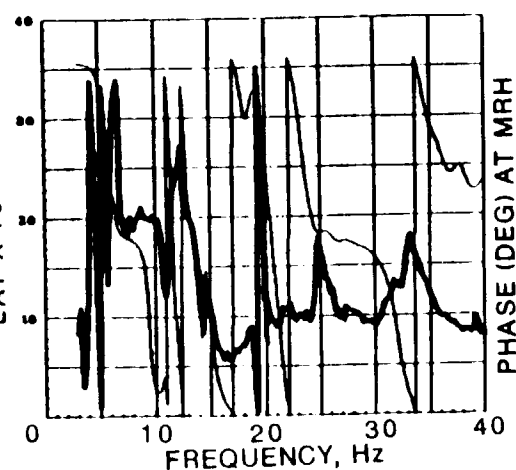
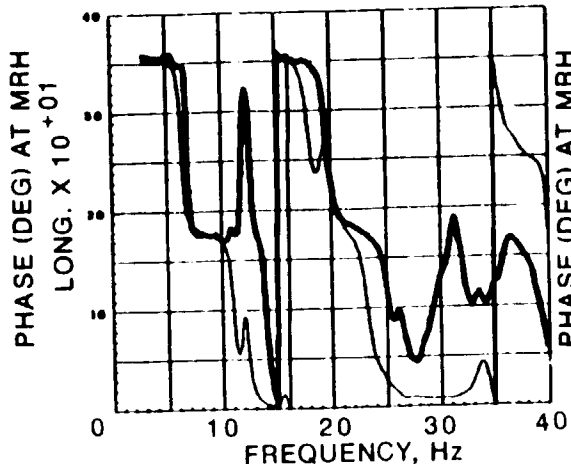
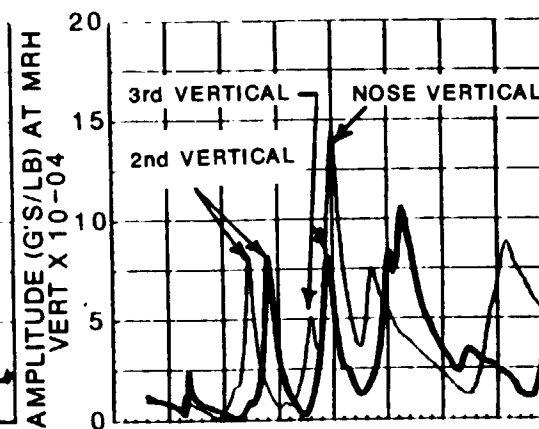
#### LONGITUDINAL RESPONSE



#### LATERAL RESPONSE



#### VERTICAL RESPONSE



## UH-60A Frequency Response: NASTRAN Versus Shake Test

### Main Rotor Head Vertical Excitation Response at Main Rotor Shaft Base (MRSB)

The main rotor shaft base longitudinal shows that NASTRAN predicts a mode at 20 HZ that is not present in the test frequency response. Examination of the mode shape shows it to be a mostly nose vertical mode. The lateral response at the main rotor shaft shows an additional test mode at 15 Hz. This is most likely the cockpit / cabin torsion mode which has considerable main transmission roll motion.

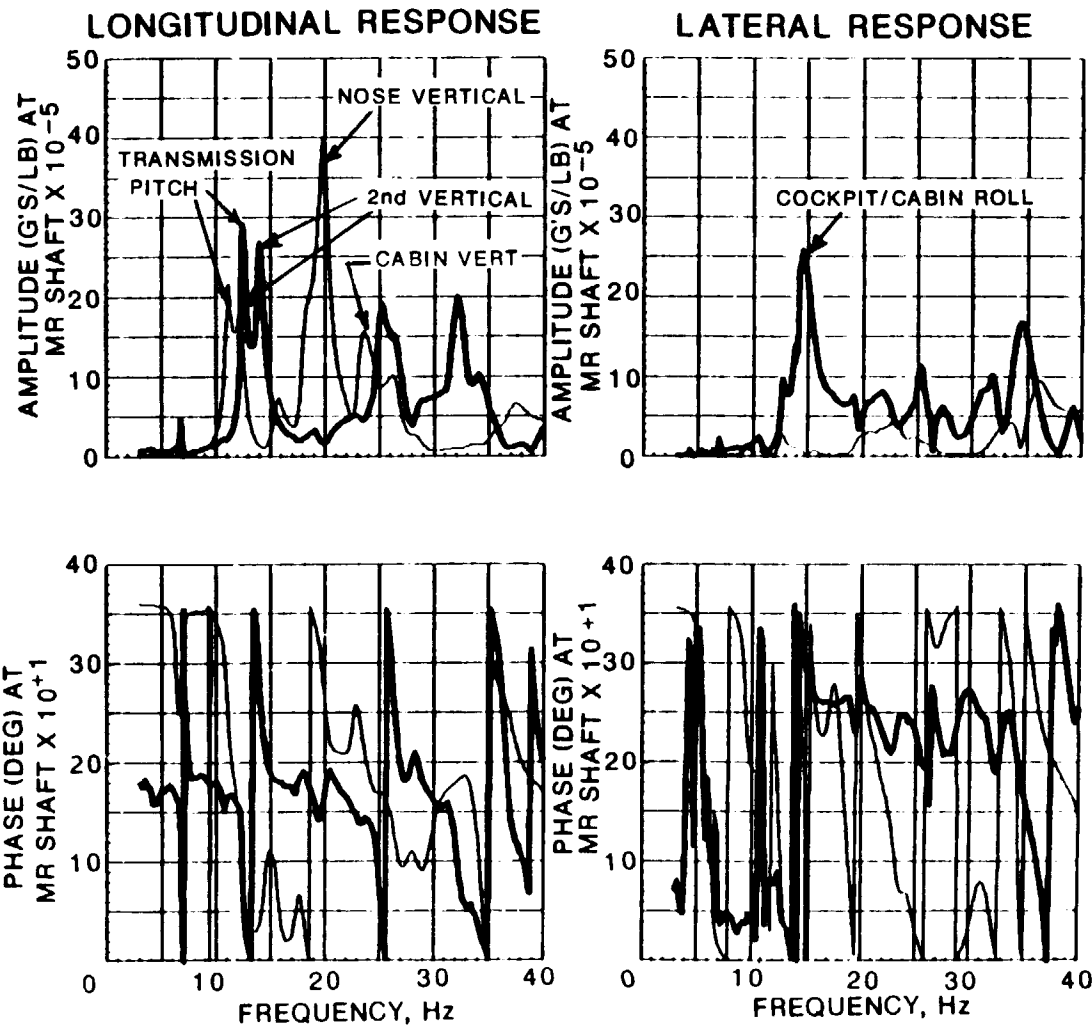


# UH-60A FREQUENCY RESPONSE: NASTRAN VERSUS SHAKE TEST

## MRH VERT. EXCITATION

### RESPONSE LOCATION: MRSB

— ANALYSIS  
— TEST



## UH-60A Frequency Response: NASTRAN Versus Shake Test

### Main Rotor Head Vertical Excitation Response at Cockpit Floor Right (CPIT-RT)

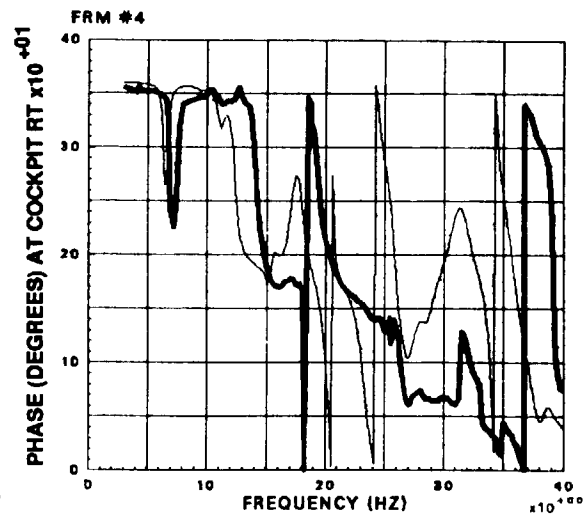
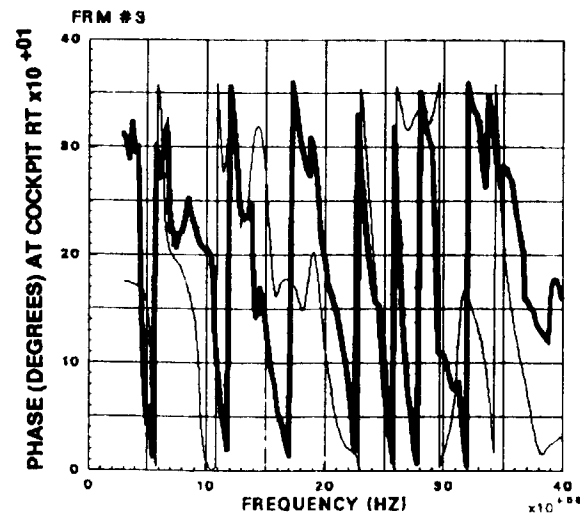
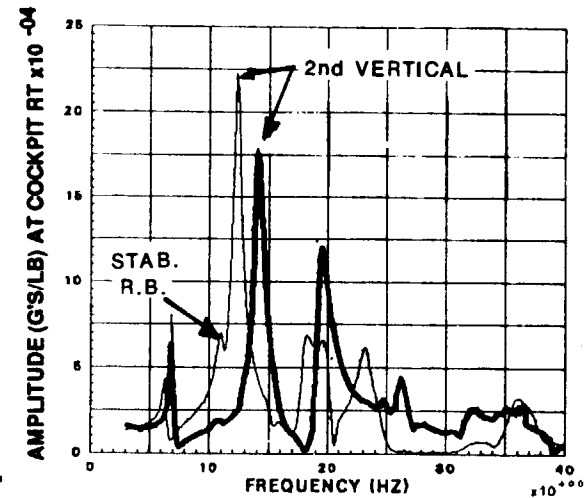
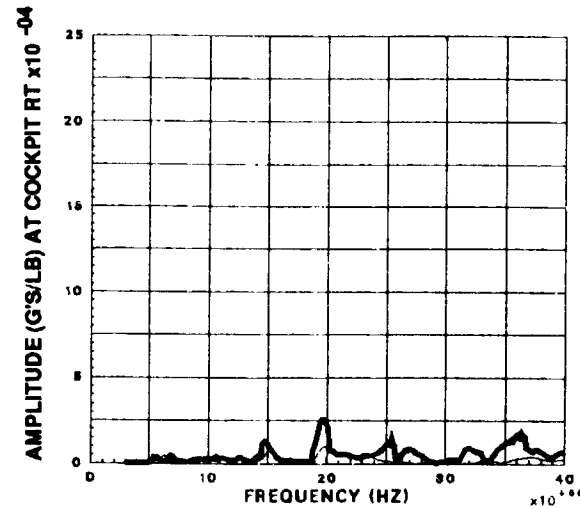
The cockpit floor vertical response shown below shows good amplitude agreement for the second vertical bending mode.

# UH-60A FREQUENCY RESPONSE: NASTRAN VERSUS SHAKE TEST

## MRH VERT. EXCITATION

RESPONSE LOCATION: CPIT-RT

— ANALYSIS  
— TEST



LONGITUDINAL

LATERAL

VERTICAL

## UH-60A Frequency Response: NASTRAN Versus Shake Test

### Main Rotor Head Vertical Excitation Response at Station 295 Floor Right (CPIT-RT)

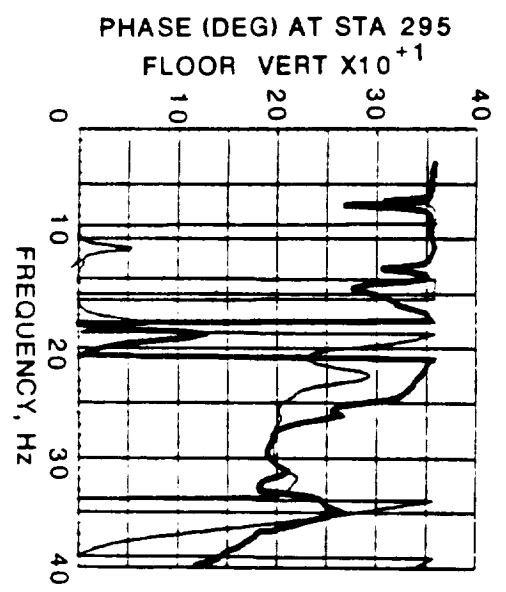
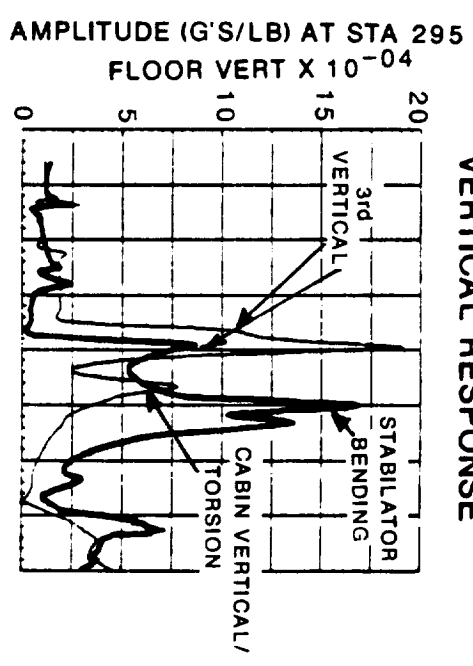
The station 295 floor vertical response shows good amplitude agreement for the third vertical mode. The NASTRAN predicted cabin vertical and torsion modes are present at 23 Hz with no test modes, and the test stabilator vertical bending mode is present at 25 Hz.

# UH-60A FREQUENCY RESPONSE: NASTRAN VERSUS SHAKE TEST MRH VERT. EXCITATION RESPONSE LOCATION: 295-FLR

— ANALYSIS

— TEST

## VERTICAL RESPONSE

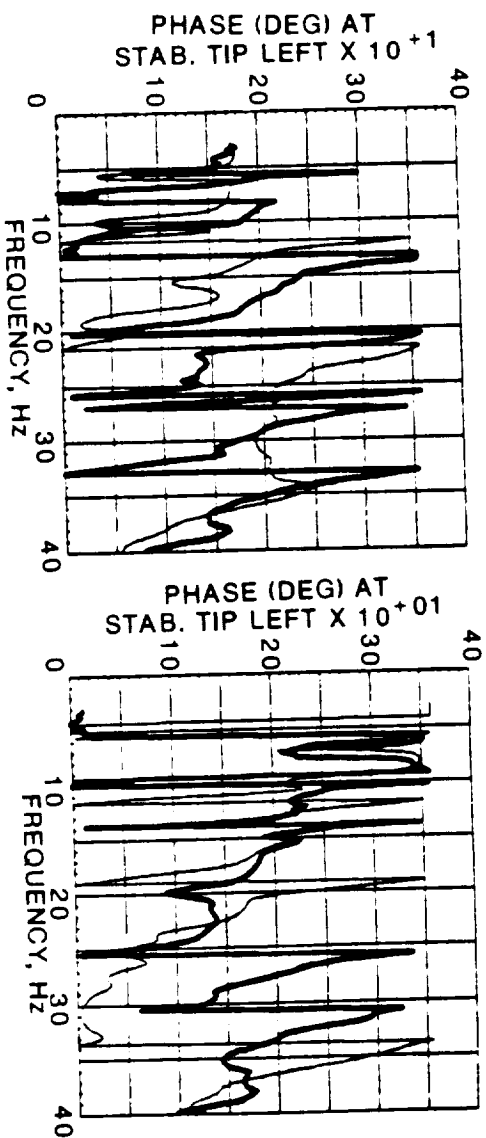
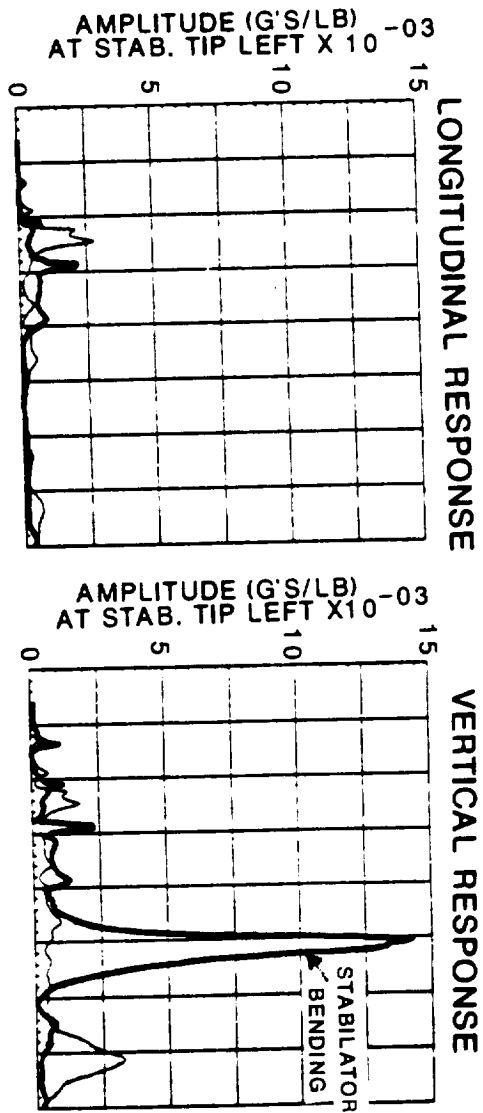


## UH-60A Frequency Response: NASTRAN Versus Shake Test

### Main Rotor Head Vertical Excitation Response at Stabilator Tip Left (STAB-LT)

The stabilator vertical response shows very well the test vertical bending mode response at 25 Hz with no accompanying NASTRAN mode.

# UH-60A FREQUENCY RESPONSE: NASTRAN VERSUS SHAKE TEST MRH VERT. EXCITATION RESPONSE LOCATION: STAB.-LT — ANALYSIS — TEST



## UH-60A Frequency Response: NASTRAN Versus Shake Test

### Main Rotor Head Vertical Excitation Response at Tail Rotor Gearbox (TRGB)

The tail rotor gearbox response is dominated by the second vertical bending and transmission pitch modes.

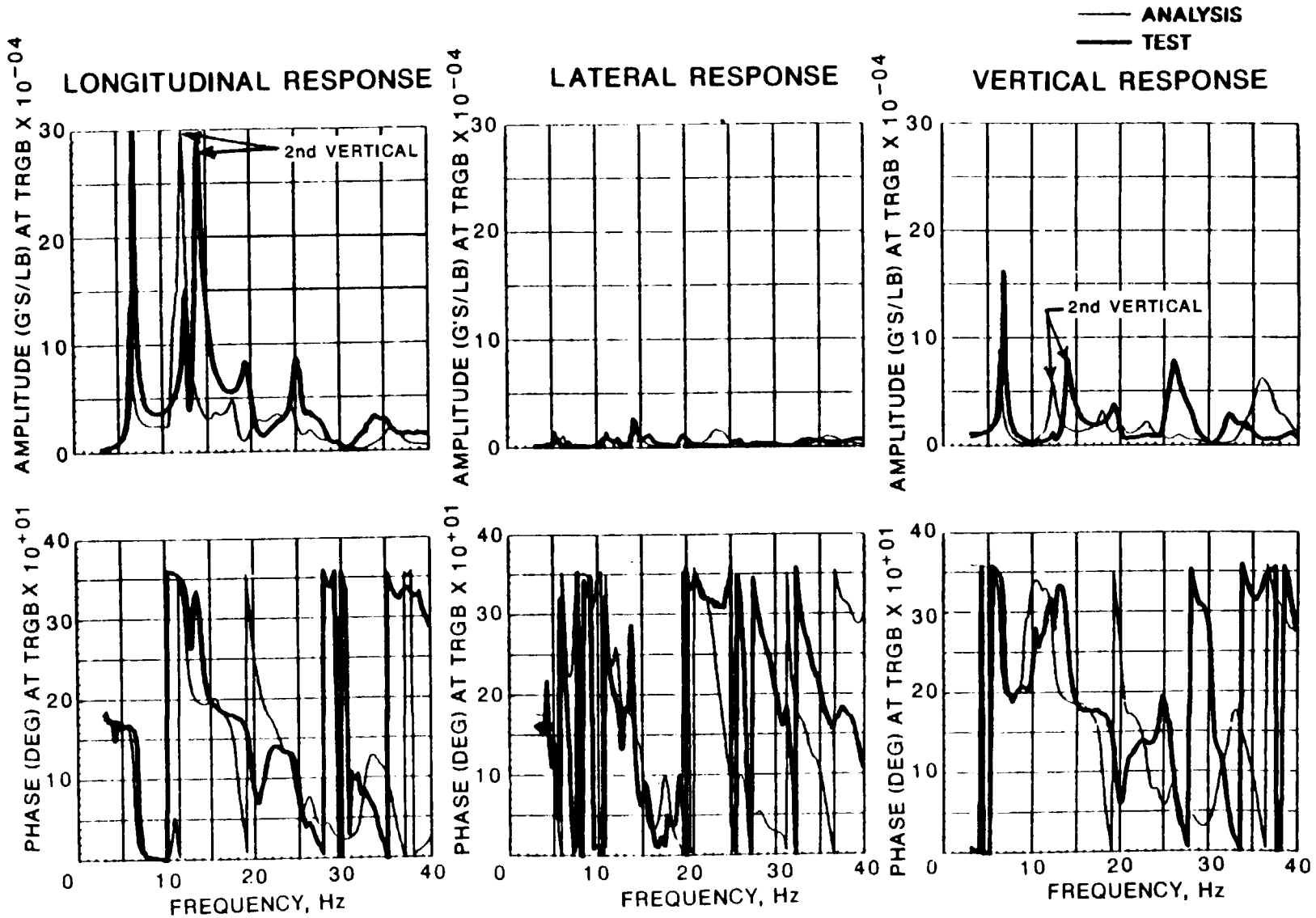


# UH-60A FREQUENCY RESPONSE: NASTRAN VERSUS SHAKE TEST

## MRH VERT. EXCITATION

### RESPONSE LOCATION: TRGB

223





## SECTION 8.0

### NASTRAN VS. SHAKE TEST: MODAL PROPERTIES

## Modal Frequency Comparison

The accompanying figure summarizes the frequencies obtained from finite element analysis compared to modes obtained from analysis of the test data. Modes were matched by close examination of the frequency response comparisons plots and the mode shape illustrations.

Due to non-linearities in the structure as well as some other factors, slightly different frequencies and mode shapes are obtained when exciting the structure in different directions. This table therefore lists the modes obtained from each excitation direction separately with a column at the end summarizing the modes using the most appropriate excitation / response combination. The table also includes the damping estimates (% critical) obtained from the modal analysis of the test data.

The error of the NASTRAN calculated frequencies is seen to be 12% or less for modes that appear to match from analysis and test. This is a great improvement over previous (pre-DAMVIBS) correlation efforts. There are several modes from NASTRAN between 20.0 and 23.5 Hz and several from test at 23.1 to over 30 Hz. These modes do not appear to match up well in either frequency or mode shape, but are most likely determined by similar structural characteristics of the structure.

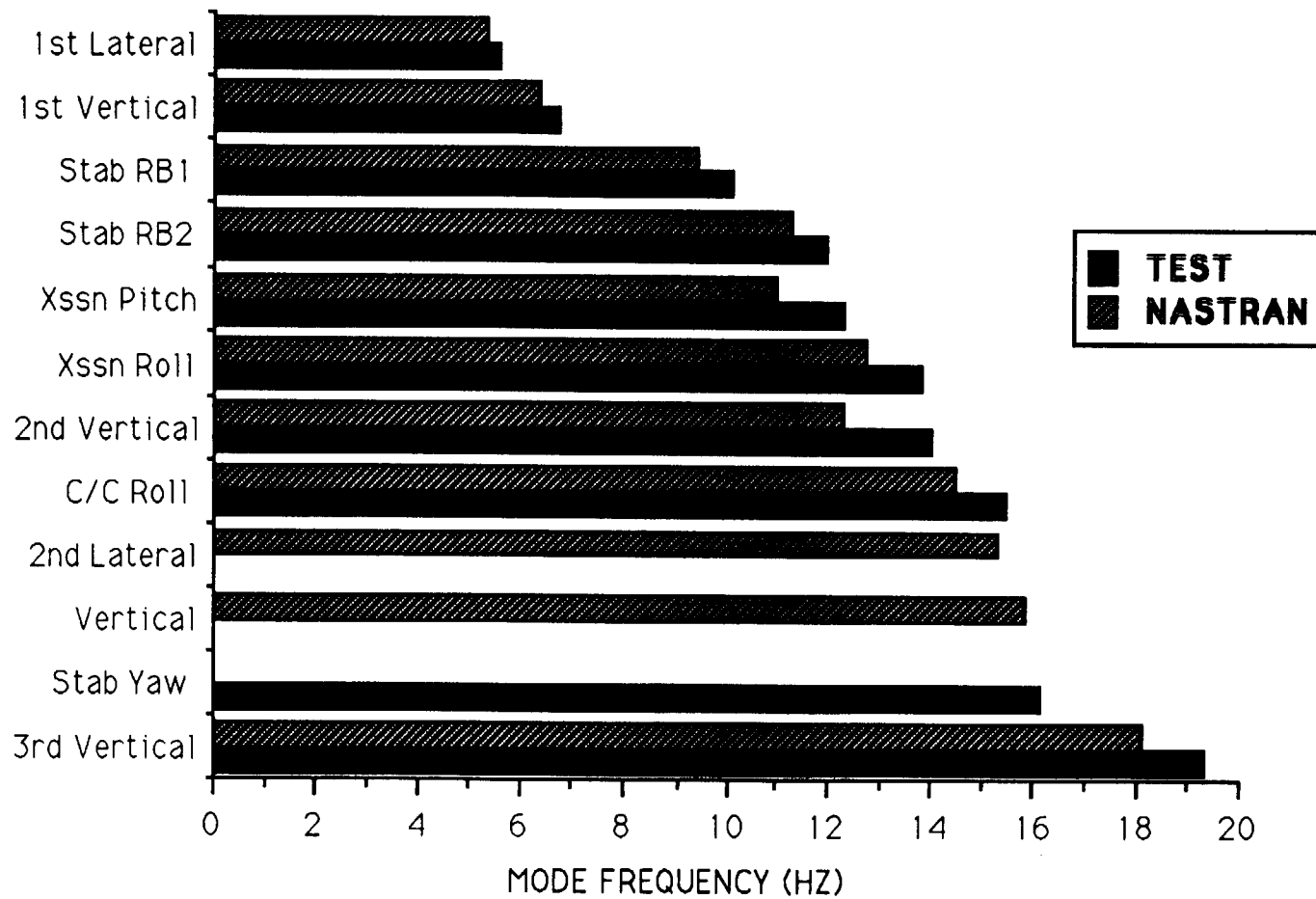
# MODAL FREQUENCY COMPARISON

Mode No.	Mode Shape	Test Frequency			Test (Avg)	NASTRAN	% Error of NASTRAN (n-t)/t	%Critical Damping		
		FX	FY	FZ				FX	FY	FZ
1	1st Lateral Bending		5.58		5.58	5.34	-4%		1.03%	
2	1st Vertical Bending	6.76		6.82	6.79	6.36	-6%	0.98%		1.25%
3	Stabilator RB	10.59	10.12		10.36	9.43	-9%	4.00%	2.93%	
4	Stabilator RB	11.94			11.94	11.16	-7%	1.95%		
5	Xssn Pitch	12.32		12.56	12.44	11.00	-12%	1.36%		1.41%
6	Xssn Roll/ 2nd Lateral		13.81		13.81	12.74	-8%		2.69%	
7	2nd Vertical Bending	13.96		14.05	14.01	12.34	-12%	2.64%		2.15%
8	Cockpit/ Cabin Roll		15.41		15.41	14.48	-6%		2.84%	
9	2nd lateral					15.32				
10	Vertical					15.84				
11	Stabilator Yaw	16.14			16.14			3.09%		
12	3rd Vertical / Xssn Vert	19.32		19.40	19.36	18.07	-7%	2.14%		2.28%
13	Cabin Shear/ 3rd vert					19.52				
14	Nose Vert/ Long					20.00				
15	Cockpit Roll/ Lateral					20.65				
16	?					21.39				
17	?					22.71				
18	Cockpit/ Cabin Torsion					23.29				
19	Cabin Vertical					23.40				
20	Cabin Torsion					23.53				
21	?	23.16			23.16			5.94%		
22	Stabilator Vert Bend.	25.22		25.07	25.15	24.53		1.69%		1.90%
23		25.64			25.64			1.88%		
24		26.58		26.39	26.49	26.60		1.65%		2.12%
25		28.36			28.36	28.50		2.84%		
26		30.57	30.65		30.61			2.18%	2.27%	
27		32.07		32.76	32.42	32.09		2.21%		1.89%
28		33.78			33.78			2.09%		
29		34.52			34.52	34.48		3.21%		
30		37.10			37.10			3.82%		
31		38.67		39.66	39.17			3.34%		1.89%

## Test Modes Versus Analysis Modes

The figure below summarizes the modal frequencies obtained from both test and analysis. It is evident from this plot that the NASTRAN calculated frequency is in general lower than that obtained from test. The modes with the best agreement are the 1st lateral and vertical bending modes, stabilator rigid body modes, transmission roll, cockpit / cabin roll and third vertical. The modes with the most error in frequency are 2nd vertical bending and transmission pitch modes. The mode shape illustrations will hopefully lead to a better understanding of why the modes differ in frequency and mode shape and where modification to the model would be effective in improving the correlation.

# TEST MODES VERSUS ANALYSIS MODES



## Mode Shape Comparisons

### First Lateral Bending

Mode shape comparisons are used to see where mode shapes differ and hopefully give an indication of where the finite element model can be modified to get better frequency and mode shape matching.

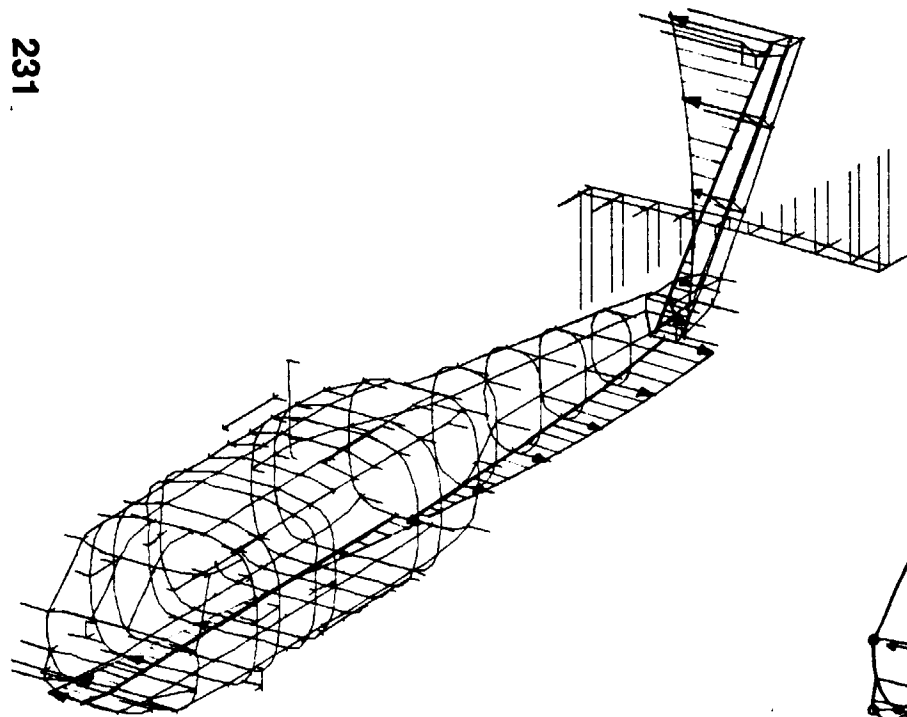
This figure illustrates the first lateral bending mode. NASTRAN under-predicts the frequency of this mode by about 4%. The mode shape is very similar except perhaps at the center of the pylon where the test shows a bit more motion than is likely. The test damping estimate for this mode is 1.0% critical.



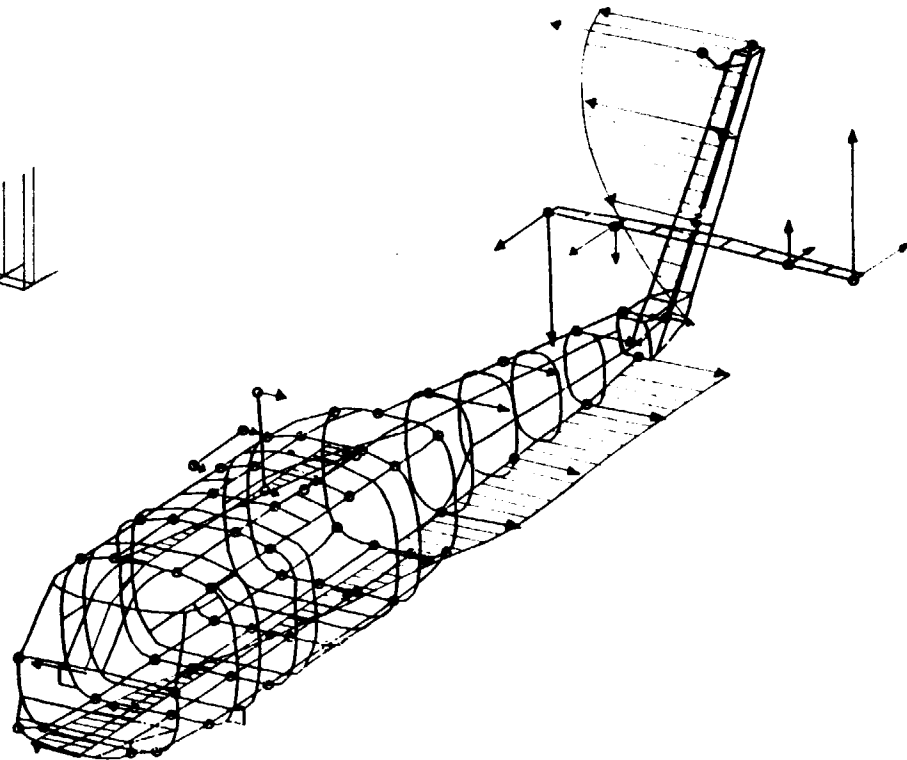
# MODE SHAPE COMPARISONS

## FIRST LATERAL BENDING

**NASTRAN**  
 **$f = 5.3 \text{ Hz}$**



**TEST**  
 **$f = 5.5 \text{ Hz}$**   
**DAMPING = 1.0%**



## Mode Shape Comparisons

### First Vertical Bending

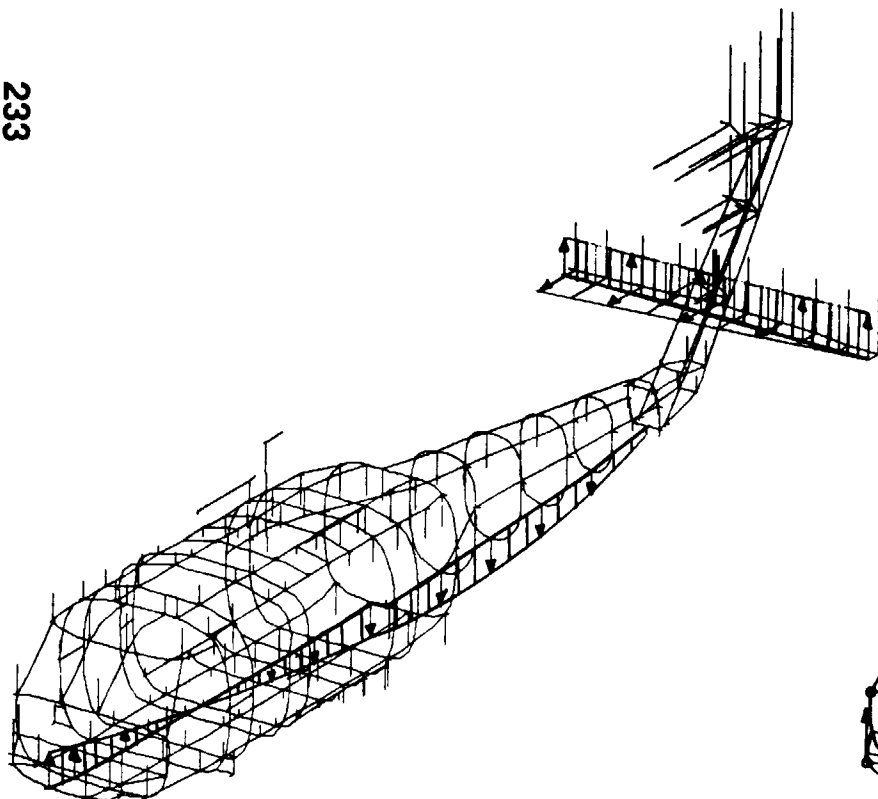
For the first vertical bending mode the frequency error is about 6%. The mode shapes compare very well with the only difference being in the amount of stabilator yaw. The test mode shape in this area looks to be more symmetric (no yaw) than the NASTRAN. The damping for this mode is again 1% critical.

# MODE SHAPE COMPARISONS

## FIRST VERTICAL BENDING

**NASTRAN**

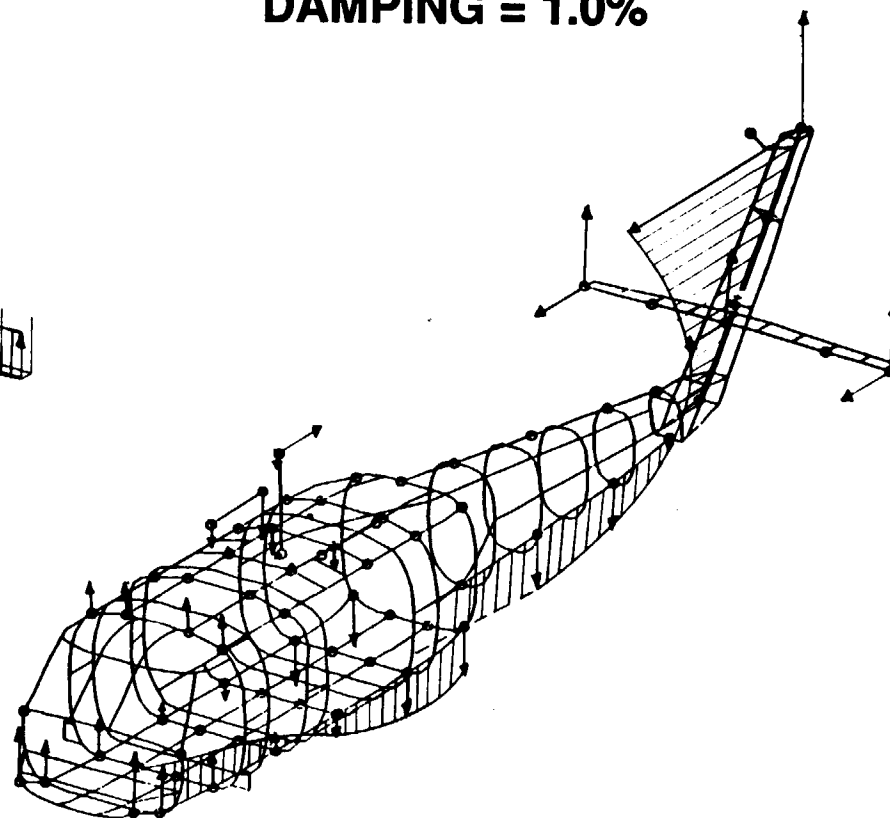
**$f = 6.4$  Hz**



**TEST**

**$f = 6.8$  Hz**

**DAMPING = 1.0%**



## Mode Shape Comparisons

### Stabilator Rigid Body 1

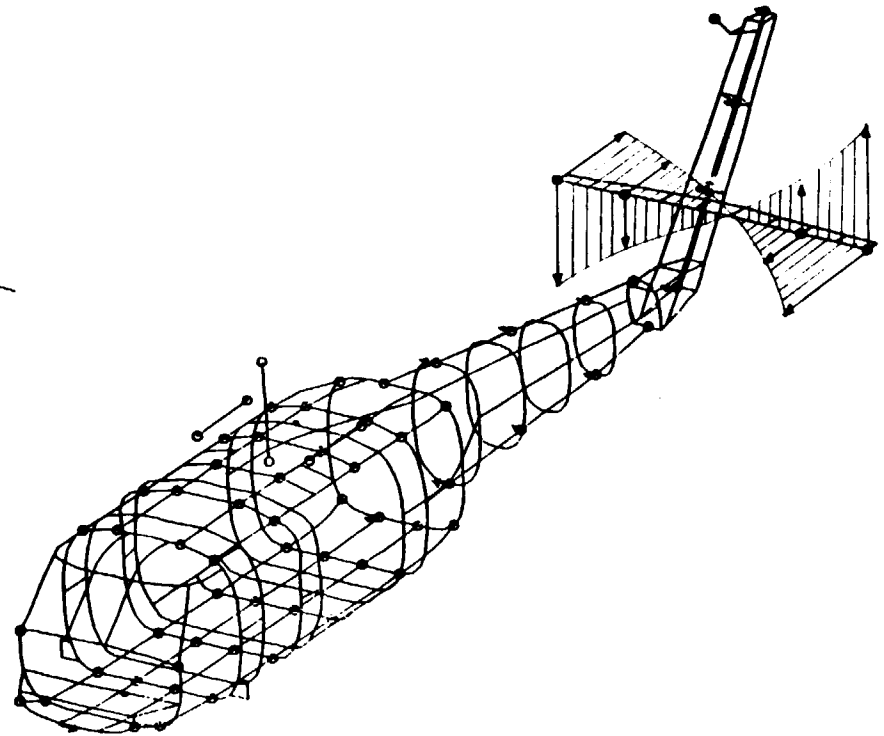
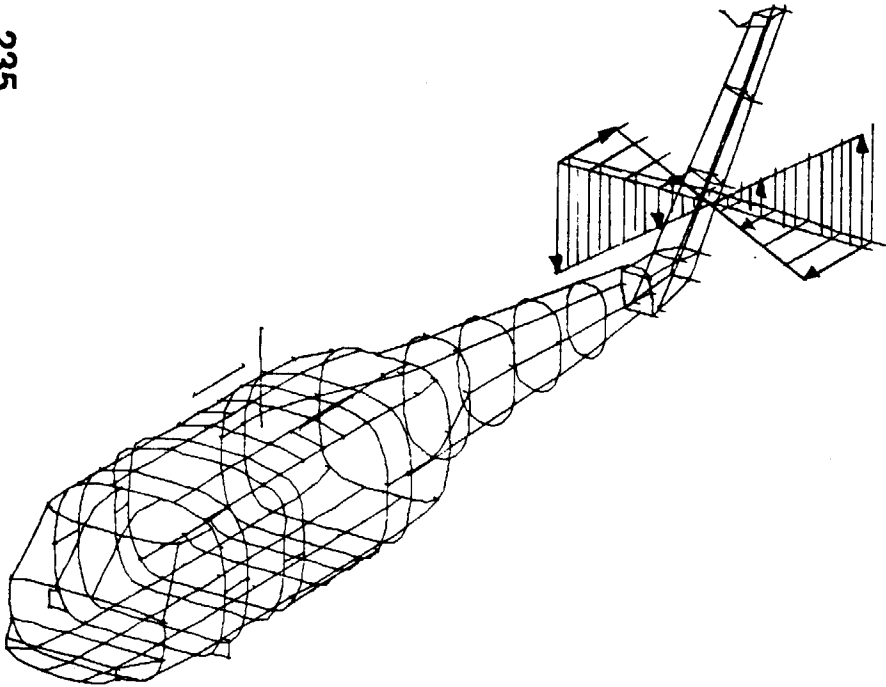
The stabilator rigid body modes (there are usually two for the UH-60) show not as good agreement as the fundamental bending modes. The mode shape of the first mode appears to have good agreement but the frequency error is 9%. The NASTRAN mode shows slightly more roll than yaw while the test mode appears to be equally in roll and yaw. Damping for this mode is 2.9% critical.

# MODE SHAPE COMPARISONS STABILATOR RIGID BODY 1

**NASTRAN**  
 **$f = 9.4$  Hz**

**TEST**  
 **$f = 10.1$  Hz**  
**DAMPING = 2.9%**

235



## Mode Shape Comparisons

### Transmission Pitch

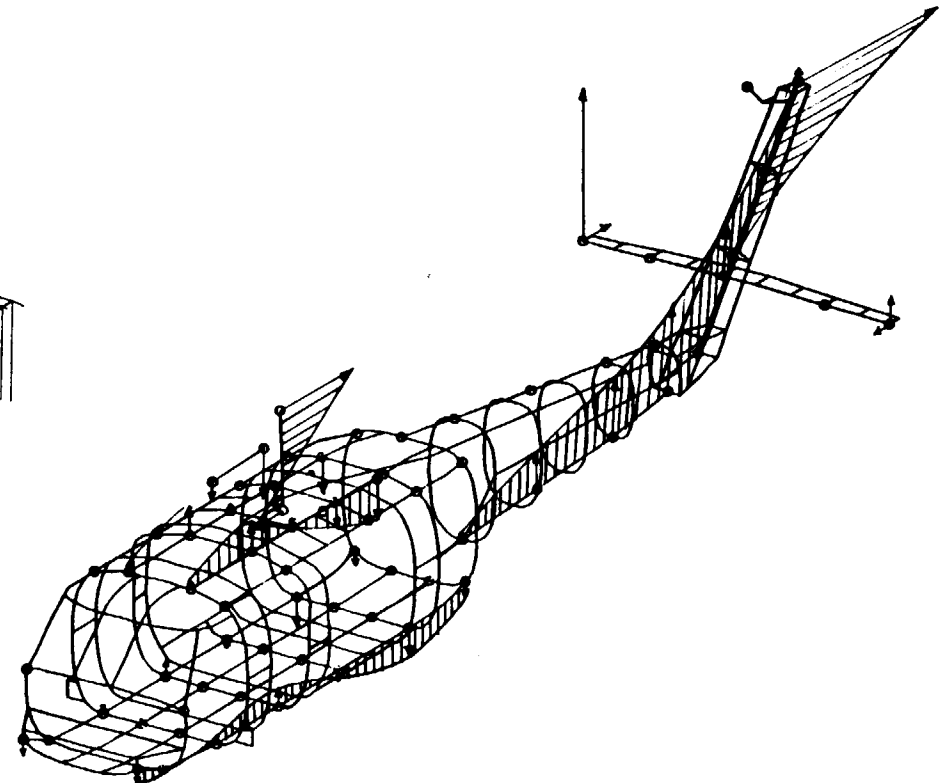
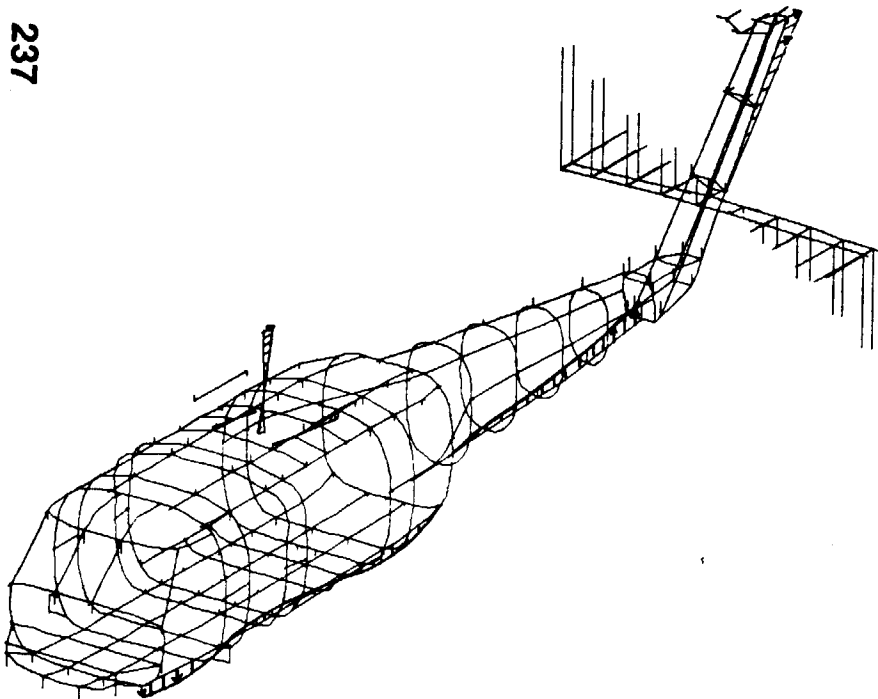
The transmission pitch mode has a frequency error of 12%. To explain this large discrepancy, the first inclination would be to assume that the transmission support structure is not modeled accurately. This mode does however have a lot of motion in the cabin, pylon and stabilator. Examination of the mode shapes shows that the biggest difference in the mode shapes is the stabilator roll motion. The NASTRAN mode appears to have more stabilator motion and the rest of the airframe appears to have lower amplitudes. Damping for this mode is 1.4% critical.

# MODE SHAPE COMPARISONS TRANSMISSION PITCH

**NASTRAN**  
 **$f = 11.0$  Hz**

**TEST**  
 **$f = 12.3$  Hz**  
**DAMPING = 1.4%**

237



## Mode Shape Comparisons

### Second Vertical Bending

The second vertical bending mode is characterized by in-phase motion of the nose and tail (bottom of the pylon) areas with another node point occurring at about one third of the pylon height. This mode also has considerable transmission pitch motion. The NASTRAN and test mode shape agree very well although the frequency error is 12%. Damping for this mode is 2.6% critical.

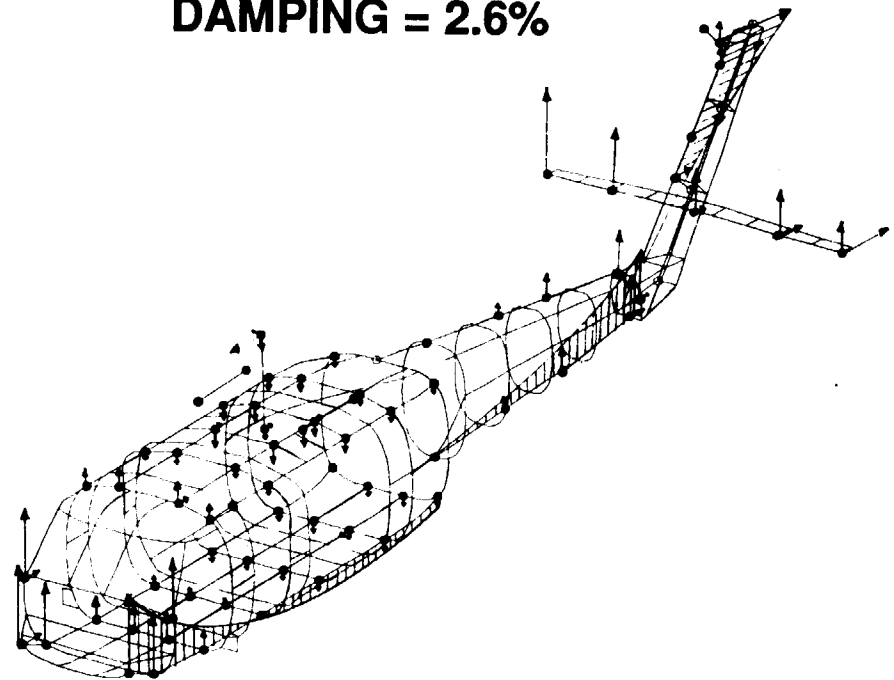
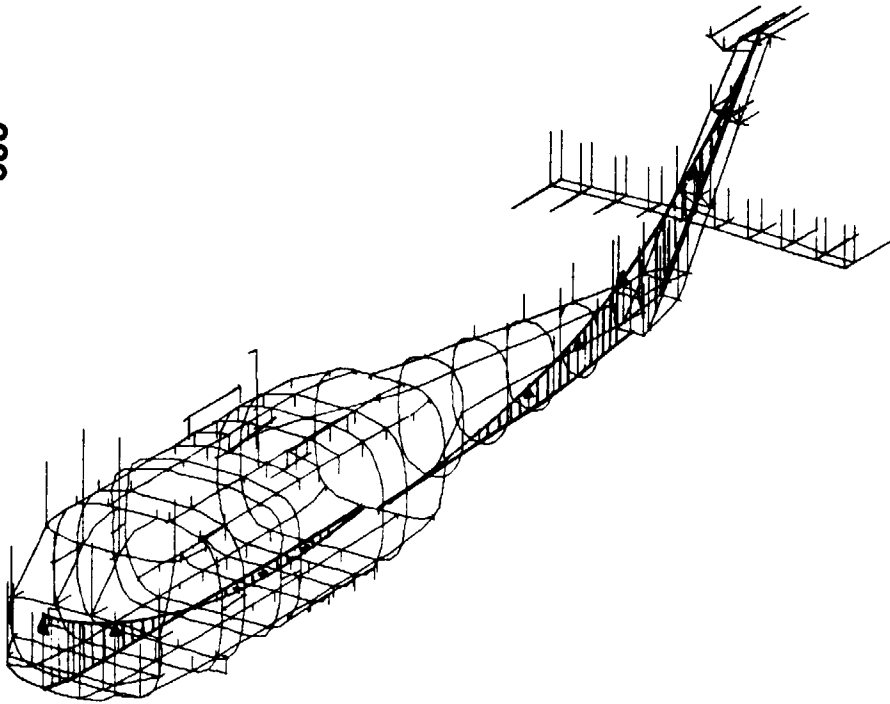


# MODE SHAPE COMPARISONS SECOND VERTICAL BENDING

**NASTRAN**  
 **$f = 12.3 \text{ Hz}$**

**TEST**  
 **$f = 14.0 \text{ Hz}$**   
**DAMPING = 2.6%**

239



## Mode Shape Comparisons

### Transmission Roll

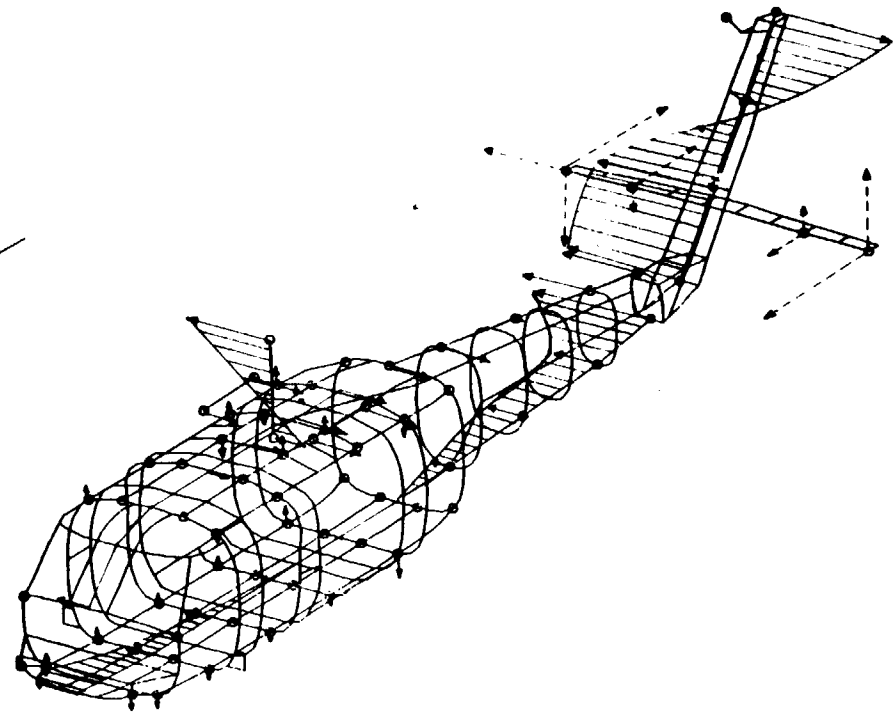
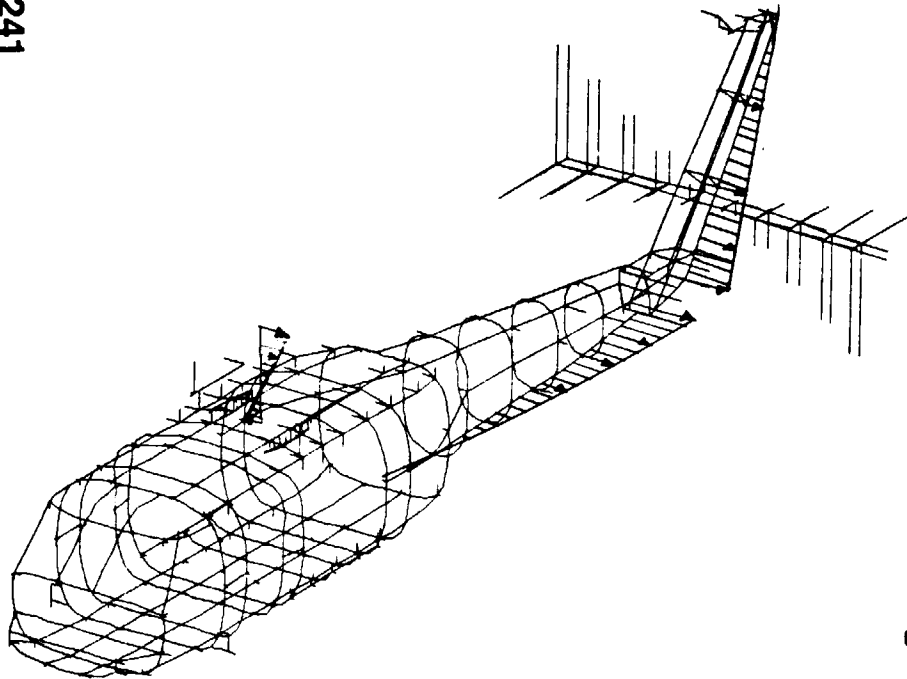
The transmission roll mode illustrated here has, like the transmission pitch mode, very distinct motion in the fuselage. The frequency error from NASTRAN to test is 8%. The two mode shapes show similar motion in the transmission and center cabin areas (although plotted out-of-phase). The differences in the mode shapes are evident in the forward cockpit lateral and the tail rotor gearbox motion. Stabilator motion is seen to be similar. Damping for this mode is 2.7% critical.

# MODE SHAPE COMPARISONS TRANSMISSION ROLL

**NASTRAN**  
 **$f = 12.7 \text{ Hz}$**

**TEST**  
 **$f = 13.8 \text{ Hz}$**   
**DAMPING = 2.7%**

241



## Mode Shape Comparisons

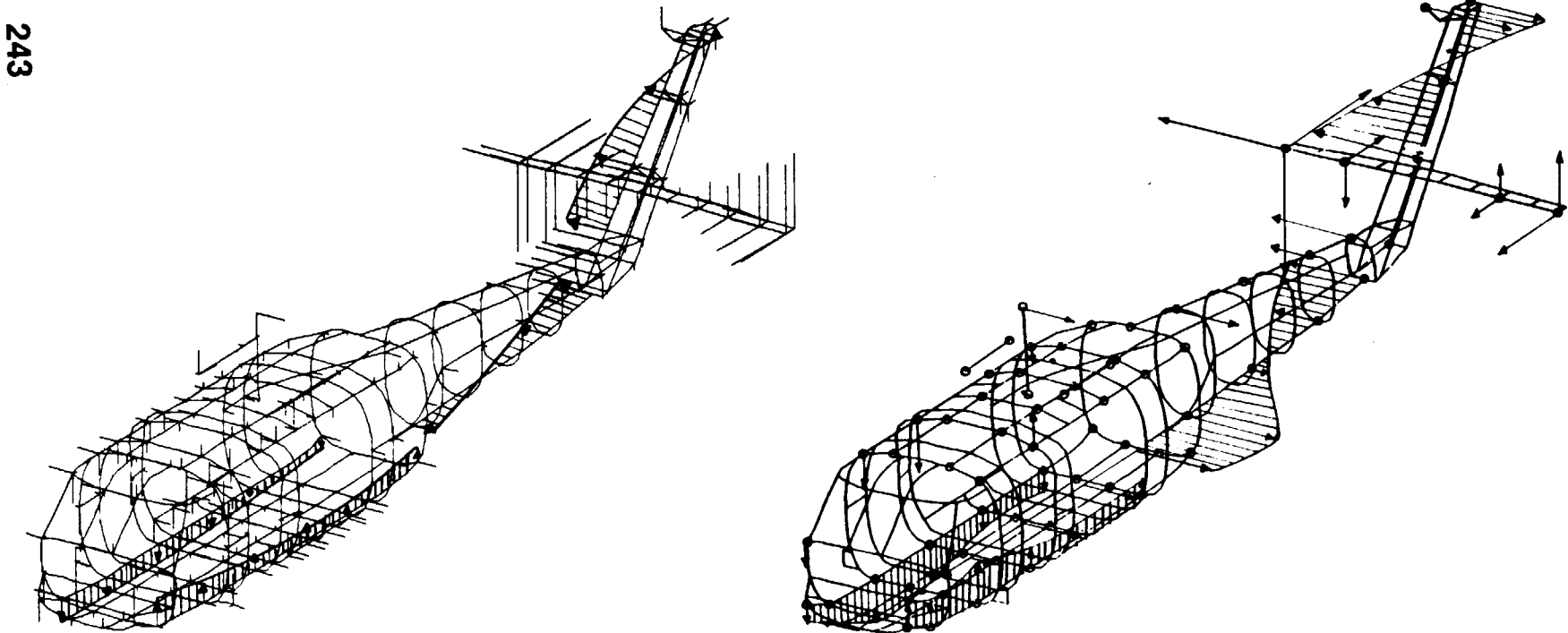
### Cockpit / Cabin Roll

The figure below illustrates the cockpit cabin roll mode. The frequency error for this mode is 6%. The mode shapes from test and analysis are very similar especially in the transmission area, cabin and stabilator. Small differences are evident in the forward cockpit lateral response where the test shows more lateral (right) motion than NASTRAN does. The damping for this mode is 2.8%.

# MODE SHAPE COMPARISONS COCKPIT / CABIN ROLL

**NASTRAN**  
 **$f = 14.5 \text{ Hz}$**

**TEST**  
 **$f = 15.4 \text{ Hz}$**   
**DAMPING = 2.8%**



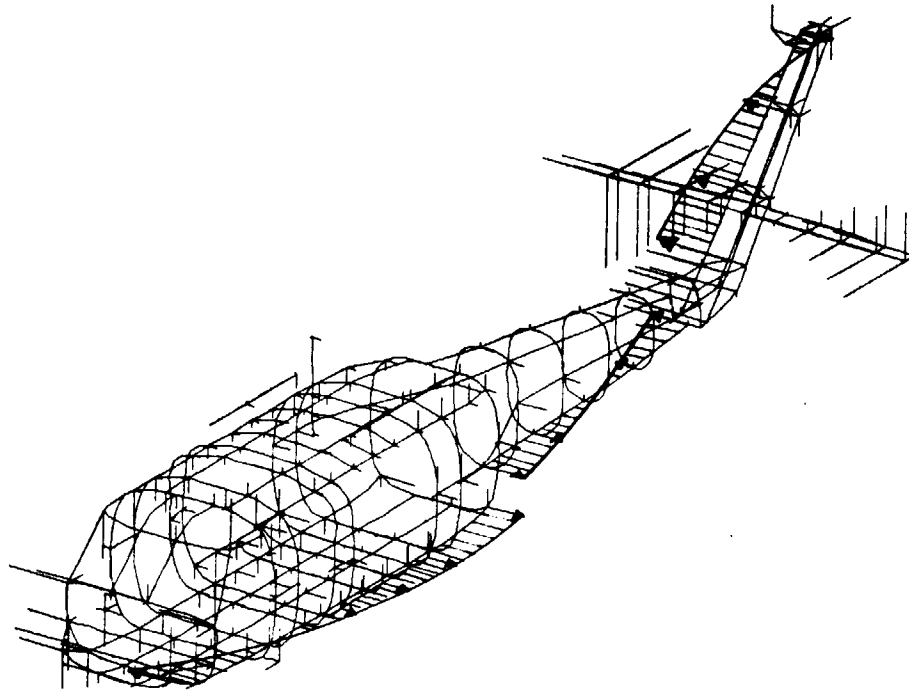
## Mode Shape Comparisons

### Second Lateral Bending

The accompanying figure presents a NASTRAN mode which appears to be a second lateral bending mode. The lateral motion of the fuselage is similar to the transmission roll mode from NASTRAN, although this mode does appear to have more lateral motion in the center cabin area. It could be that the NASTRAN model is under-predicting the transmission roll mode which is closer to second lateral in the test article. These modes appear as one mode in test.

# MODE SHAPE COMPARISONS SECOND LATERAL BENDING

**NASTRAN**  
 **$f = 15.3 \text{ Hz}$**



## Mode Shape Comparisons

### Third Vertical / Transmission Vertical

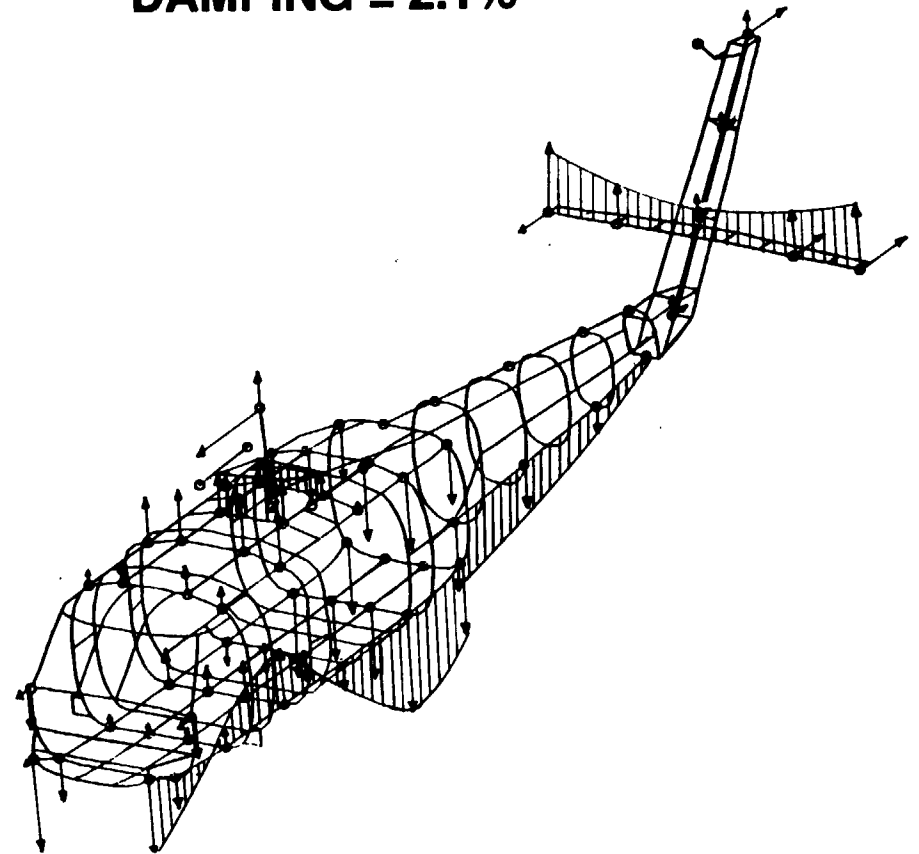
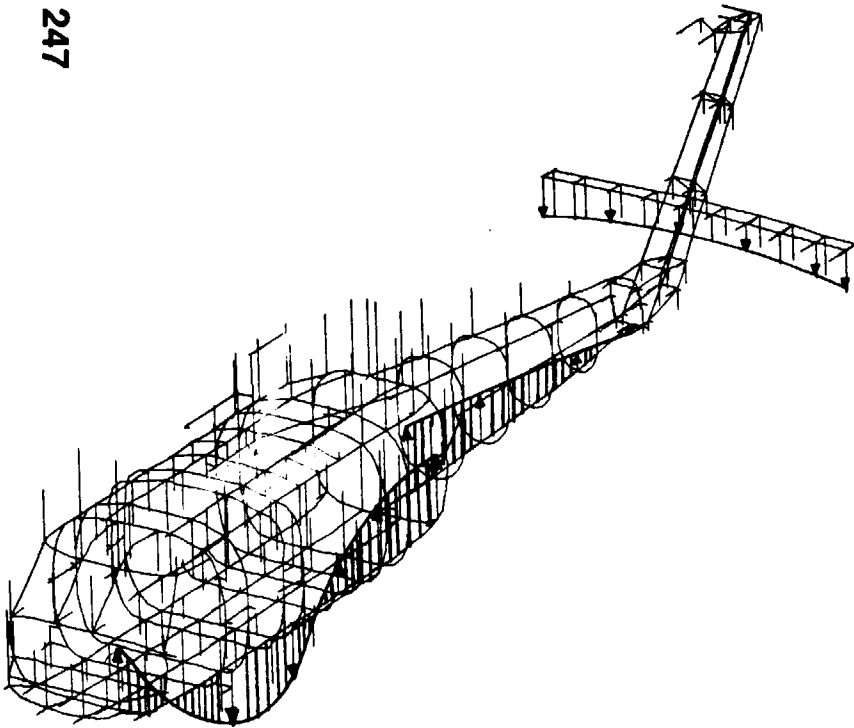
The third vertical/ bending mode comparison is presented in the accompanying slide. The frequency error for this mode is 7%. The mode shapes are seen to be very similar at most locations on the airframe. The damping for this mode is 2.1%.



# MODE SHAPE COMPARISONS THIRD VERTICAL BENDING / TRANSMISSION VERTICAL

**NASTRAN**  
 **$f = 18.1$  Hz**

**TEST**  
 **$f = 19.3$  Hz**  
**DAMPING = 2.1%**





## SECTION 9.0

# SCHEDULE AND RESOURCES

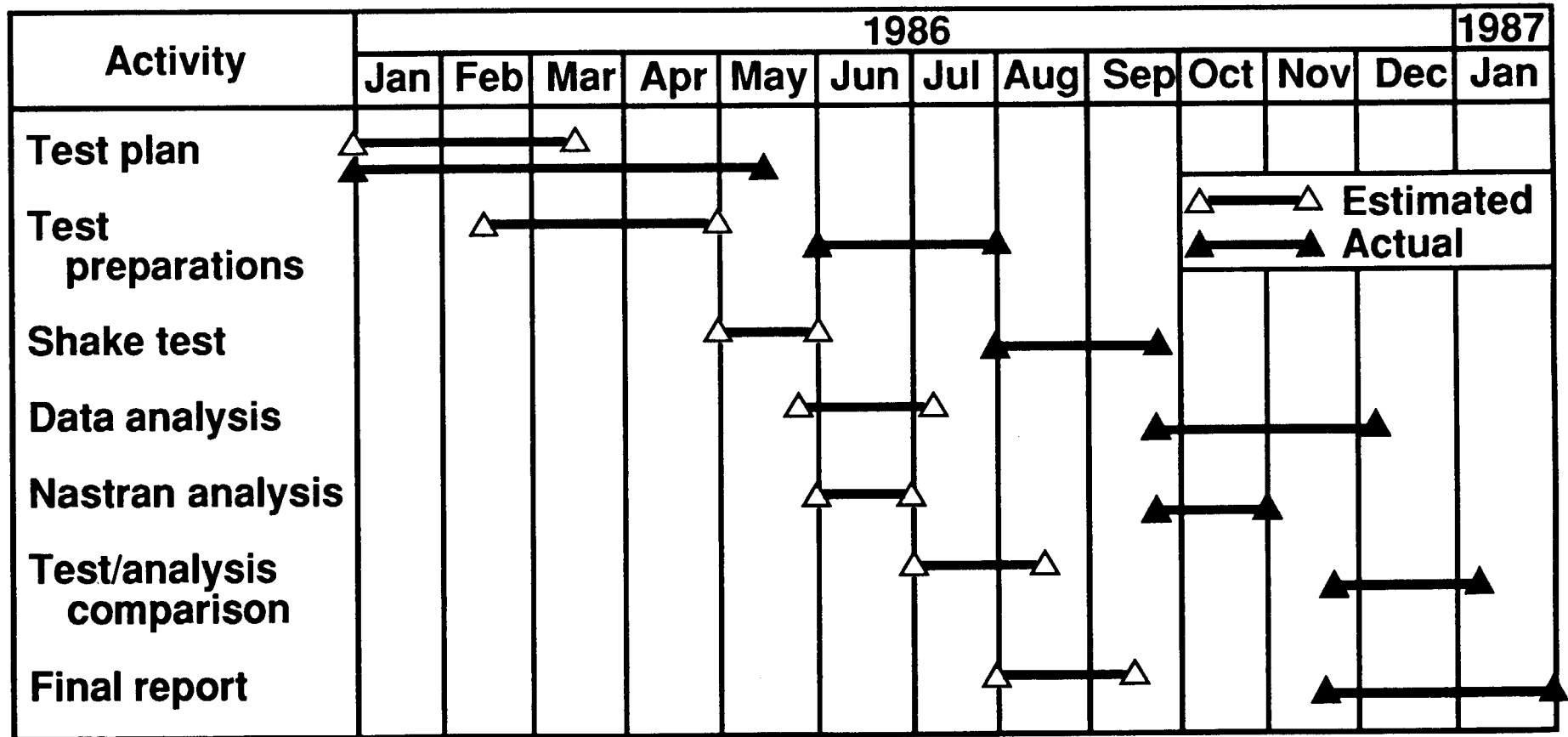
## SCHEDULE AND RESOURCES

### Comparison of Planned and Actual Schedules

The projected and actual schedules for the major activities of this task are shown in this figure. A delay in obtaining the test aircraft was the major cause of the increase in the overall elapsed time.

# SCHEDULE AND RESOURCES

## COMPARISON OF PLANNED AND ACTUAL SCHEDULES



## SCHEDULE AND RESOURCES

### Comparison of Estimated and Actual Manhours

This table summarizes the estimated and actual manhour expenditures to accomplish the major activities of this task. Actual manhours spent were about 25% less than those estimated.

## SCHEDULE AND RESOURCES

### COMPARISON OF ESTIMATED AND ACTUAL MANHOURS

		<u>Engineering</u>		<u>Manufacturing</u>	
		<u>Estimated</u>	<u>Actual</u>	<u>Estimated</u>	<u>Actual</u>
Test plan		600	460		
Test preparations		840	660	860	550
Shake test		1120	690	640	330
253 Data analysis		400	370		
Nastran analysis		200	160		
Test/analysis comparison		120	240		
Final report		300	380		
		<u>3580</u>	<u>2960</u>	<u>1500</u>	<u>880</u>

Combined totals: Estimated = 5080

Actual = 3840





## **SECTION 10.0**

## **CONCLUSIONS**

## CONCLUSIONS

Frequency response functions (FRF's) were measured on a production UH-60A aircraft for 127 response components at 72 locations. Test modal properties (frequency, shape, and damping) were then identified, by curve-fitting, from these FRF's. Modal damping values were found to range from 1% to 4% critical, for all the modes but one. Local modes of the support system were found to couple with aircraft modes, which deserves further investigation.

Test FRF's and modal properties were compared with values calculated from the NASTRAN finite element model. NASTRAN under-predicts the modal frequencies by 4% to 12%, with the largest deviations being for the main transmission pitch mode and the second vertical bending mode.

## **CONCLUSIONS**

- **Frequency response functions (FRF's) were measured on a production UH-60A aircraft for 127 motions at 72 locations**
- **Test modal properties (frequency, shape, and damping) were identified by curve-fitting the above**
- **Modal damping values were found to range from 1% to 4% critical, for all the modes but one**
- **Local modes of support system were not isolated from aircraft modes and should be further investigated**
- **Test FRF's and modal properties were compared with values calculated from the NASTRAN finite element model**
- **NASTRAN under-predicts the modal frequencies by 4% to 12%, with the largest under-predictions being for the main transmission pitch mode and the second vertical bending mode**



259

## SECTION 11.0

## REFERENCES





## Report Documentation Page

1. Report No. NASA CR-181993		2. Government Accession No.		3. Recipient's Catalog No.	
4. Title and Subtitle GROUND SHAKE TEST OF THE UH-60A HELICOPTER AIRFRAME AND COMPARISON WITH NASTRAN FINITE ELEMENT MODEL PREDICTIONS				5. Report Date MARCH 1990	
				6. Performing Organization Code	
7. Author(s) G.R. HOWLAND, J.A. DURNO, AND W.J. TWOMEY				8. Performing Organization Report No.	
				10. Work Unit No. 505-63-51-01	
9. Performing Organization Name and Address UNITED TECHNOLOGIES CORPORATION SIKORSKY AIRCRAFT DIVISION 6900 MAIN STREET STRATFORD, CT 06601-1381				11. Contract or Grant No. NAS1-17499	
				13. Type of Report and Period Covered CONTRACTOR REPORT	
12. Sponsoring Agency Name and Address NATIONAL AERONAUTICS AND SPACE ADMINISTRATION LANGLEY RESEARCH CENTER HAMPTON, VA 23665-5225				14. Sponsoring Agency Code	
15. Supplementary Notes LANGLEY TECHNICAL MONITOR: RAYMOND G. KVATERNIK FINAL REPORT (FOR TASK NO. 3 OF THE CONTRACT)					
16. Abstract  Sikorsky Aircraft, together with the other major helicopter airframe manufacturers, is engaged in a study to improve the use of finite element analysis to predict the dynamic behavior of helicopter airframes, under a rotorcraft structural dynamics program called DAMVIBS ( <u>D</u> esign <u>A</u> nalysis <u>M</u> ethods for <u>V</u> ibration <u>S</u> ), sponsored by the NASA Langley Research Center.  This report presents the test plan and test results for a shake test of the UH-60A BLACK HAWK helicopter. It also presents a comparison of test results with results obtained from analysis using a NASTRAN finite element model.					
17. Key Words (Suggested by Author(s)) AIRFRAME VIBRATIONS, UH-60A HELICOPTER FINITE ELEMENT, GROUND VIBRATION TEST, NASTRAN, DYNAMICS				18. Distribution Statement UNCLASSIFIED - UNLIMITED  SUBJECT CATEGORY 39	
19. Security Classif. (of this report) UNCLASSIFIED		20. Security Classif. (of this page) UNCLASSIFIED		21. No. of pages 262	22. Price A12

## REFERENCES

1. Ewins, D. J.: Modal Testing: Theory and Practice, 1984, John Wiley and Sons, Inc., New York.
2. Dinyovszky, P., and Twomey, W. J.: Plan, Formulate, and Discuss a NASTRAN Finite Element Model of the UH-60A Helicopter Airframe. NASA CR 181975, February, 1990.